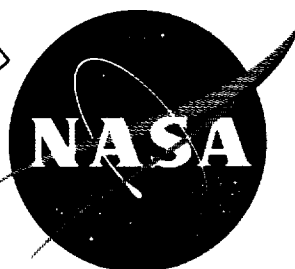
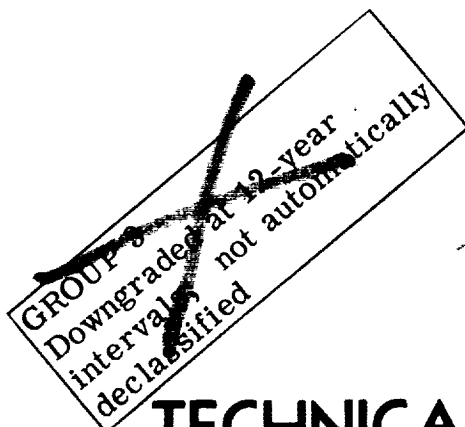


~~CONFIDENTIAL~~

NASA TM X-809

NASA TM X-809


 X63-14178
 CLASSIFICATION CHANGED
 UNCLASSIFIED

 40-nasa
 By Authority of 22-274 Date 5 JUL 1972

TECHNICAL MEMORANDUM

CASE FILE COPY

X-809

TRANSONIC AERODYNAMIC CHARACTERISTICS OF THE DYNA-SOAR
 GLIDER AND TITAN III LAUNCH-VEHICLE CONFIGURATION
 WITH VARIOUS FIN ARRANGEMENTS

By Ralph P. Bielat

Langley Research Center
 Langley Station, Hampton, Va.

Declassified by authority of NASA
 Classification Change Notice No. 218
 Dated 30 SEP 1972

CLASSIFIED DOCUMENT - TYPE UNCLASSIFIED

This document contains information affecting the national defense of the United States within the meaning of the Espionage Laws, Title 18, U.S.C., Sec. 793 and 794, and the transmission or revelation of which in any manner to an unauthorized person is prohibited by law.

NATIONAL AERONAUTICS AND SPACE ADMINISTRATION
 WASHINGTON

April 1963

~~CONFIDENTIAL~~

1. The first part of the document discusses the importance of maintaining accurate records of all transactions and activities. It emphasizes the need for transparency and accountability in financial reporting.

2. The second part of the document outlines the various methods and techniques used to collect and analyze data. It includes a detailed description of the experimental procedures and the statistical analysis performed.

3. The third part of the document presents the results of the study. It includes a series of tables and graphs that illustrate the findings of the research. The data shows a clear trend of increasing activity over time.

4. The fourth part of the document discusses the implications of the findings. It suggests that the results have significant implications for the field of study and may lead to further research in this area.

5. The fifth part of the document concludes the study. It summarizes the key findings and provides a final statement on the importance of the research.

~~CONFIDENTIAL~~

NATIONAL AERONAUTICS AND SPACE ADMINISTRATION

TECHNICAL MEMORANDUM X-809

TRANSONIC AERODYNAMIC CHARACTERISTICS OF THE DYNA-SOAR

GLIDER AND TITAN III LAUNCH-VEHICLE CONFIGURATION

WITH VARIOUS FIN ARRANGEMENTS*

By Ralph P. Bielat

SUMMARY

An investigation was conducted at transonic speeds in the Langley 8-foot transonic pressure tunnel to obtain the static longitudinal and lateral aerodynamic characteristics of the Dyna-Soar glider and Titan III launch-vehicle configuration with various fin arrangements. The Mach number range extended from 0.70 to 1.30, the angle-of-attack range from approximately -11° to 9° , and the angle-of-sideslip range from approximately -8° to 8° . The Reynolds number per foot ranged from approximately 3.50×10^6 to 4.22×10^6 during the tests.

The wind-tunnel results indicated that the only configurations which possibly may have satisfactory longitudinal or directional stability characteristics were those with either the medium or large fin arrangements. However, large unstable pitching-moment characteristics were evident at angles of attack above about $\pm 6^{\circ}$ for all configurations with the fins. All of the configurations had positive effective dihedral throughout the test Mach number range at positive angles of attack.

INTRODUCTION

A research program has been carried out at transonic and supersonic speeds at the Langley Research Center to develop fin configurations which would satisfy the stability requirements for the Dyna-Soar and Titan III launch-vehicle combination during a portion of the launch phase. The Titan III launch vehicle is composed of a modified Titan II which is referred to as the Titan III core and two coplanar solid-propellant strap-on bottles which are attached to the core. The launch vehicle with various sized fins in combination with the Dyna-Soar glider was tested in the Langley 8-foot transonic pressure tunnel at Mach numbers from 0.70 to 1.30 for angles of attack ranging from -11° to 9° and angles of sideslip ranging from -8° to 8° . Additional tests with glider elevon deflections of 0° and -4° were also made. A bulbous nose shape was also investigated

* Title, Unclassified.

~~CONFIDENTIAL~~

with the Titan III launch vehicle with small fins. The Reynolds number per foot ranged from approximately 3.50×10^6 to 4.22×10^6 during the tests.

SYMBOLS

The data presented herein are referred to the body axes system with the origin for the configuration located at model station 20.209. (See fig. 1.) The coefficients and symbols used herein are defined as follows:

C_A	axial-force coefficient, $\frac{\text{Axial force}}{qS}$
$C_{A,\alpha=0}$	axial-force coefficient at $\alpha = 0^\circ$
C_l	rolling-moment coefficient, $\frac{\text{Rolling moment}}{qSd}$
C_m	pitching-moment coefficient, $\frac{\text{Pitching moment}}{qSd}$
C_N	normal-force coefficient, $\frac{\text{Normal force}}{qS}$
C_n	yawing-moment coefficient, $\frac{\text{Yawing moment}}{qSd}$
C_Y	side-force coefficient, $\frac{\text{Side force}}{qS}$
$C_{l\beta}$	effective-dihedral parameter measured at $\beta = \pm 2^\circ$, $\frac{\partial C_l}{\partial \beta}$, per deg
$C_{m\alpha}$	slope of pitching-moment-coefficient curve measured at $\alpha = \pm 2^\circ$, $\frac{\partial C_m}{\partial \alpha}$, per deg
$C_{N\alpha}$	normal-force-curve slope measured at $\alpha = \pm 2^\circ$, $\frac{\partial C_N}{\partial \alpha}$, per deg
$C_{n\beta}$	directional-stability parameter measured at $\beta = \pm 2^\circ$, $\frac{\partial C_n}{\partial \beta}$, per deg
$C_{Y\beta}$	side-force parameter measured at $\beta = \pm 2^\circ$, $\frac{\partial C_Y}{\partial \beta}$, per deg
d	Titan core diameter, 2.403 in.

M free-stream Mach number
q free-stream dynamic pressure
R Reynolds number per foot
r radius, in.
S reference area, 0.0315 sq ft
x distance forward of base of model, in.
 α angle of attack, referred to reference line, deg
 β angle of sideslip, referred to plane of symmetry, deg
 δ_e elevon deflection, positive when trailing edge is down, deg

Subscripts:

cg center of gravity
cp center of pressure

MODEL DESCRIPTION

The models of the present investigation were 1/50-scale configurations of the Titan III launch vehicle in combination with a Dyna-Soar glider (basic configuration) and with a bulbous nose shape. The elevons on the glider could be deflected 0° and -4° . Details of the models are shown in figures 1 and 2; the physical characteristics of the basic configuration and fins are given in table I. The Titan III launch vehicle consists of a modified Titan II launch vehicle with two coplanar solid-propellant strap-on bottles. Small, medium, and large fins attached to the solid-propellant strap-on bottles were used to investigate the static longitudinal and lateral aerodynamic characteristics. Details of the various pitch fins and yaw fins are shown in figure 3. Another configuration, which extended the base of the Titan II core from model station 24.486 to model station 26.859 (fig. 1), was investigated. The core extension was attached to the support sting and, hence, provided no balance load input except to the extent of the interference effects on the basic data. Photographs of the models are shown as figures 4 and 5.

APPARATUS AND PROCEDURE

Tunnel

The investigation was made in the Langley 8-foot transonic pressure tunnel. This facility is rectangular in cross section with the upper and lower walls

slotted longitudinally to allow continuous operation through the transonic-speed range with negligible effects of choking and blockage. The main tunnel drive power is varied to provide a Mach number range to 1.20 and Mach numbers to 1.30 are obtained with additional power put into a slot plenum suction system. The stagnation temperature and dewpoint were maintained at values to preclude shock condensation effects. The tunnel was operated at a stagnation pressure of 1 atmosphere; therefore, the Reynolds numbers per foot shown in figure 6 varied from 3.50×10^6 to 4.22×10^6 .

Measurements

Six-component force and moment measurements were determined by means of an electrical strain-gage balance located inside the core of the Titan III vehicle. The tests were made at Mach numbers from 0.70 to 1.30 for an angle-of-attack range from -11° to 9° , an angle-of-sideslip range from -8° to 8° , and elevon deflections of 0° and -4° . The pressures in the balance chamber and at the bases of the two coplanar solid-propellant strap-on bottles and rocket nozzles were also measured.

All tests were conducted with fixed transition on the model according to the methods described in reference 1. The strips were approximately 0.10 inch wide and were formed by sprinkling No. 60 carborundum grains around the glider $7/8$ inch back from the nose, $1/4$ inch measured perpendicular from the leading edge of the glider wing and fins, $1/4$ inch measured perpendicular from the leading edge of the pitch and yaw fins, and $3/4$ inch back from the nose on the two coplanar solid-propellant strap-on bottles. A transition strip was also applied around the bulbous nose shape $5/8$ inch back from station -5.855.

Corrections and Accuracy

No corrections to the free-stream Mach number and dynamic pressure for the effects of model and wake blockage are necessary for tests in the slotted test section of the Langley 8-foot transonic pressure tunnel. (See ref. 2.) There is a range of Mach numbers above a Mach number of 1.00 where the data are affected by reflected compressions and expansions from the test-section walls. From considerations of the results of reference 3, it is believed that for Mach numbers up to approximately 1.03 the effects of these disturbances on the measurements made in the present investigation would be negligible. No test data, however, are presented in the range ($M > 1.03$ and $M < 1.15$) where the reflected wall disturbances impinged upon the models.

The axial-force coefficient C_A was corrected by adjusting the static pressures in the balance chamber and at the bases of the two coplanar solid-propellant strap-on bottles and rocket nozzles of the models to the free-stream value. The axial-force coefficient was also corrected for a buoyant force acting over the forward portion of the model for the tests made at a Mach number of 1.30.

No sting interference corrections have been made to the data except to the extent of the partial correction for sting interference inherent in the base-pressure correction.

The angles of attack and sideslip have been corrected for the deflection of the balance and sting under load. An additional correction for flow angularity has been applied to the angles of attack and sideslip. The angles of attack, sideslip, and control deflection are estimated to be accurate to within $\pm 0.1^\circ$.

The estimated accuracy of the data at a Mach number of 0.90 and a stagnation pressure of 1 atmosphere, based primarily on the static calibrations and the repeatability of the data, is as follows:

C_N	± 0.10
C_A	± 0.032
C_m	± 0.154
C_l	± 0.023
C_n	± 0.154
C_y	± 0.10

RESULTS AND DISCUSSION

Presentation of Results

The results of this investigation are presented in the following figures:

Figure

Aerodynamic characteristics in pitch for:

Titan III launch vehicle and Dyna-Soar glider with -	
Fins off	7
Small fins	8
Medium fins	9
Large fins	10
Titan III launch vehicle and bulbous nose shape with small fins	11

Summary of static longitudinal aerodynamic characteristics:

Effect of configuration	12
Effect of core extension	13
Bulbous nose shape	14

Aerodynamic characteristics in sideslip for:

Titan III launch vehicle and Dyna-Soar glider with -	
Fins off	15
Small fins	16
Medium fins	17
Large fins	18

Small pitch fins on, yaw fins off	19
Medium fins and core extension	20
Titan III booster and bulbous nose shape with small fins	21
Summary of static lateral aerodynamic characteristics:	
Effect of configuration	22
Effect of yaw fins	23
Variation of sideslip derivatives with angle of attack:	
Effect of configuration	24
Effect of yaw fins	25
Summary of static lateral aerodynamic characteristics for configura-	
tion with small fins and bulbous nose shape	26

Longitudinal Aerodynamic Characteristics

Normal-force characteristics.- The value of the normal-force-curve slope C_{N_α} for the launch vehicle and glider configuration was low and showed little variation with Mach number (fig. 22). Addition of the various fins to the basic configuration caused substantial increases of the order of about 2.5 to approximately 3.8 times the values of the normal-force-curve slope for the configuration without fins. As might be expected, there was no effect on the normal-force-curve-slope characteristics of the basic configuration with medium fins of the addition of the launch-vehicle core extension. (See fig. 13.) Replacing the Dyna-Soar glider with a bulbous nose shape in combination with the launch vehicle with small fins resulted in a small decrease in the normal-force-curve slope. (Compare fig. 14 with fig. 12.)

Axial-force characteristics.- A comparison of the axial-force coefficients measured at $\alpha = 0^\circ$ indicates that the addition of the various fins increased the drag of the basic configuration by approximately 20 to 40 percent over the test Mach number range (fig. 12). The increase in drag is higher than would be expected, based on the increase in skin-friction area due to the fins; thus some adverse interference effects are indicated to be present. There was no effect of the core extension on the axial-force characteristics of the basic combination with medium fins (fig. 13). The bulbous nose shape and launch vehicle with small fins had about the same axial-force characteristics at $M = 0.70$ as did the basic configuration; however, at $M = 1.20$ the drag of the bulbous nose shape configuration was 20 percent higher than the drag of the Dyna-Soar configuration. (Compare fig. 14 with fig. 12.)

Pitching-moment characteristics.- The slope of the pitching-moment-coefficient curve C_{m_α} and the longitudinal center-of-pressure location x_{cp}/d forward of the base of the various configurations with the Dyna-Soar glider are shown in figure 12. In addition, the approximate location of the center-of-gravity position x_{cg}/d as a function of Mach number for the basic configuration

~~CONFIDENTIAL~~

without fins is also shown for reference in figure 12. As is evident by the values of x_{cp}/d and x_{cg}/d , the basic configuration without fins is aerodynamically unstable throughout the Mach number range of the present tests. The addition of the small fins to the launch vehicle moved the center-of-pressure position rearward approximately 4.5 diameters, the medium fins moved the center-of-pressure position rearward approximately 5.0 diameters, and only a further small gain in the rearward center-of-pressure position was realized by the addition of the large fins. Although the center-of-gravity position of the model with the various fins is not known, it is possible that the configurations with the medium and large fins on the launch vehicle could be longitudinally stable. However, it should be pointed out that the longitudinal characteristics were summarized over an angle-of-attack range of only $\pm 2^\circ$ and, as is evident by the pitching-moment characteristics for these configurations (figs. 9(c) and 10(c)), large unstable breaks in the pitching-moment coefficients occur at angles of attack greater than about $\pm 6^\circ$. Although unstable breaks in the pitching-moment coefficients also occur for the basic configuration with the small fins, the resulting change in the longitudinal center-of-pressure location associated with the unstable breaks is not as large as the changes for the configurations with the medium and large fins. Nevertheless, it can be expected that large stability problems will be experienced which will require a careful programming of the thrust vector control or other form of control if the local angles of attack exceed about $\pm 4^\circ$ because of wind shears or elastic deformation of the glider-launch-vehicle combination during the launch phase.

The longitudinal center-of-pressure location of the launch vehicle with small fins and the bulbous nose shape was about the same as that for the basic configuration with the medium and large fins. (Compare figs. 14 and 12.) However, the large unstable pitching-moment characteristics at angles of attack above -6° are still evident (fig. 11(c)).

Lateral Aerodynamic Characteristics

Directional stability characteristics.— The directional-stability derivative $C_{n\beta}$ and the directional center-of-pressure location x_{cp}/d forward of the base for the basic configuration with various fins are shown in figure 22 for $\alpha = 0^\circ$. The approximate location of the center-of-gravity position x_{cg}/d for the basic configuration without fins is also shown for reference in figure 22. The configuration without the fins, of course, was aerodynamically unstable throughout the test Mach number range, the directional center-of-pressure location being about 4.5 to 3.5 diameters ahead of the approximate center-of-gravity position. The various yaw fins caused the directional center-of-pressure position to move rearward about 4.0 to 6.0 diameters. Although a knowledge of the center-of-gravity location for the basic launch configuration with the various fins is not known, it is believed that the configurations with the medium and large fins could be directionally stable. For the configuration with the small yaw fins removed but with the small pitch fins on, the directional center-of-pressure location for Mach numbers up to 0.95 was approximately 0.75 to 1.0 diameter farther forward than that for the configuration with all fins removed. (Compare figs. 22 and 23.) In general, the directional stability for the various

~~CONFIDENTIAL~~

configurations was greater at $\alpha = 0^\circ$ with the exception of more stable values of $C_{n\beta}$ noted at $M = 1.20$ and angles of attack greater than 4° . (See figs. 24 and 25.)

The directional stability characteristics for the launch vehicle with small fins and bulbous nose shape were about the same as those noted for the launch vehicle with small fins and the Dyna-Soar glider. (Compare figs. 26 and 22.) Although the directional center-of-pressure location for the combination with the bulbous nose shape varied between 3.2 to 4.0 diameters forward of the base of the launch vehicle through the Mach number range of the present investigation, it is possible that this configuration could be aerodynamically stable.

The side-force derivative $C_{Y\beta}$ for the various configurations was only slightly affected by changes in Mach number (figs. 22, 23, and 26) or by changes in angle of attack (figs. 24 and 25). It will be noted that the various fins provided substantial incremental increases in $C_{Y\beta}$ throughout the test Mach number range (fig. 22).

Effective dihedral. - At 0° angle of attack, all of the configurations indicated either zero or negative effective dihedral ($+C_{l\beta}$) throughout the test Mach number range (figs. 22, 23, and 26). However, with an increase in angle of attack, the configurations had positive effective dihedral ($-C_{l\beta}$). (See figs. 24 and 25.)

SUMMARY OF RESULTS

The results of a wind-tunnel investigation at transonic speeds to determine the static longitudinal and lateral aerodynamic characteristics of the Dyna-Soar glider and Titan III launch vehicle with several fin configurations are summarized as follows:

1. The only configurations that may have satisfactory longitudinal and directional stability characteristics were those that had either the medium or large fins on the launch vehicle. With regard to the longitudinal stability characteristics, however, large unstable pitching-moment characteristics were evident at angles of attack above about $\pm 6^\circ$ for the configurations with fins on.
2. All of the configurations indicated positive effective dihedral throughout the test Mach number range at positive angles of attack.

Langley Research Center,
National Aeronautics and Space Administration,
Langley Station, Hampton, Va., February 4, 1963.

~~CONFIDENTIAL~~

REFERENCES

1. Braslow, Albert L., and Knox, Eugene C.: Simplified Method for Determination of Critical Height of Distributed Roughness Particles for Boundary-Layer Transition at Mach Numbers From 0 to 5. NACA TN 4363, 1958.
2. Wright, Ray H., and Ward, Vernon G.: NACA Transonic Wind-Tunnel Test Sections. NACA Rep. 1231, 1955. (Supersedes NACA RM L8J06.)
3. Wright, Ray H., Ritchie, Virgil S., and Pearson, Albin O.: Characteristics of the Langley 8-Foot Transonic Tunnel With Slotted Test Section. NACA Rep. 1389, 1958. (Supersedes NACA RM L51H10 by Wright and Ritchie and RM L51K14 by Ritchie and Pearson.)

~~CONFIDENTIAL~~

TABLE I.- PHYSICAL CHARACTERISTICS OF MODEL

Glider body (without transition section):	
Length along glider center line, in.	6.803
Width, in.	1.26
Incidence, deg	1.0
Glider wing:	
Aspect ratio	1.258
Overall span, in.	5.00
Leading-edge sweepback, deg	72.80
Trailing-edge sweepback, deg	10.43
Total lifting area, sq ft	0.138
Glider vertical fins:	
Aspect ratio	1.123
Span, in.	1.416
Area per fin, sq ft	0.0124
Leading-edge sweepback, deg	55.0
Transition section:	
Length, in.	1.952
Maximum diameter, in.	2.403
Planform half-angle at booster intersection, deg	28.0
Planform half-angle at glider intersection, deg	6.0
Top profile angle at booster intersection, deg	9.1
Bottom profile angle at booster intersection, deg	20.7
Launch-vehicle body core:	
Length (not including transfer section), in.	20.784
Length of transfer section, in.	3.055
Overall length (including transfer section), in.	23.839
Maximum diameter, in.	2.403
Solid-propellant strap-on bottles:	
Overall length, in.	19.655
Length of nose section, in.	2.785
Radius of rounded nose, in.	0.480
Maximum diameter, in.	2.420
Launch-vehicle fins:	
Aspect ratio	3.00
Taper ratio	0.50
Thickness ratio of midchord, percent	6.0
Leading-edge sweepback angle, deg	12.5
Area per fin (pitch), sq ft:	
Small	0.080
Medium	0.140
Large	0.170
Area per fin (yaw), sq ft:	
Small	0.0128
Medium	0.0225
Large	0.0273

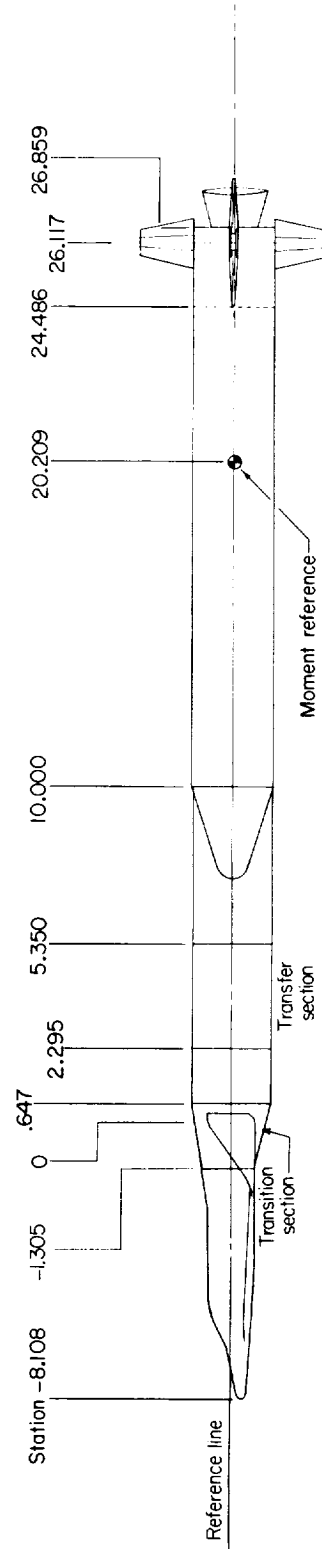
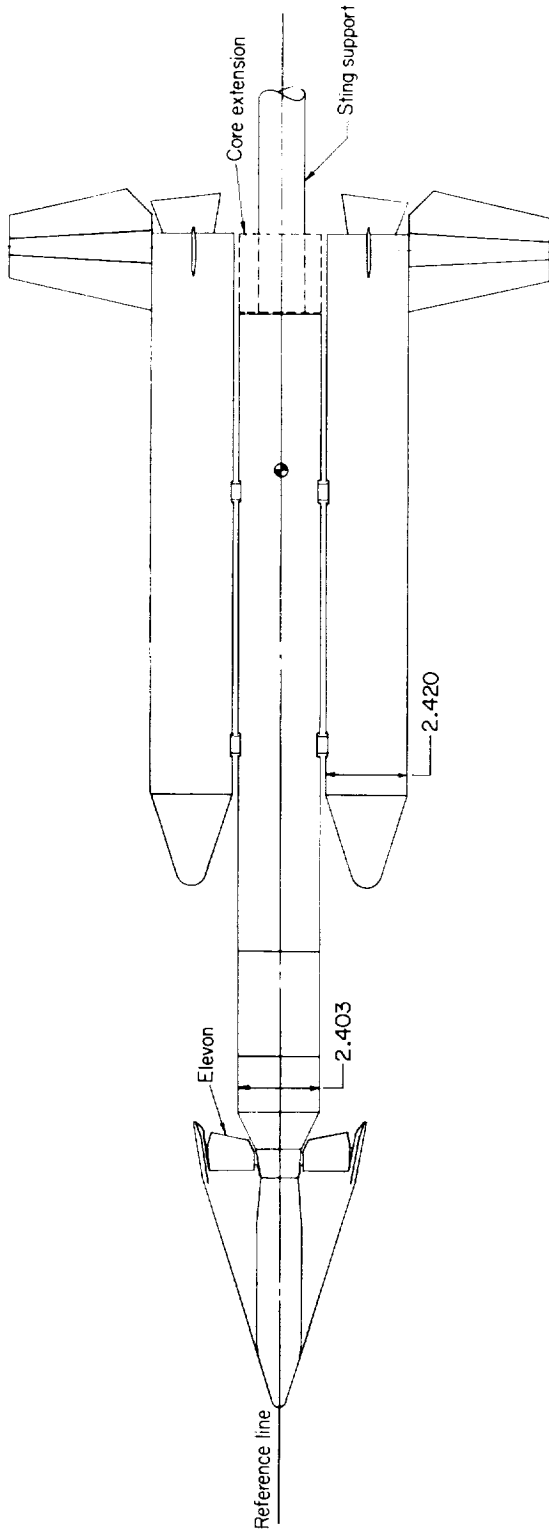


Figure 1.- Detailed drawing of Titan III launch vehicle with fin arrangement and with Dyna-Soar glider. All dimensions are in inches.

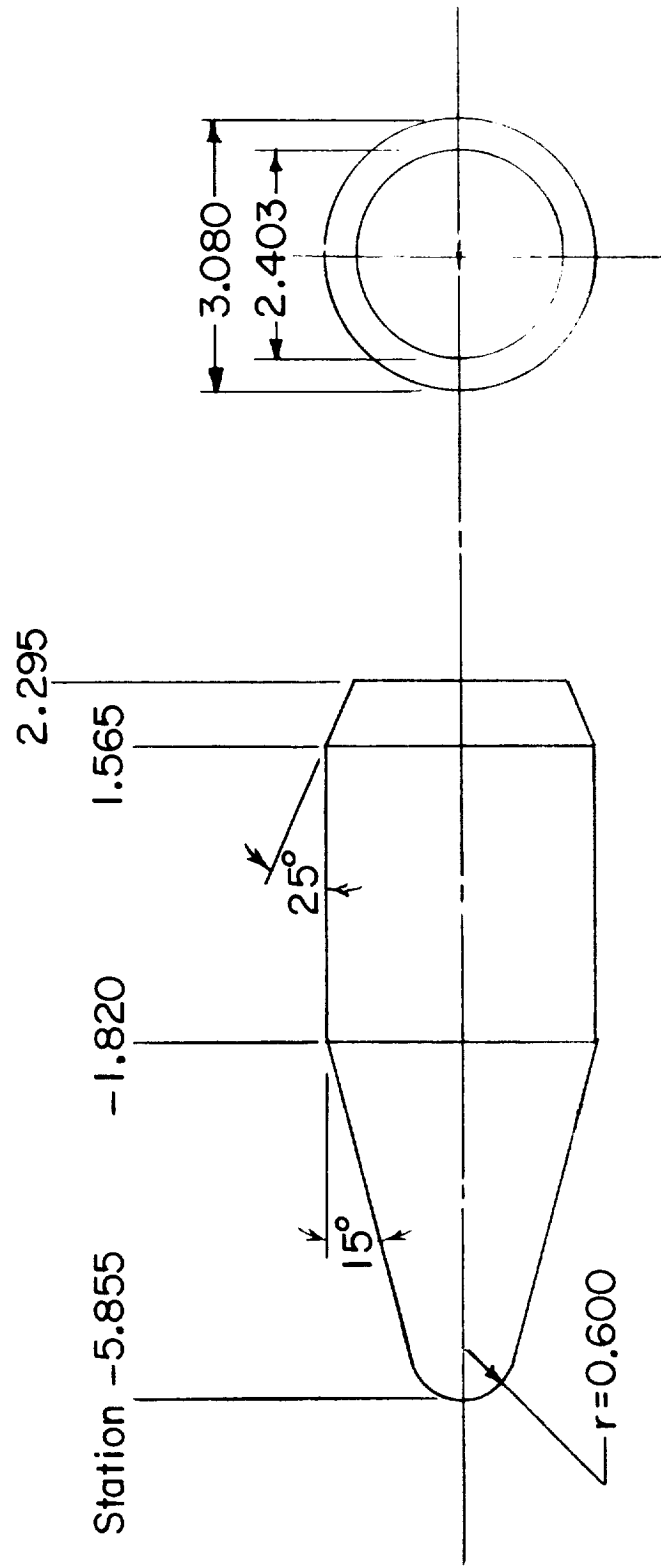
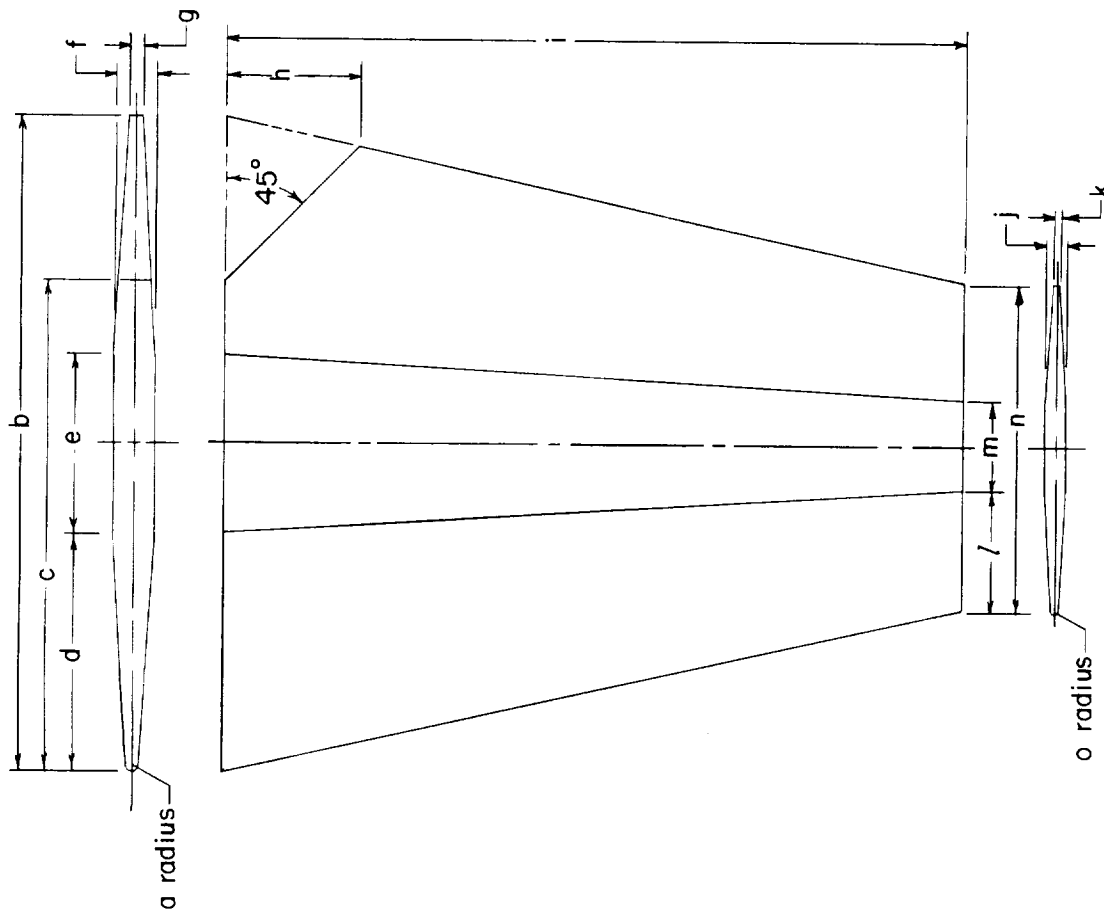


Figure 2.- Details of bulbous nose shape. All dimensions are in inches unless otherwise specified.

CONFIDENTIAL

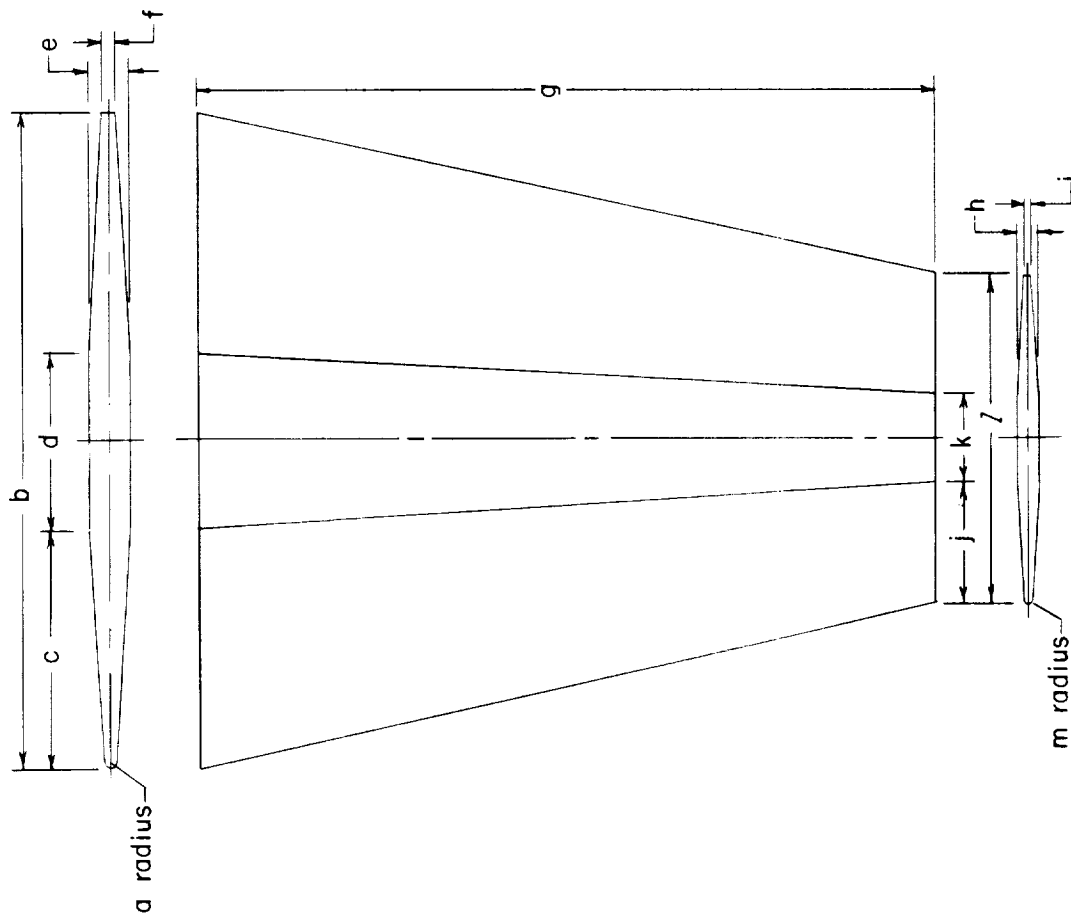


Pitch fins

a	Small	Medium	Large
	Radius equals $\frac{1}{2} g$		
b	3.748	4.960	5.464
c	2.820	3.730	4.111
d	1.374	1.818	2.004
e	1.000	1.324	1.456
f	.225	.298	.328
g	.075	.099	.109
h	.760	1.006	1.108
i	4.220	5.580	6.152
j	.112	.149	.164
k	.037	.050	.055
l	.687	.909	1.002
m	.500	.662	.728
n	1.874	2.480	2.732
o	Radius equals $\frac{1}{2} k$		

(a) Pitch fins.

Figure 3.- Details of fins. All dimensions are in inches unless otherwise specified.



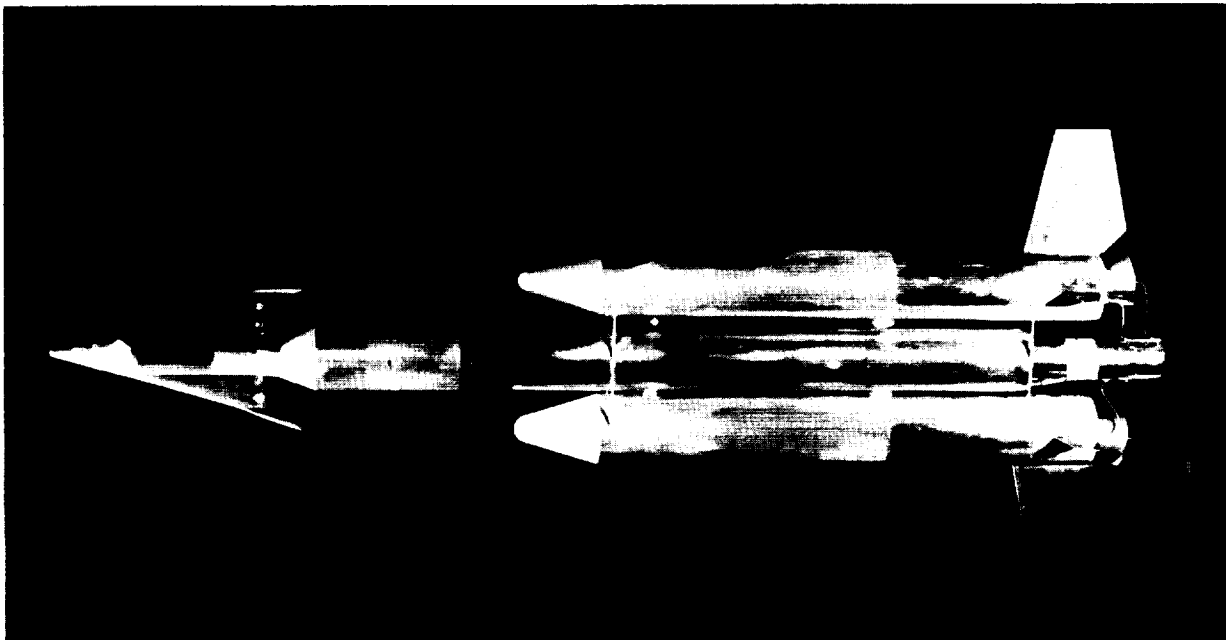
Yaw fins

	Small	Medium	Large
a	Radius equals $\frac{1}{2} f$		
b	1.482	1.960	2.160
c	.543	.719	.792
d	.396	.522	.576
e	.089	.118	.130
f	.030	.039	.043
g	1.666	2.204	2.430
h	.044	.059	.065
i	.015	.020	.022
j	.272	.359	.396
k	.197	.272	.288
l	.741	.980	1.080
m	Radius equals $\frac{1}{2} i$		

(b) Yaw fins.

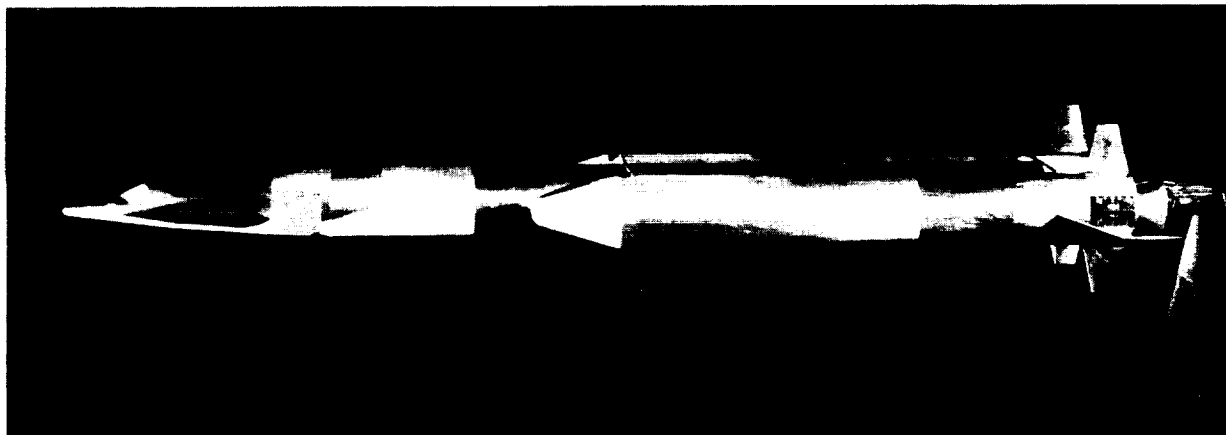
Figure 3.- Concluded.

~~CONFIDENTIAL~~



Plan view

L-62-5201



Side view

L-62-5203

Figure 4.- Titan III launch vehicle with small fins and with Dyna-Soar glider.

~~CONFIDENTIAL~~

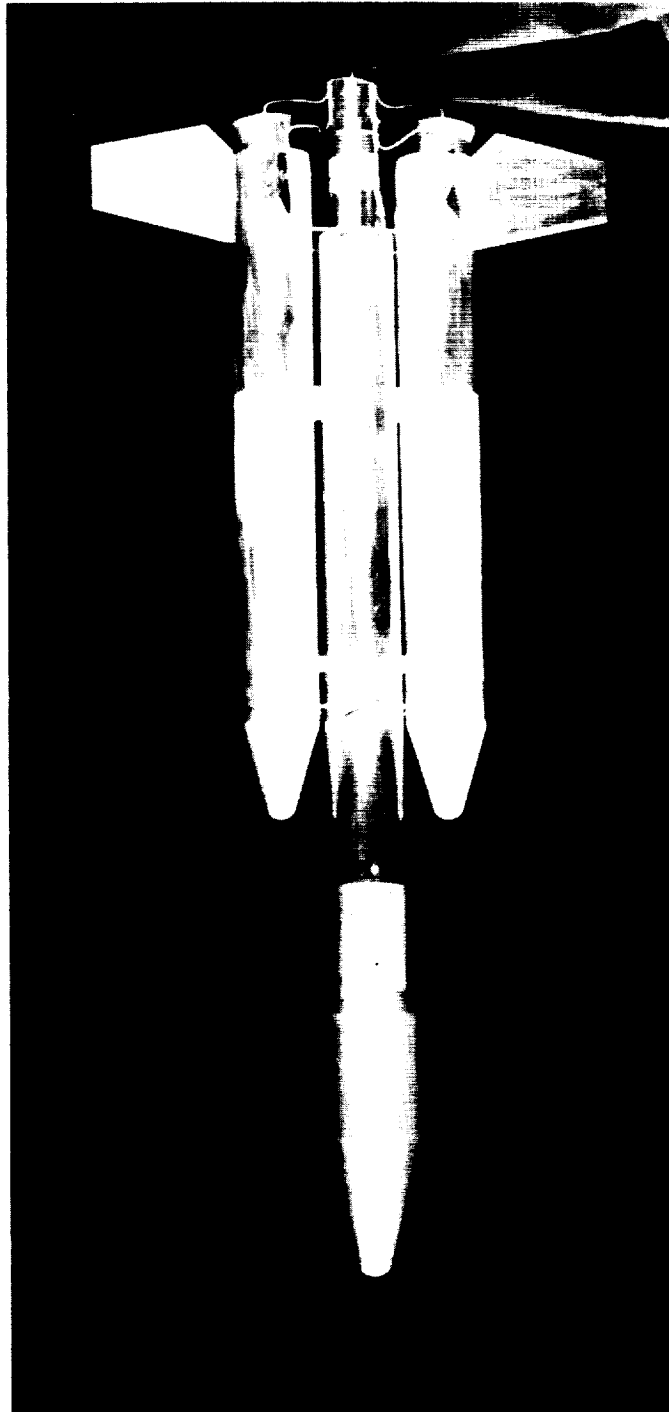


Figure 5.- Titan III launch vehicle with small fins and with bulbous nose shape.

L-62-5202

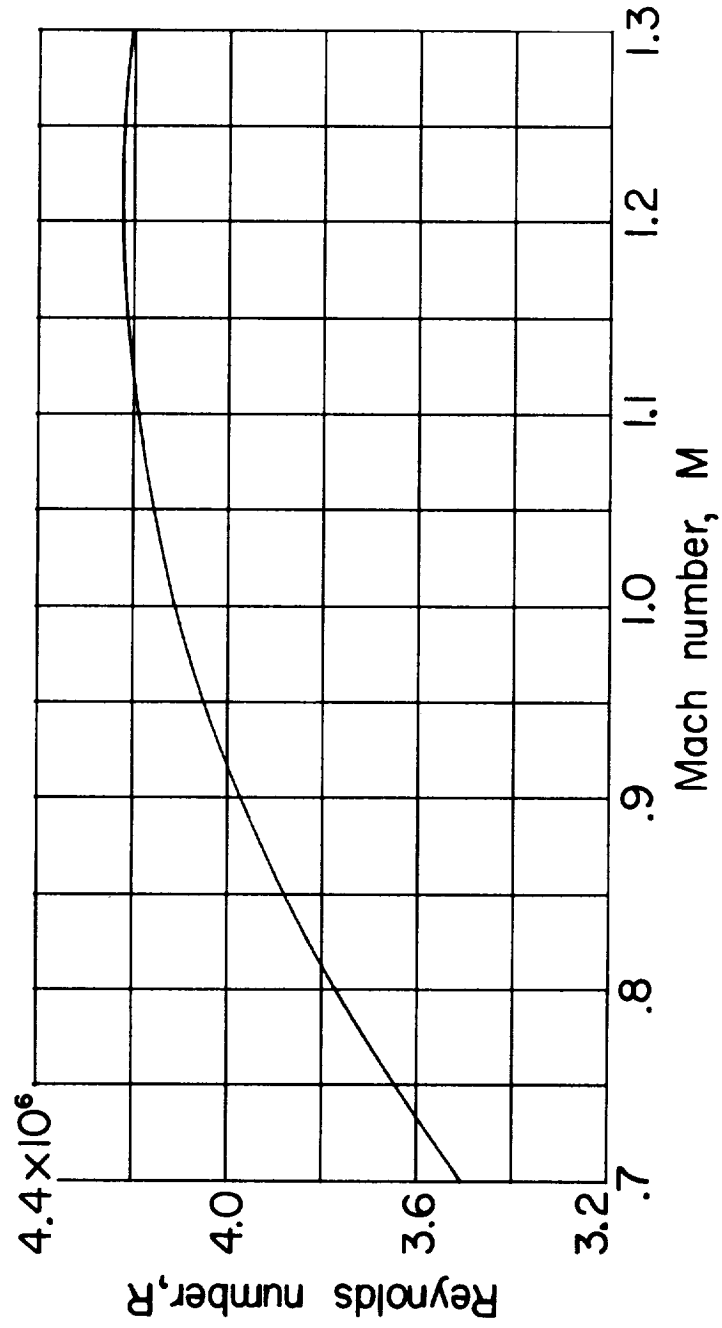


Figure 6.- Variation of test Reynolds number (per unit length) with Mach number.

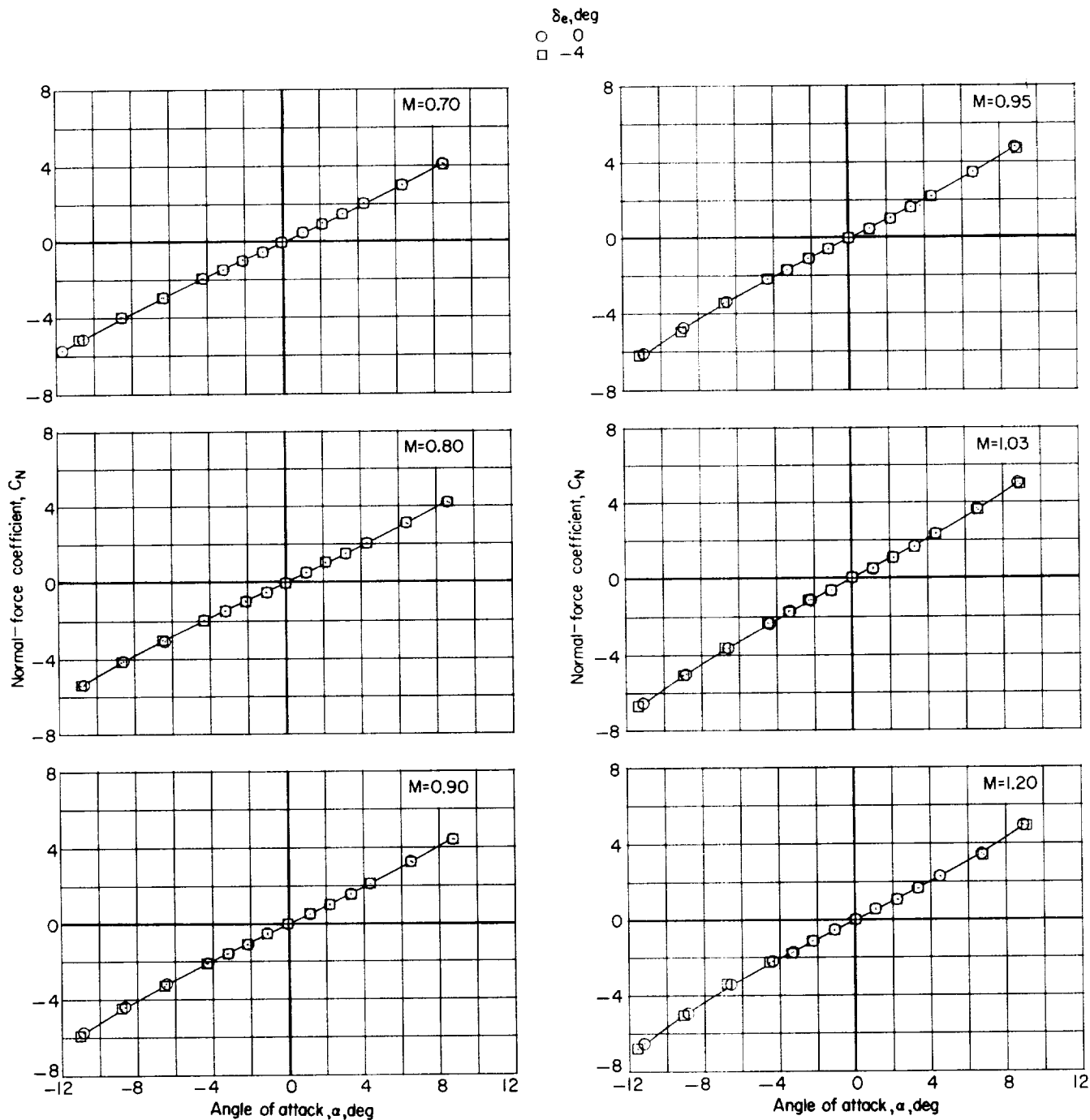


Figure 7.- Effect of elevon deflection on aerodynamic characteristics in pitch for the Titan III launch vehicle and Dyna-Soar glider (basic) configuration without fins.

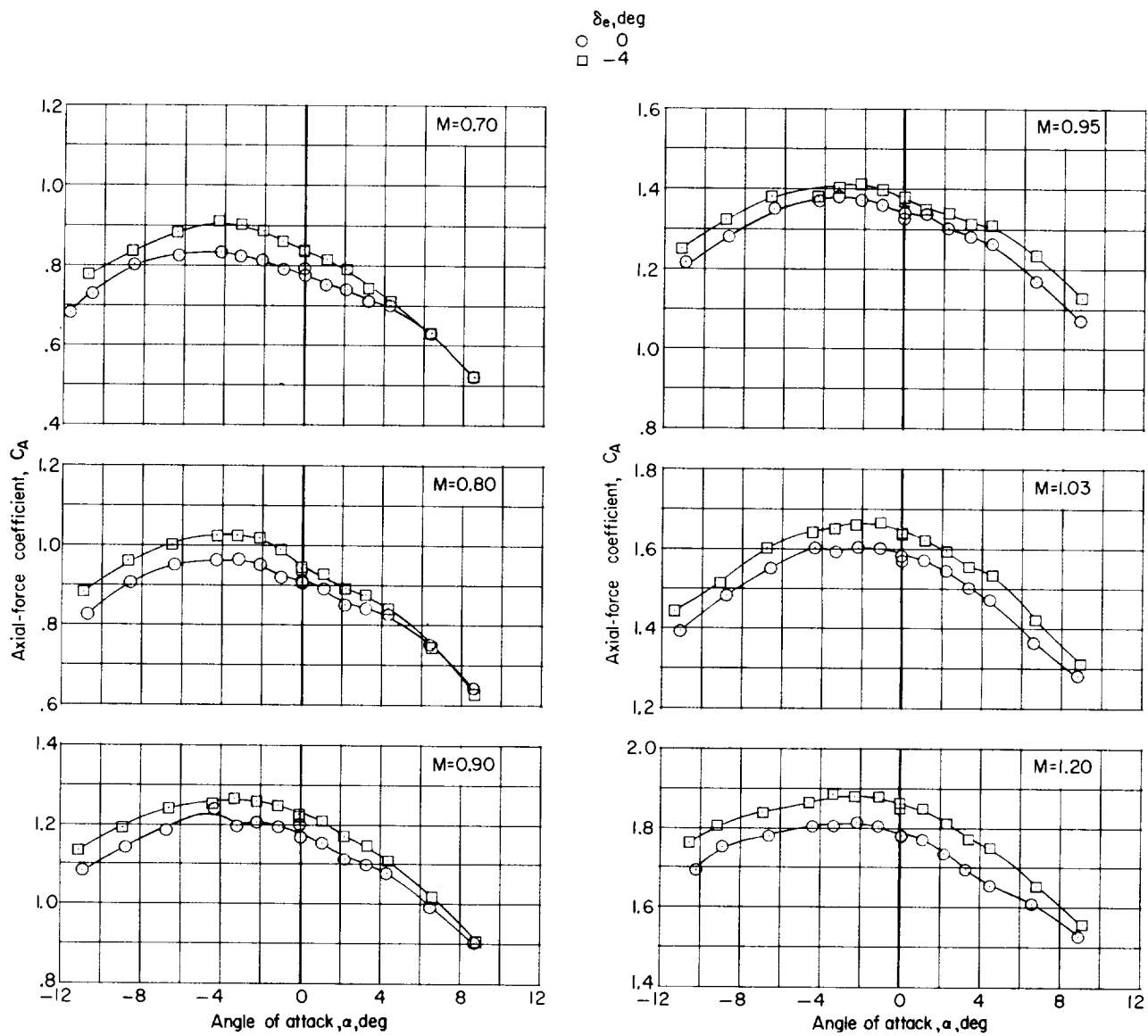
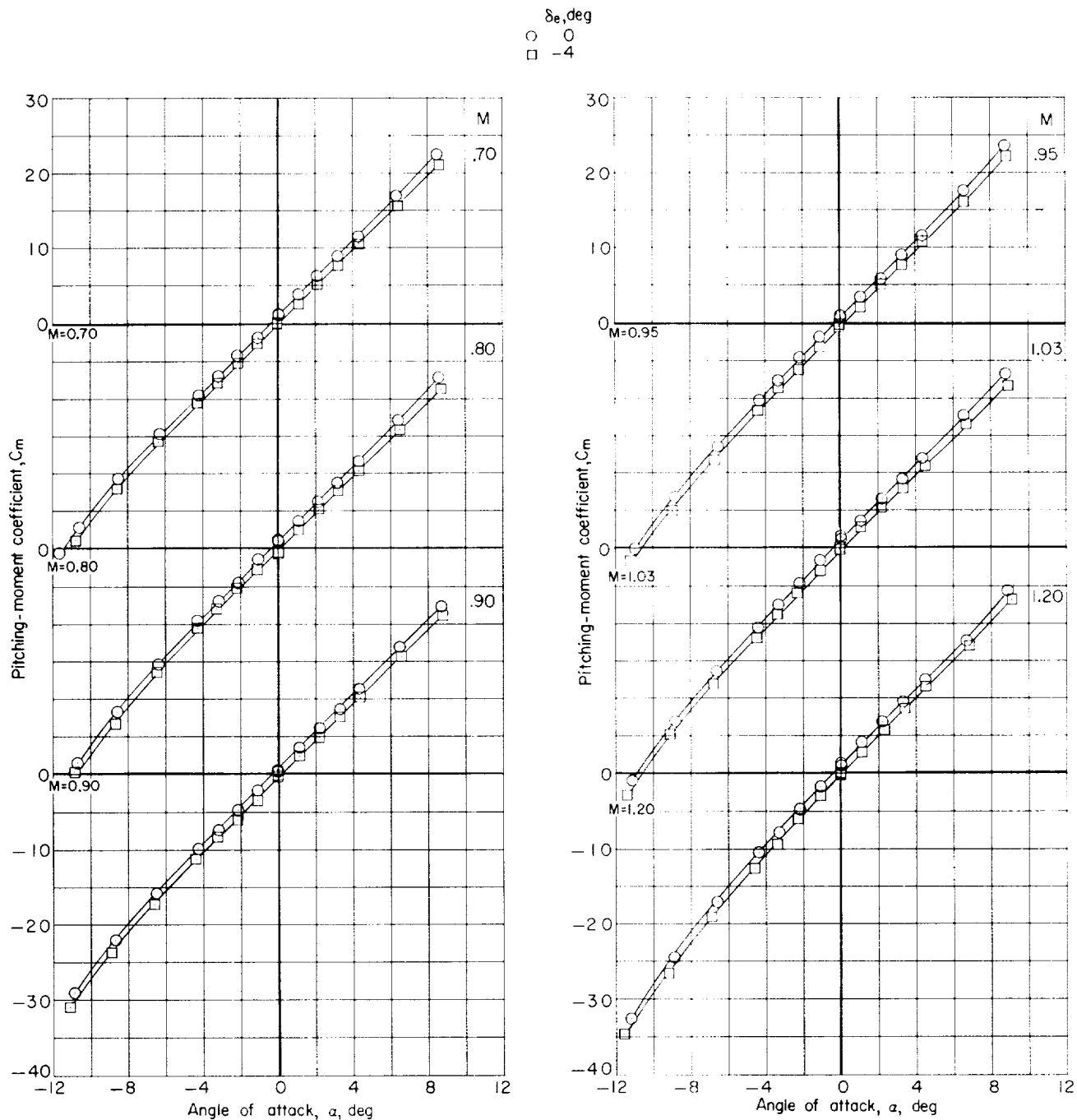
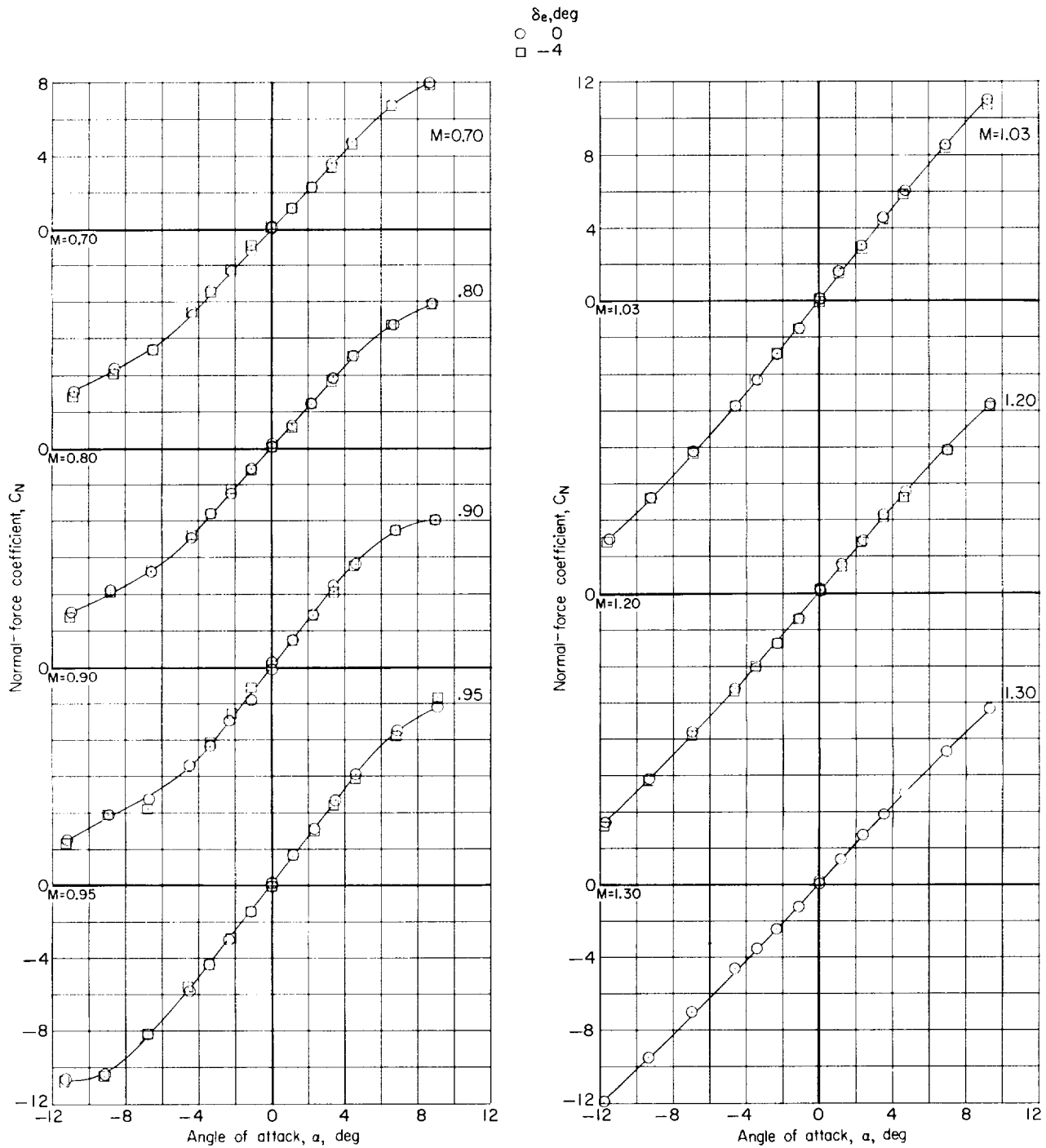


Figure 7.- Continued.



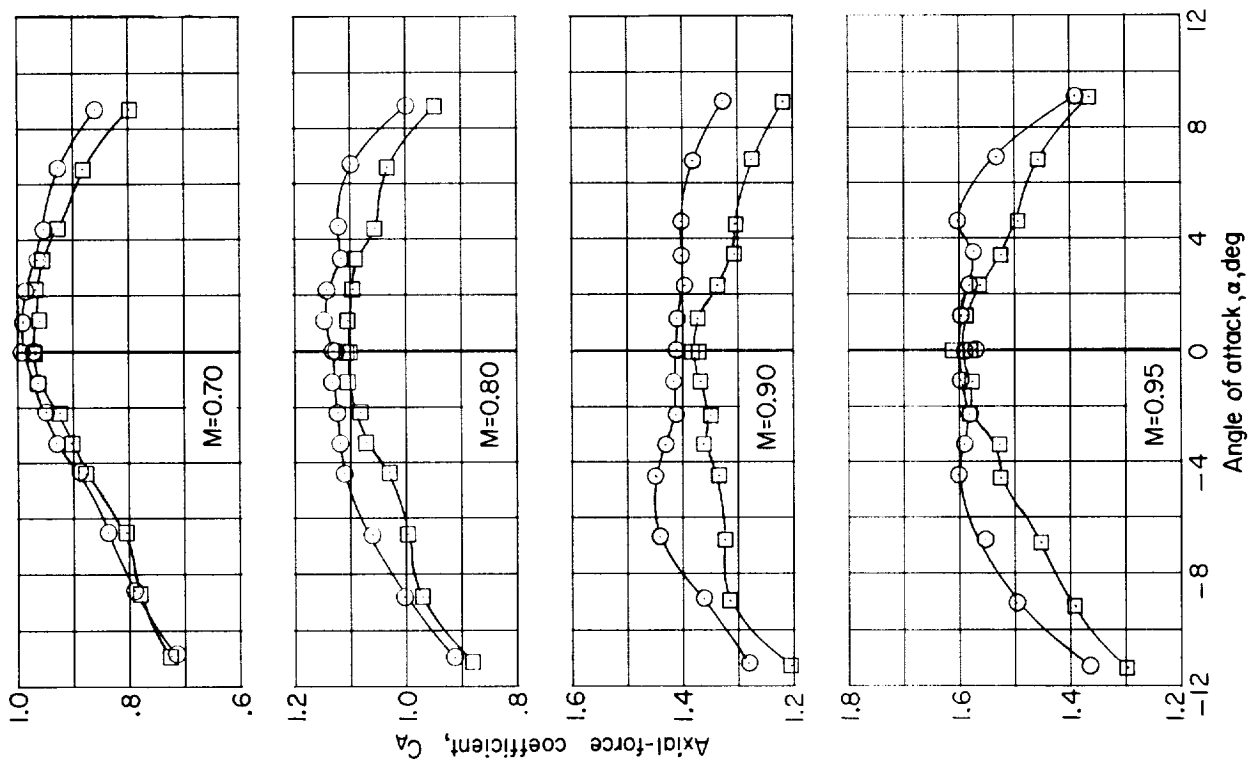
(c) Pitching-moment coefficient.

Figure 7.- Concluded.

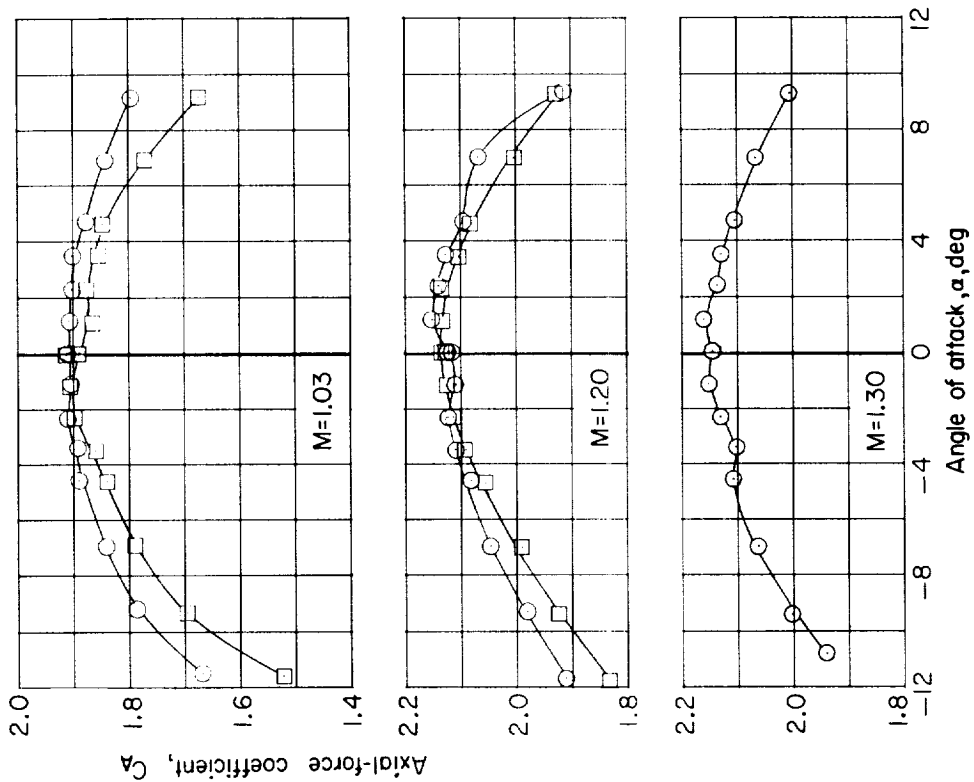


(a) Normal-force coefficient.

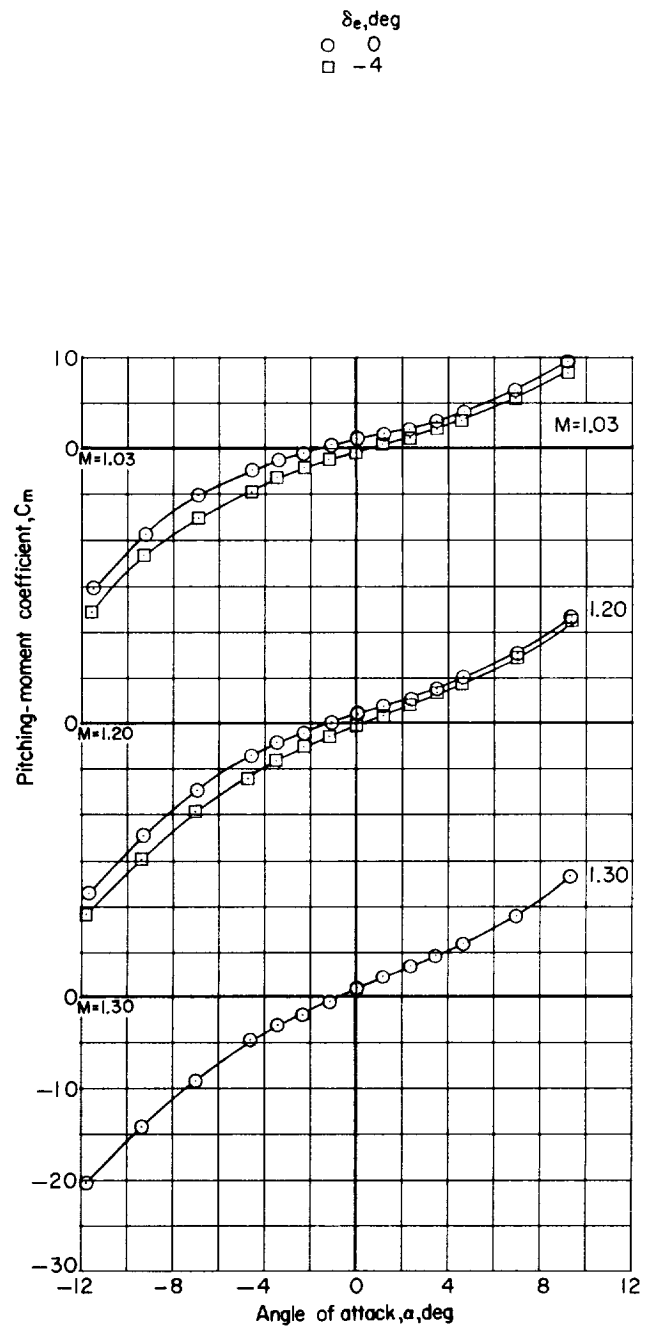
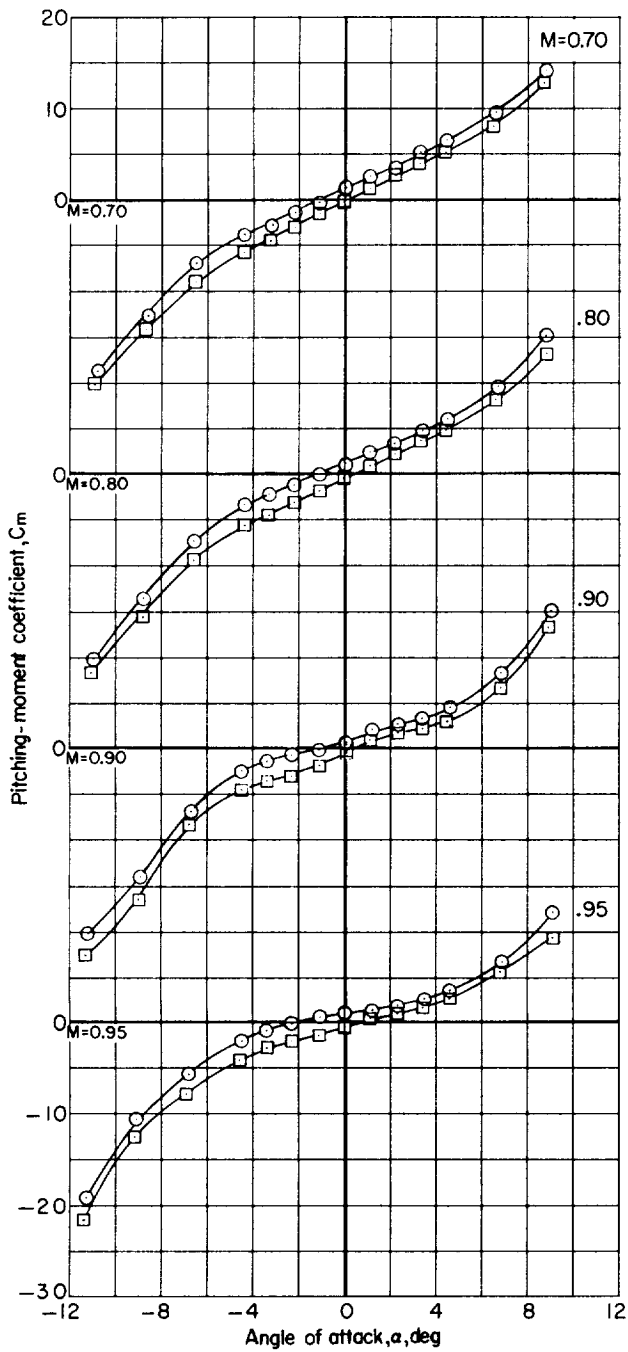
Figure 8.- Effect of elevon deflection on aerodynamic characteristics in pitch for the basic configuration with small fins.



(b) Axial-force coefficient.
Figure 8.- Continued.



δ_e, deg
○ 0
□ -4



(c) Pitching-moment coefficient.

Figure 8.- Concluded.

~~CONFIDENTIAL~~

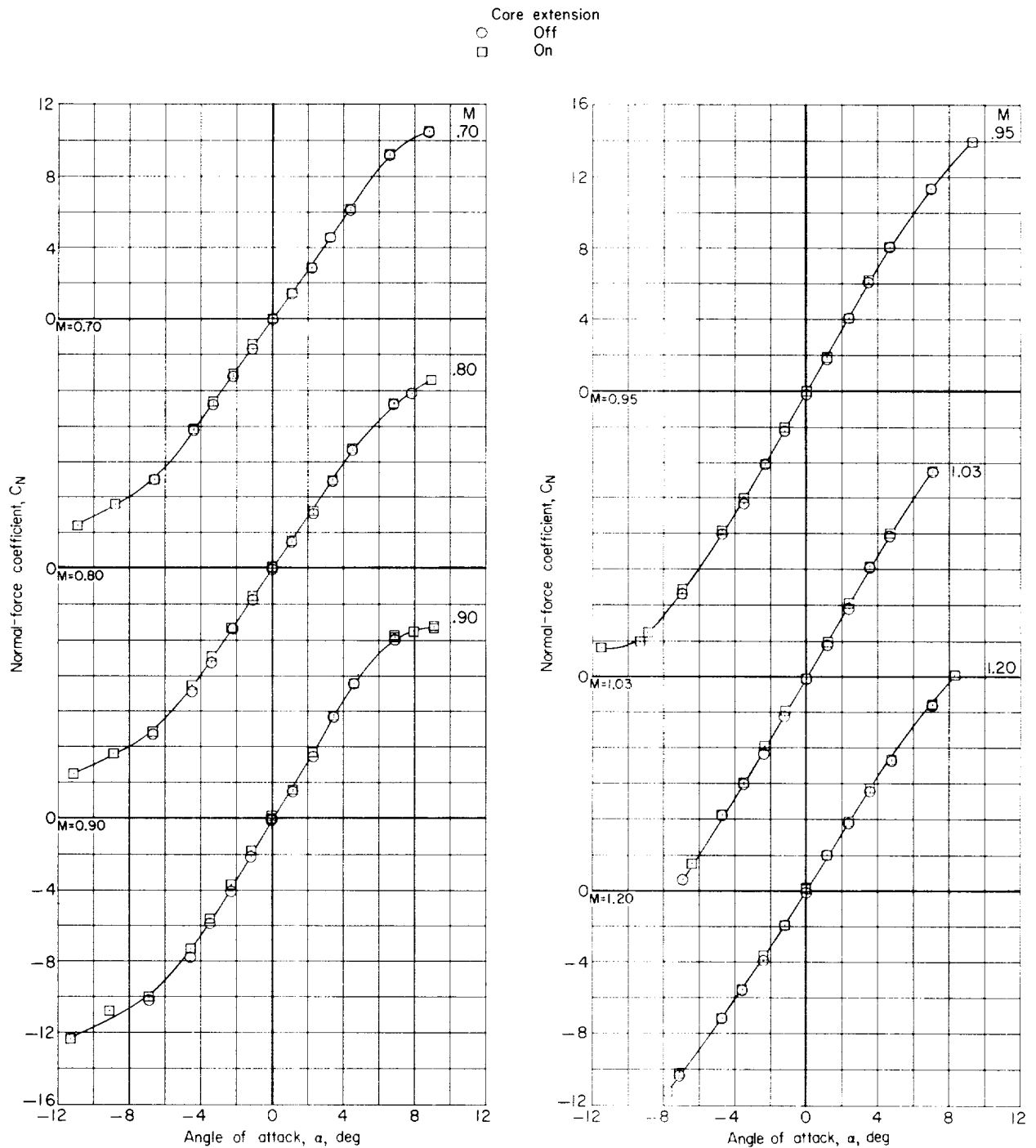
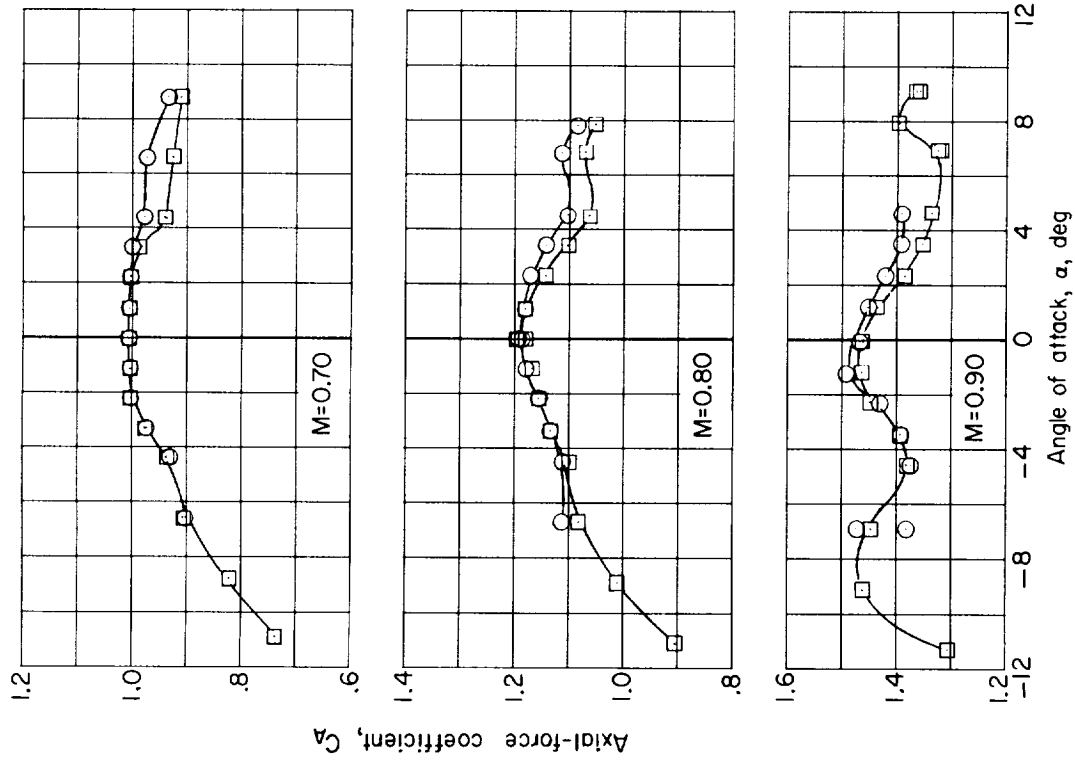
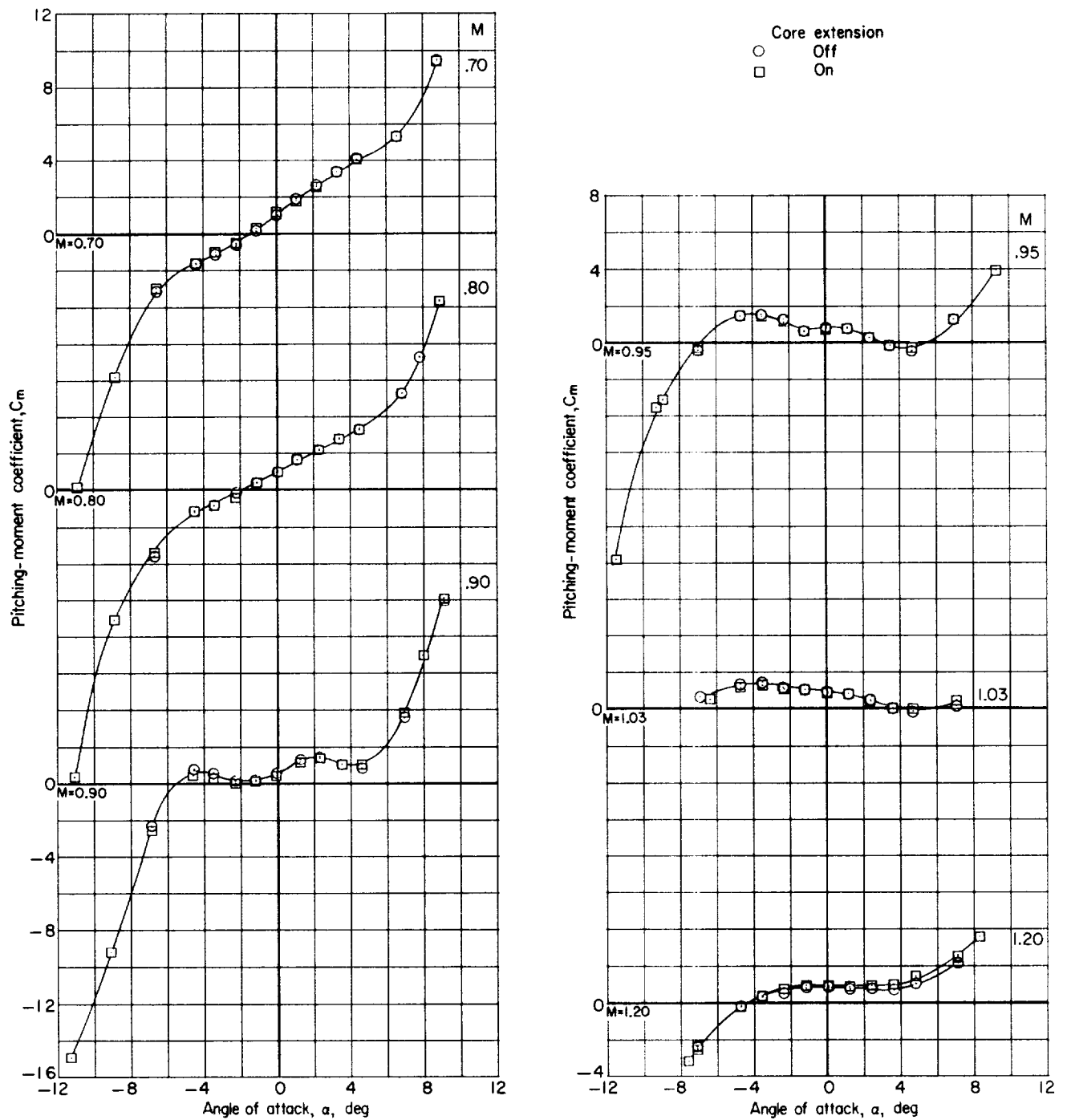


Figure 9.- A comparison of the aerodynamic characteristics in pitch of the basic configuration with medium fins with and without core extension. $\delta_e = 0^\circ$.

~~CONFIDENTIAL~~

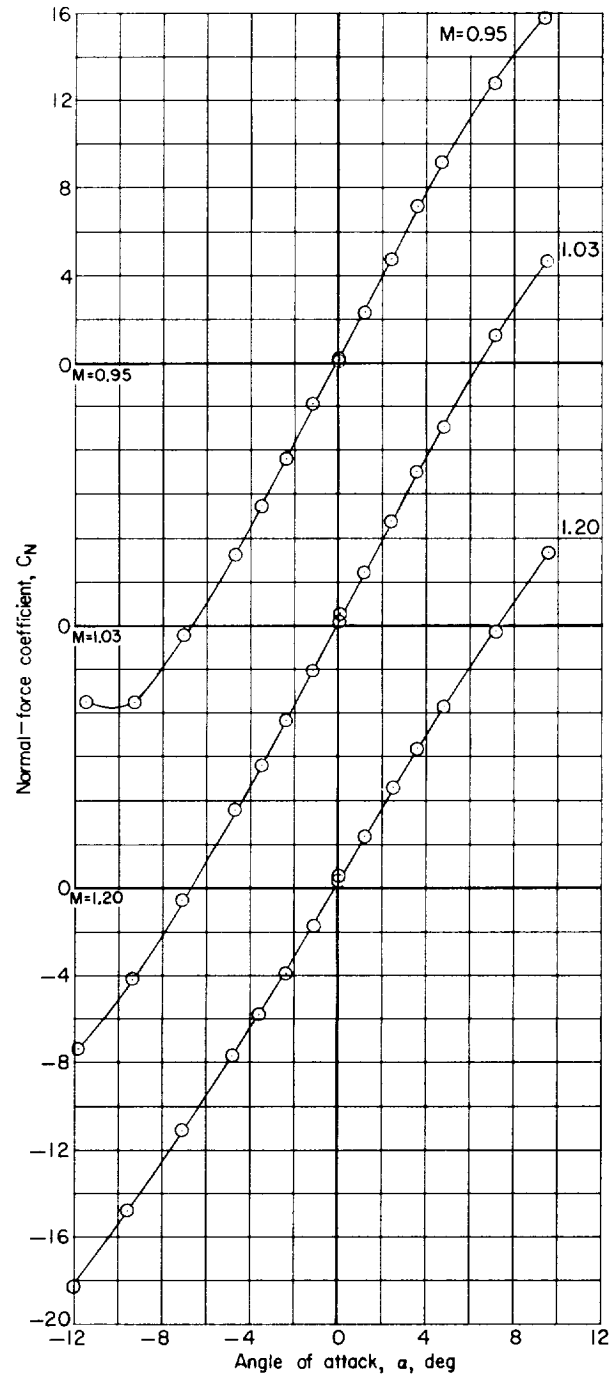
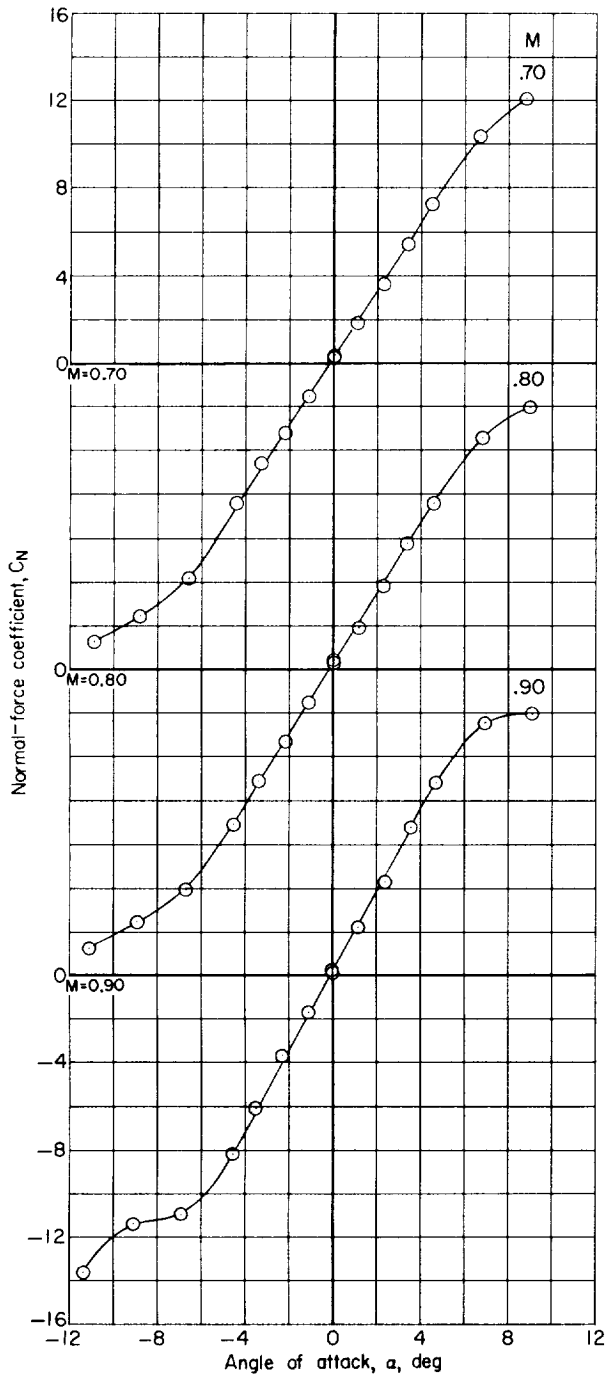


(b) Axial-force coefficient.
Figure 9.- Continued.



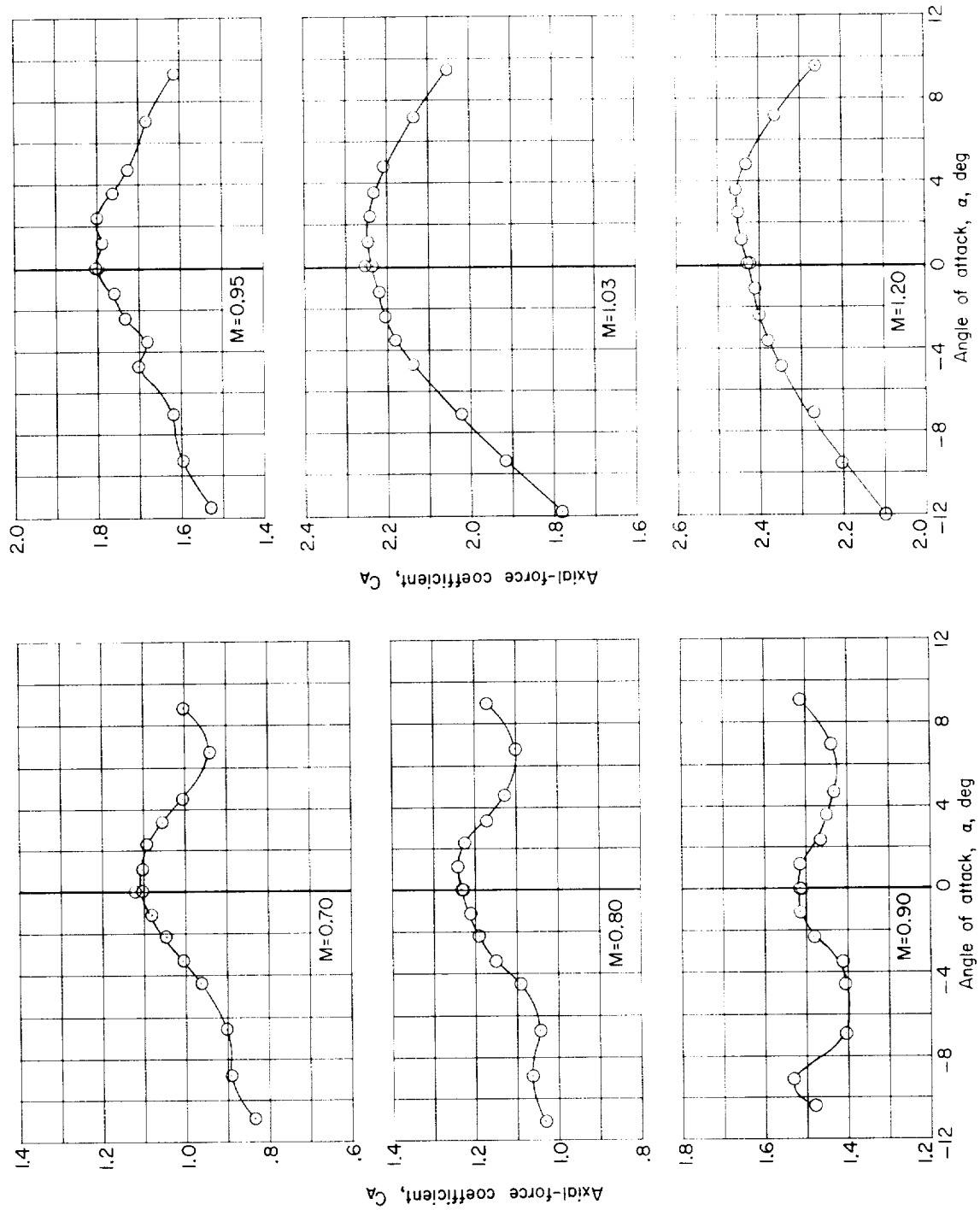
(c) Pitching-moment coefficient.

Figure 9.- Concluded.



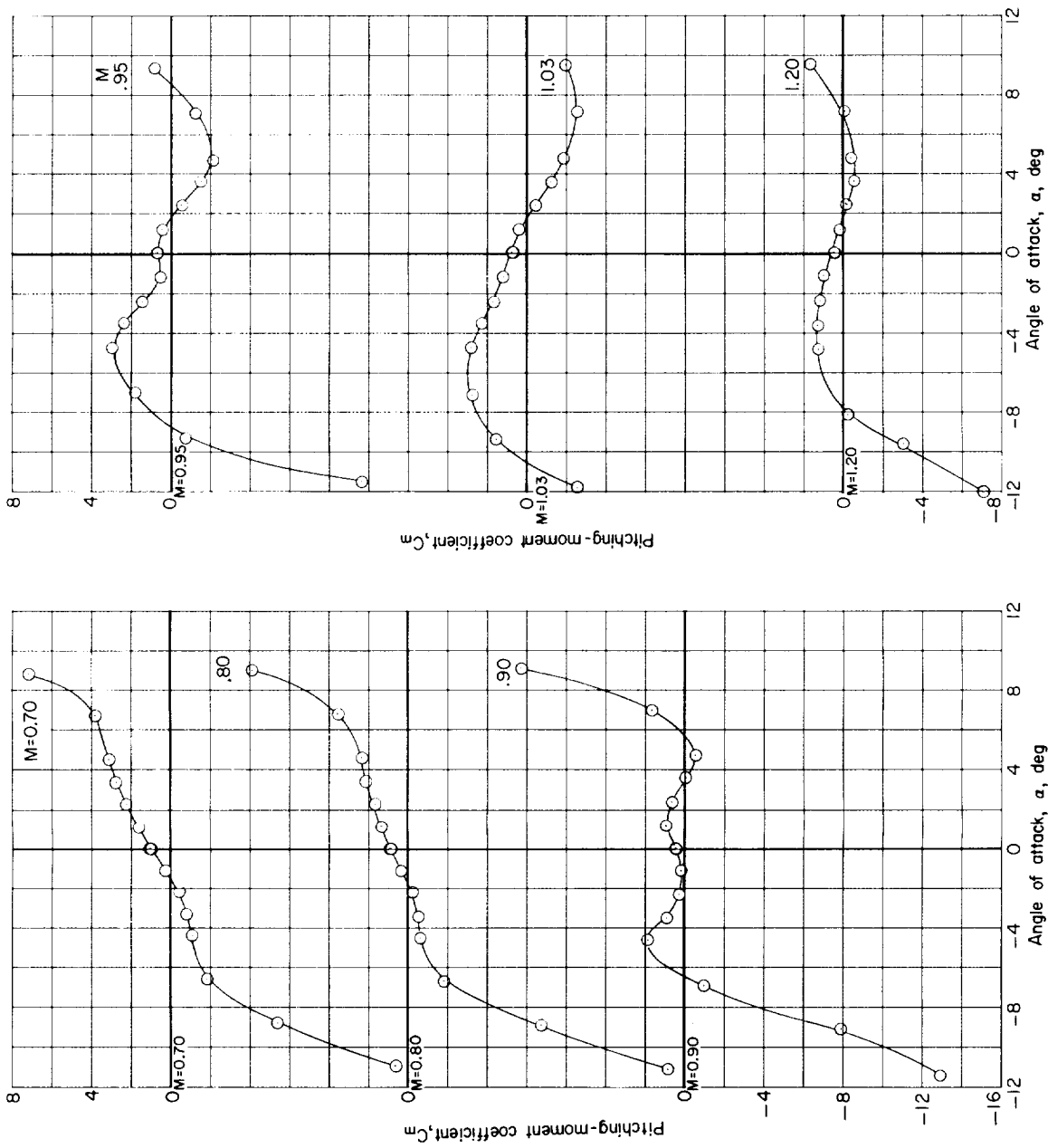
(a) Normal-force coefficient.

Figure 10.- Aerodynamic characteristics in pitch for the basic configuration with large fins.
 $\delta_e = 0^\circ$.



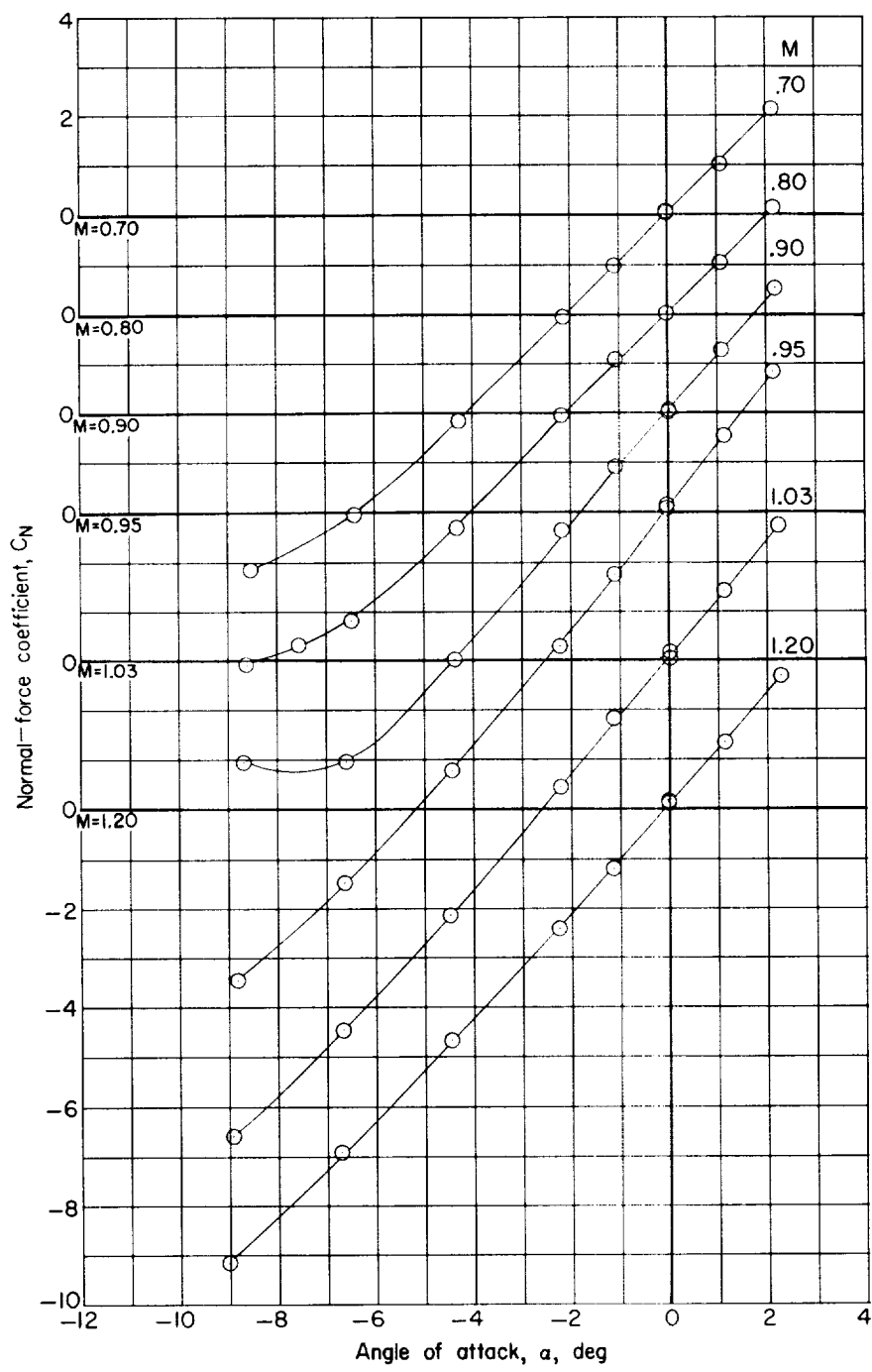
(b) Axial-force coefficient.

Figure 10.- Continued.



(c) Pitching-moment coefficient.

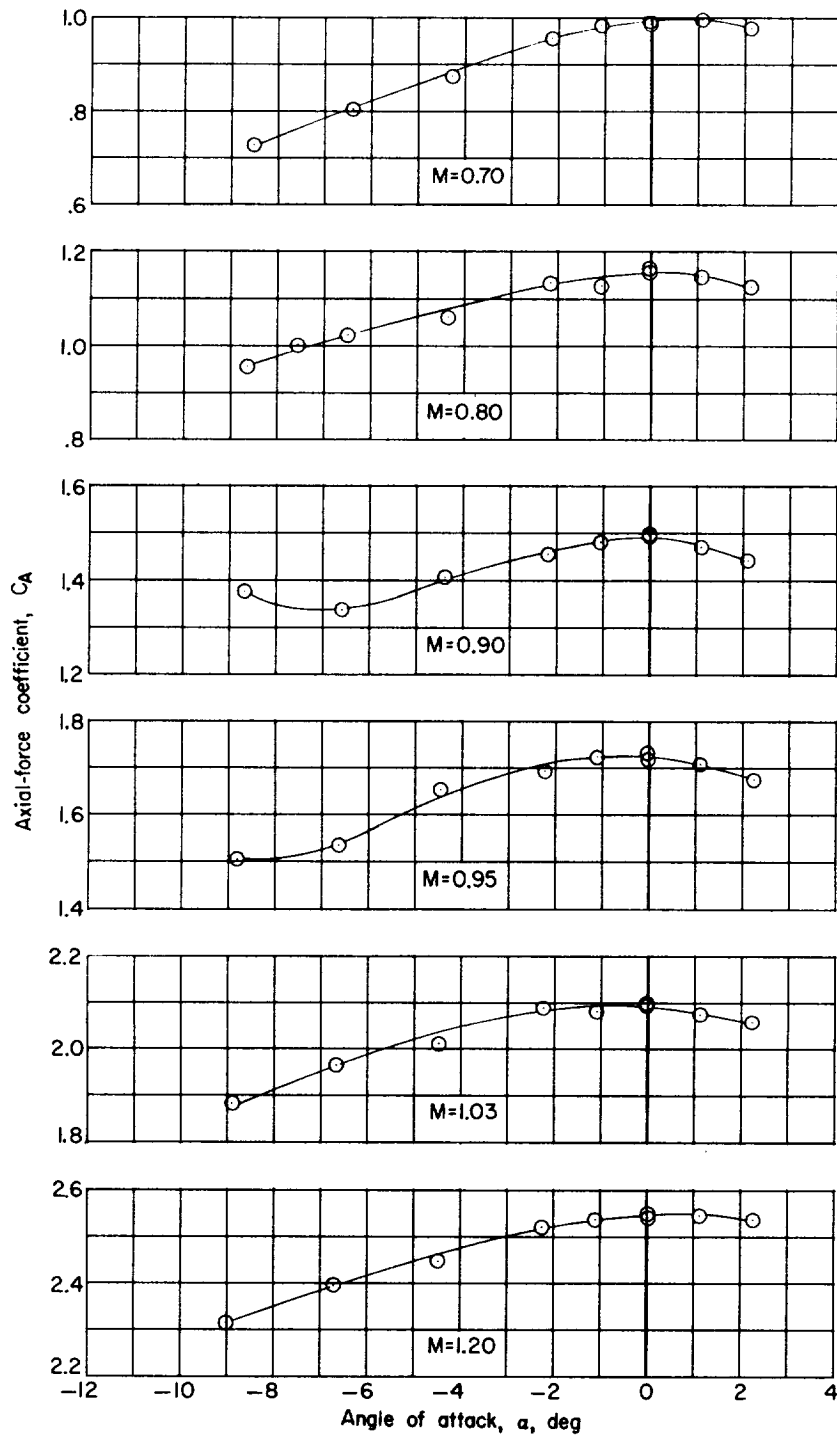
Figure 10.- Concluded.



(a) Normal-force coefficient.

Figure 11.- Aerodynamic characteristics in pitch of the Titan III launch-vehicle configuration with small fins and with bulbous nose shape.

~~CONFIDENTIAL~~

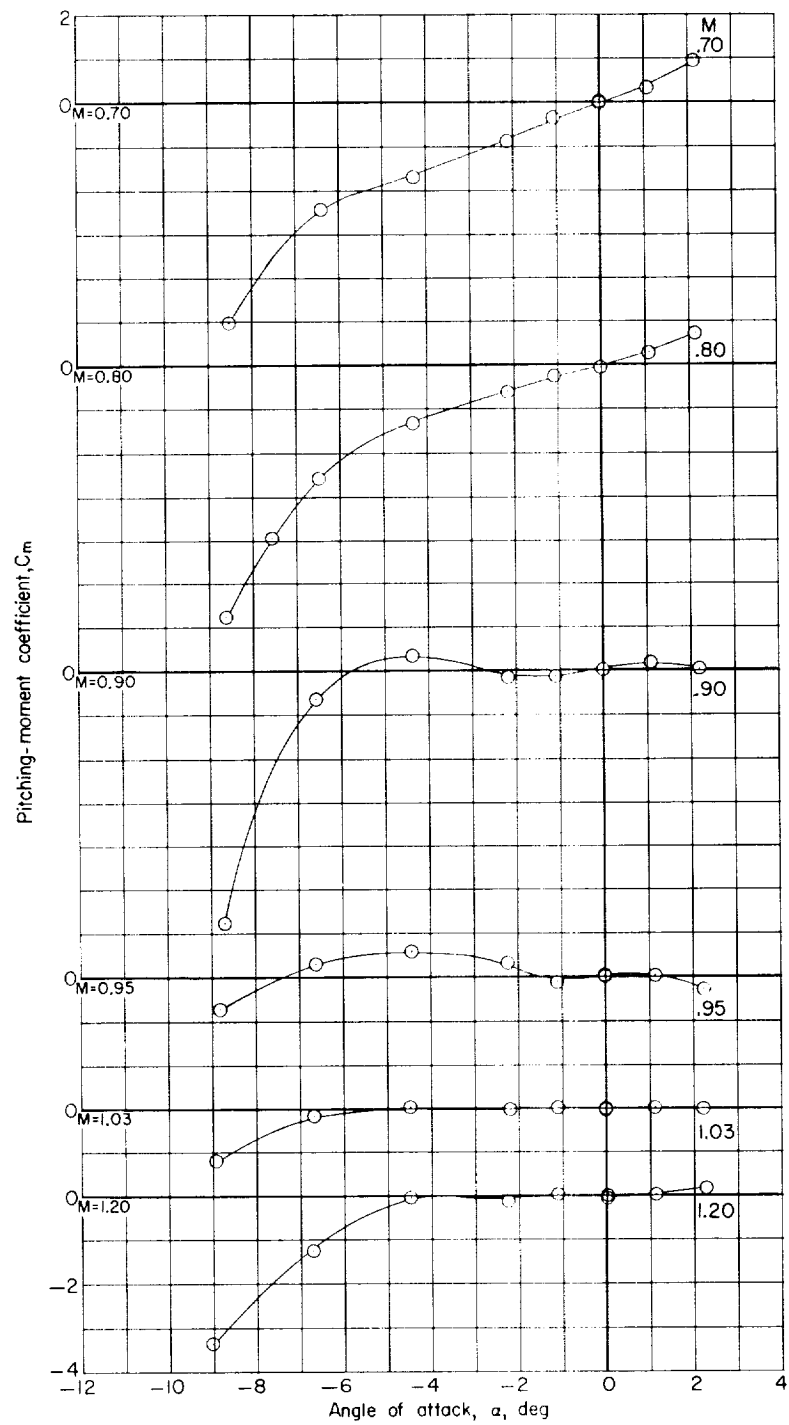


(b) Axial-force coefficient.

Figure 11.- Continued.

~~CONFIDENTIAL~~

CONFIDENTIAL



(c) Pitching-moment coefficient.

Figure 11.- Concluded.

CONFIDENTIAL

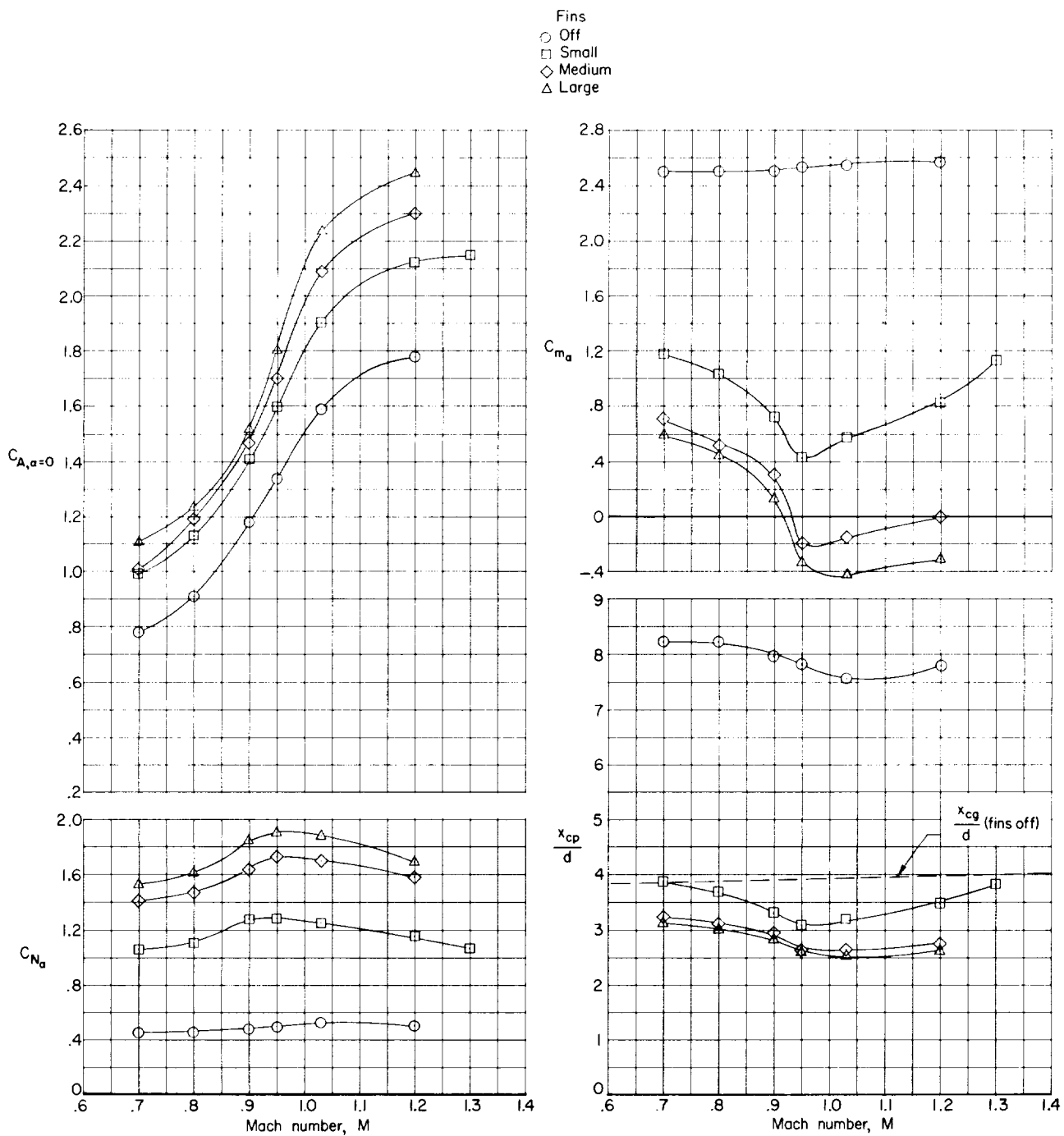


Figure 12.- Summary of static longitudinal aerodynamic characteristics of several Titan III launch vehicle and Dyna-Soar glider configurations.

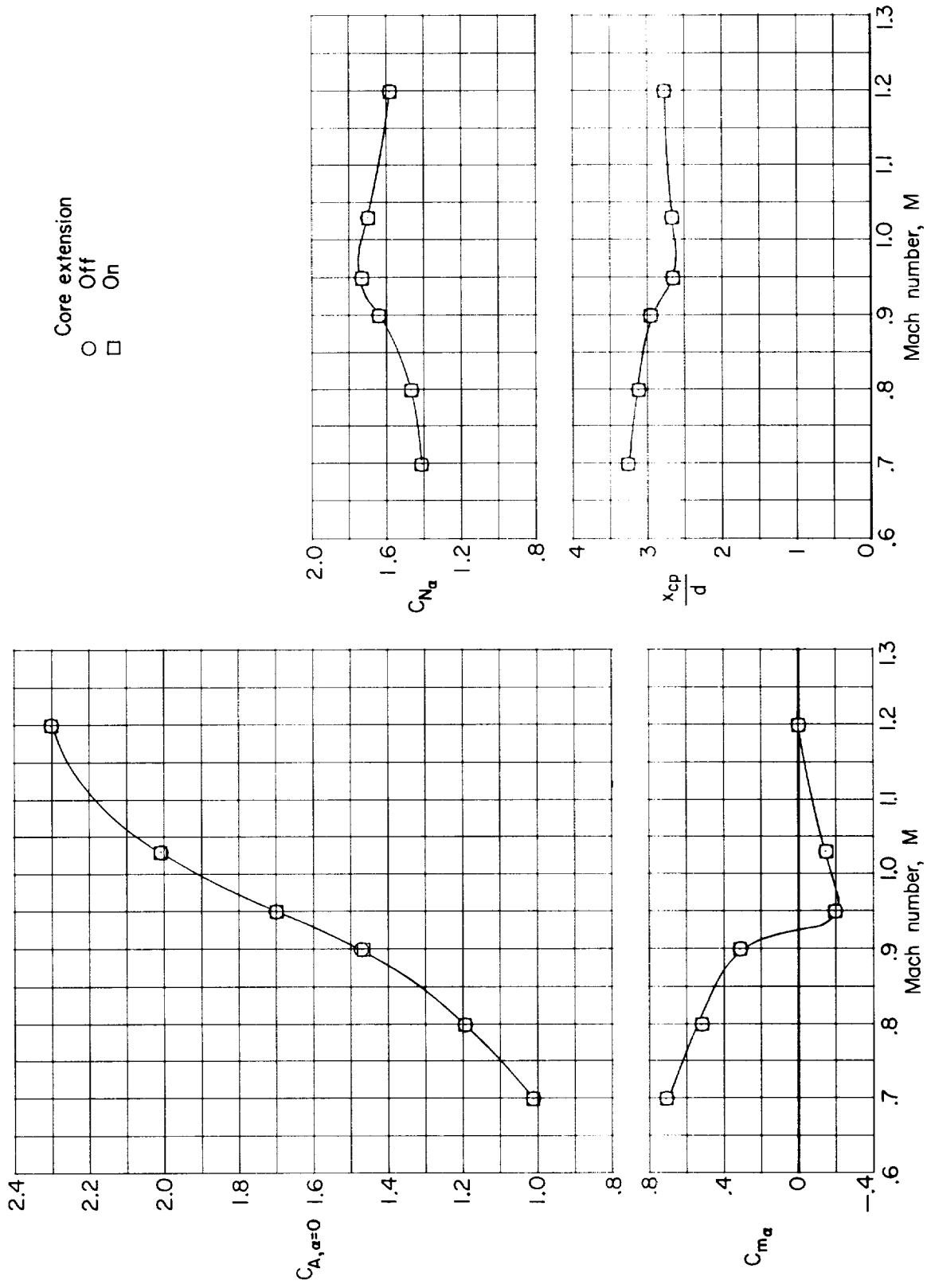


Figure 13.- Summary of the static longitudinal aerodynamic characteristics of the basic configuration with medium fins and with and without core extension.

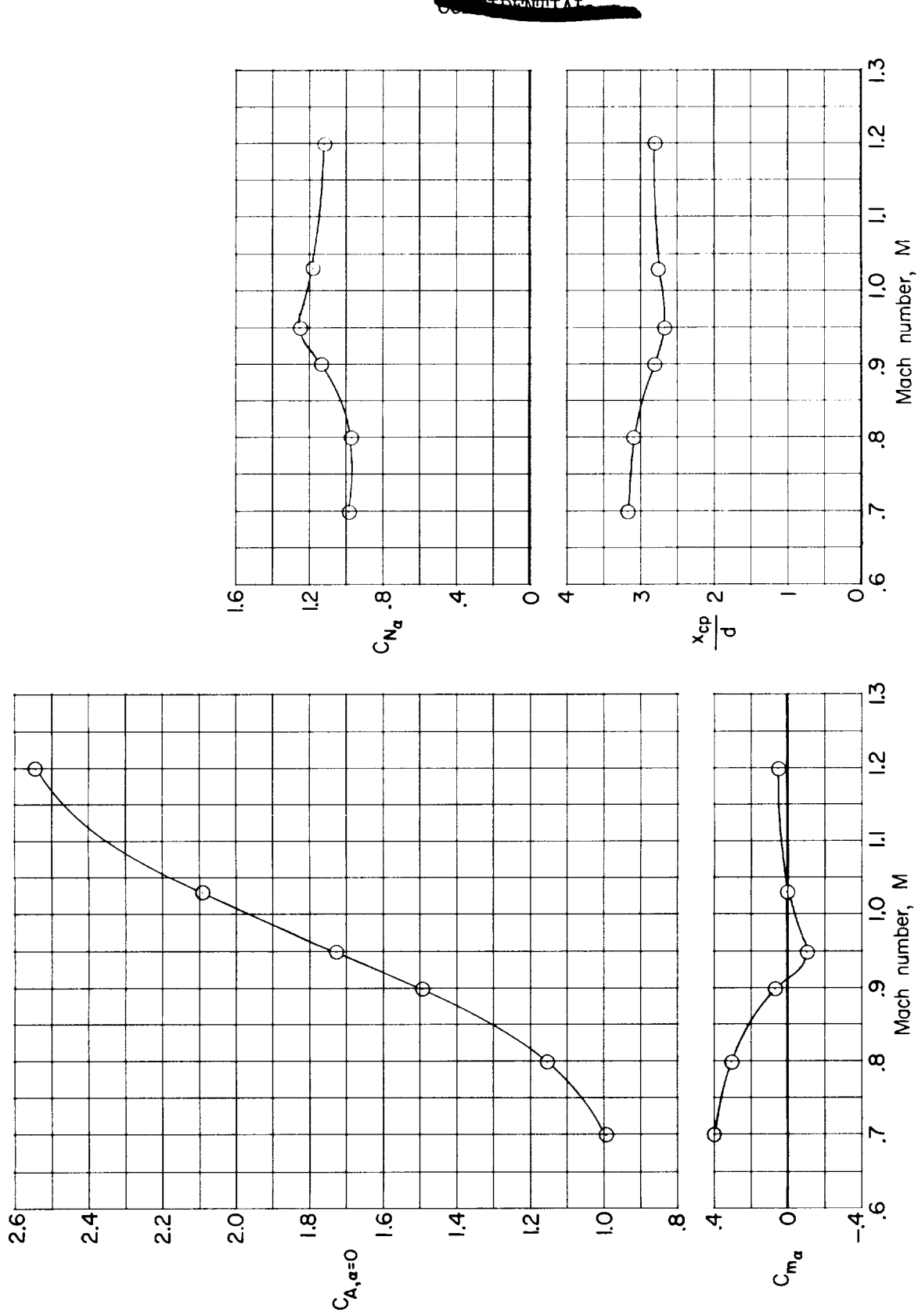


Figure 14.- Summary of the static longitudinal aerodynamic characteristics for the Titan III launch-vehicle configuration with small fins and with bulbous nose shape.

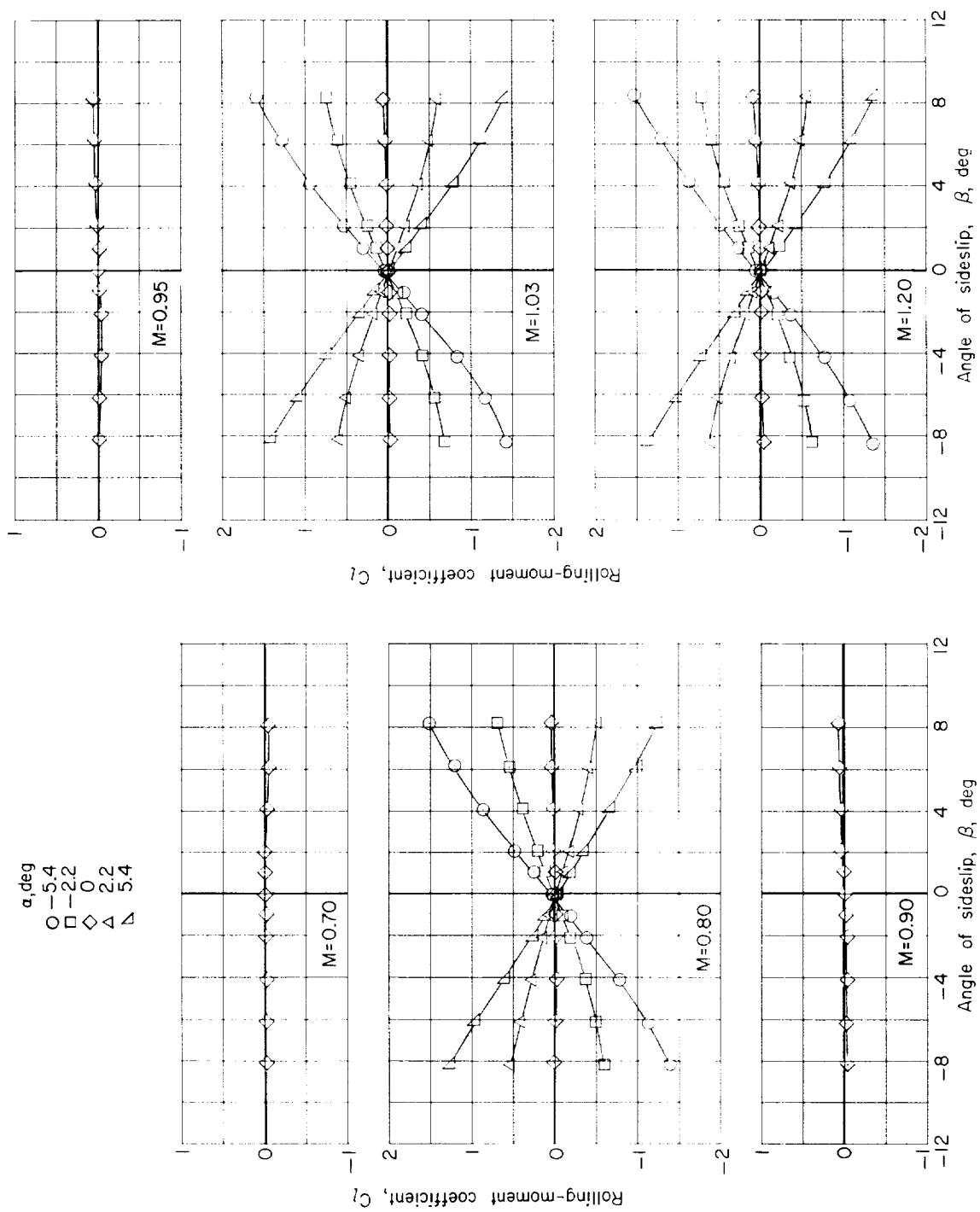


Figure 15.- Aerodynamic characteristics in sideslip of the basic configuration without fins. $\delta_e = 0^\circ$.

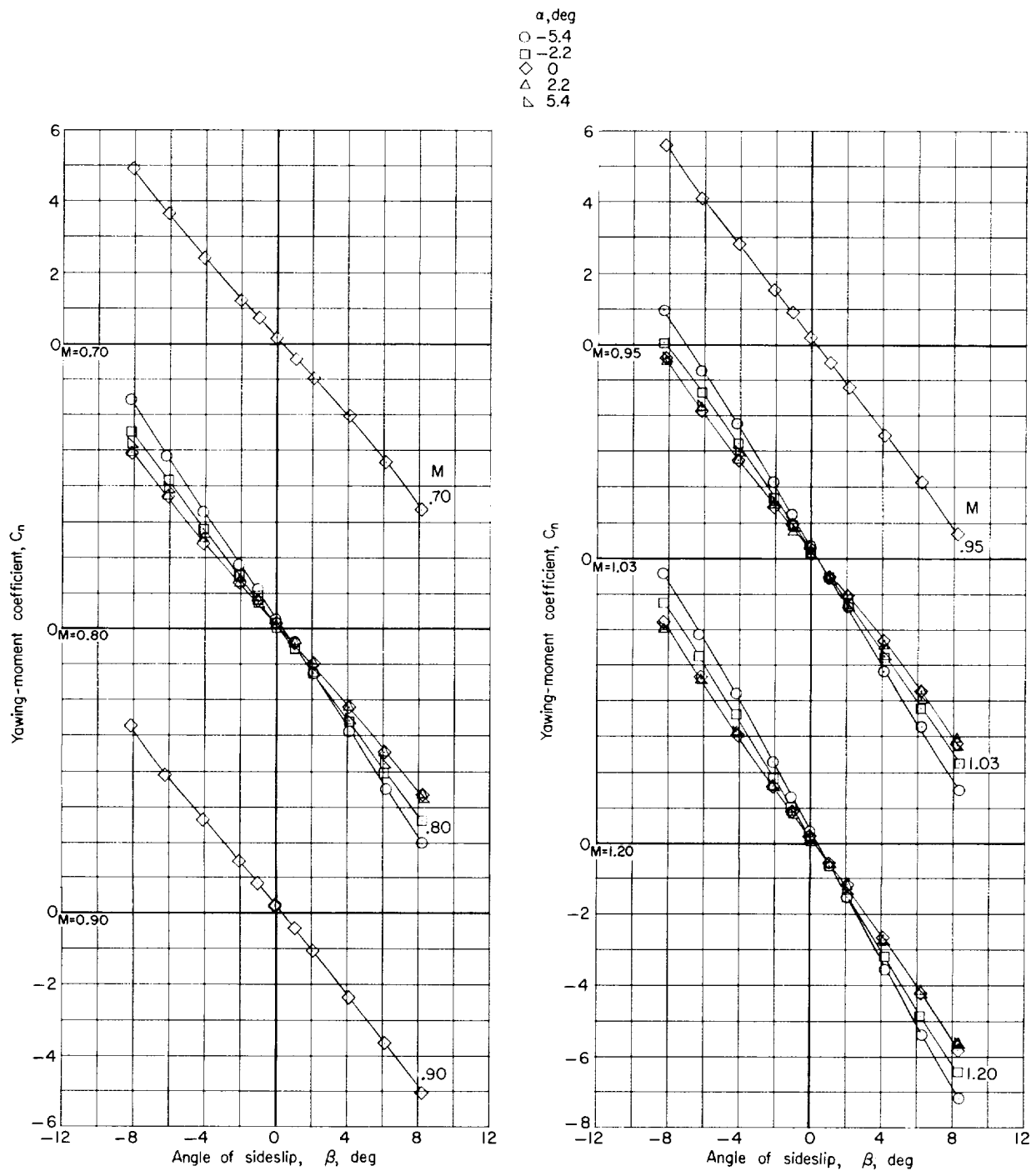
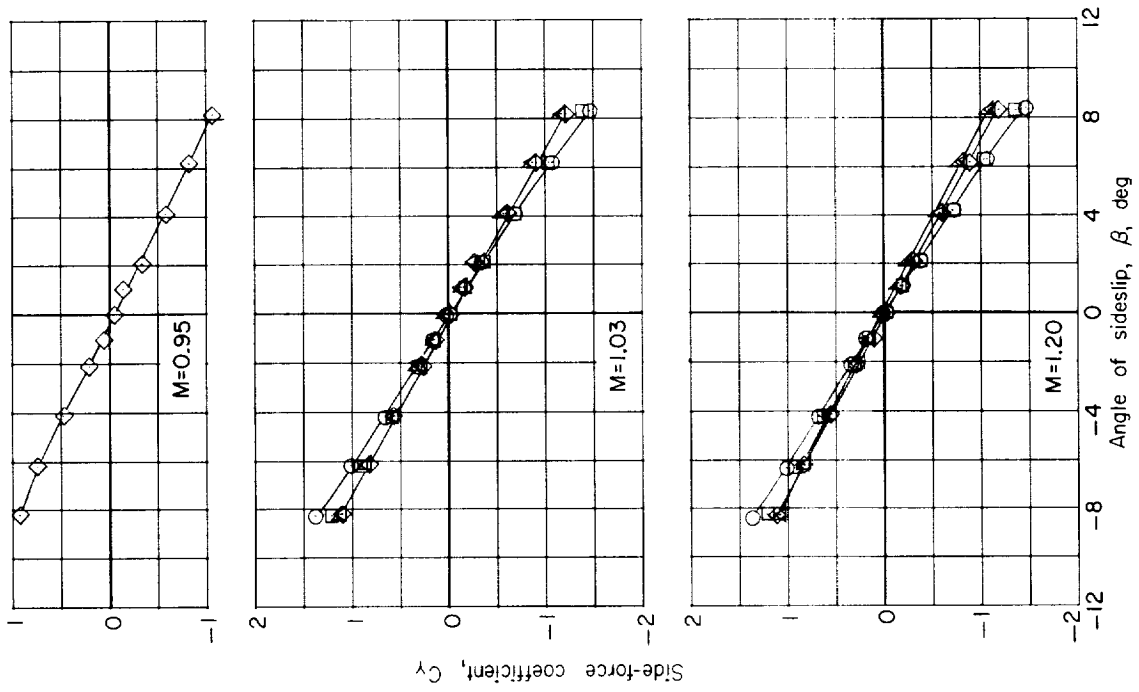
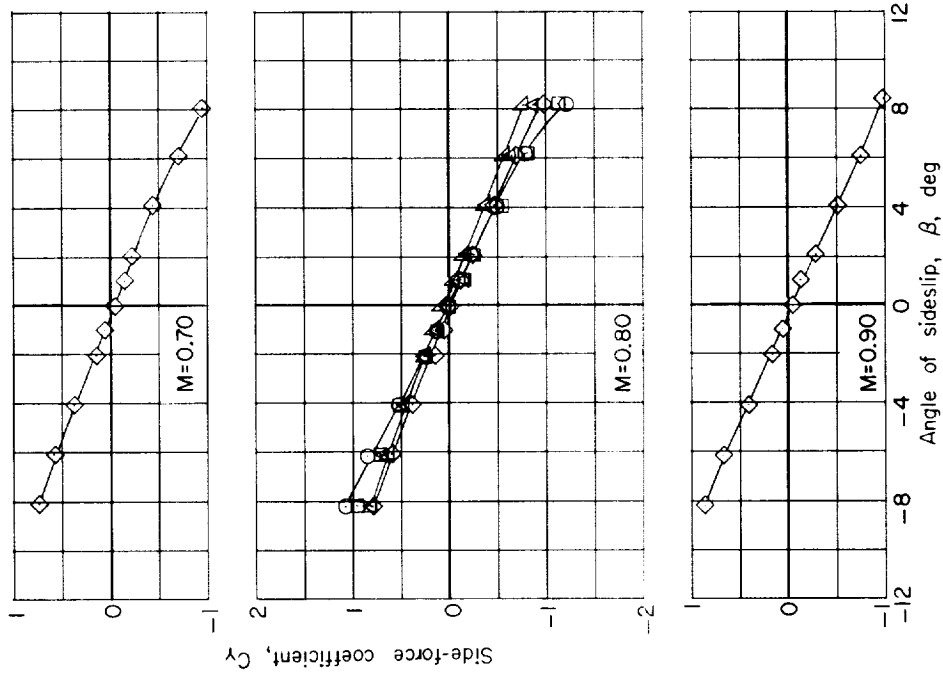


Figure 15.- Continued.

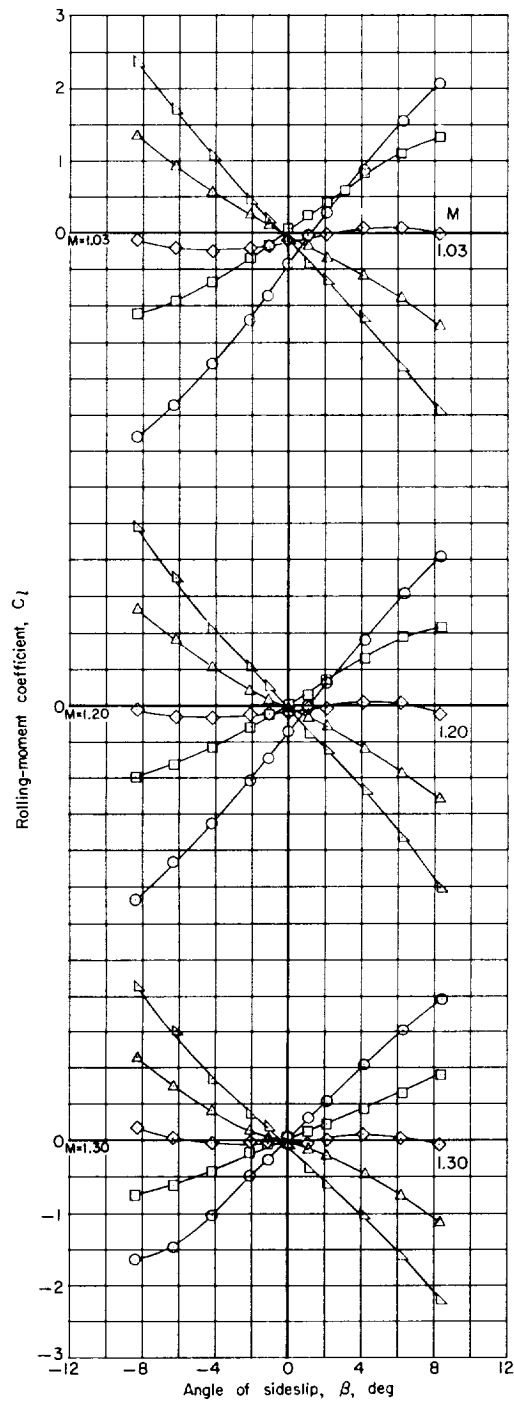
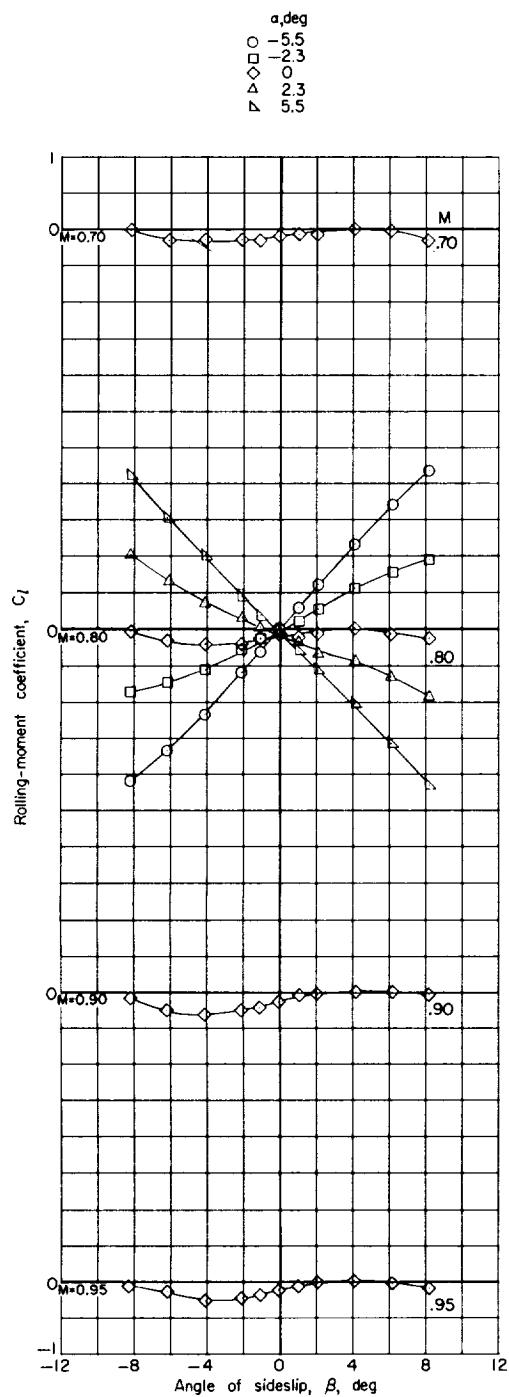


α , deg
 O -5.4
 □ -2.2
 ◇ 0
 △ 2.2
 ▲ 5.4



(c) Side-force coefficient.

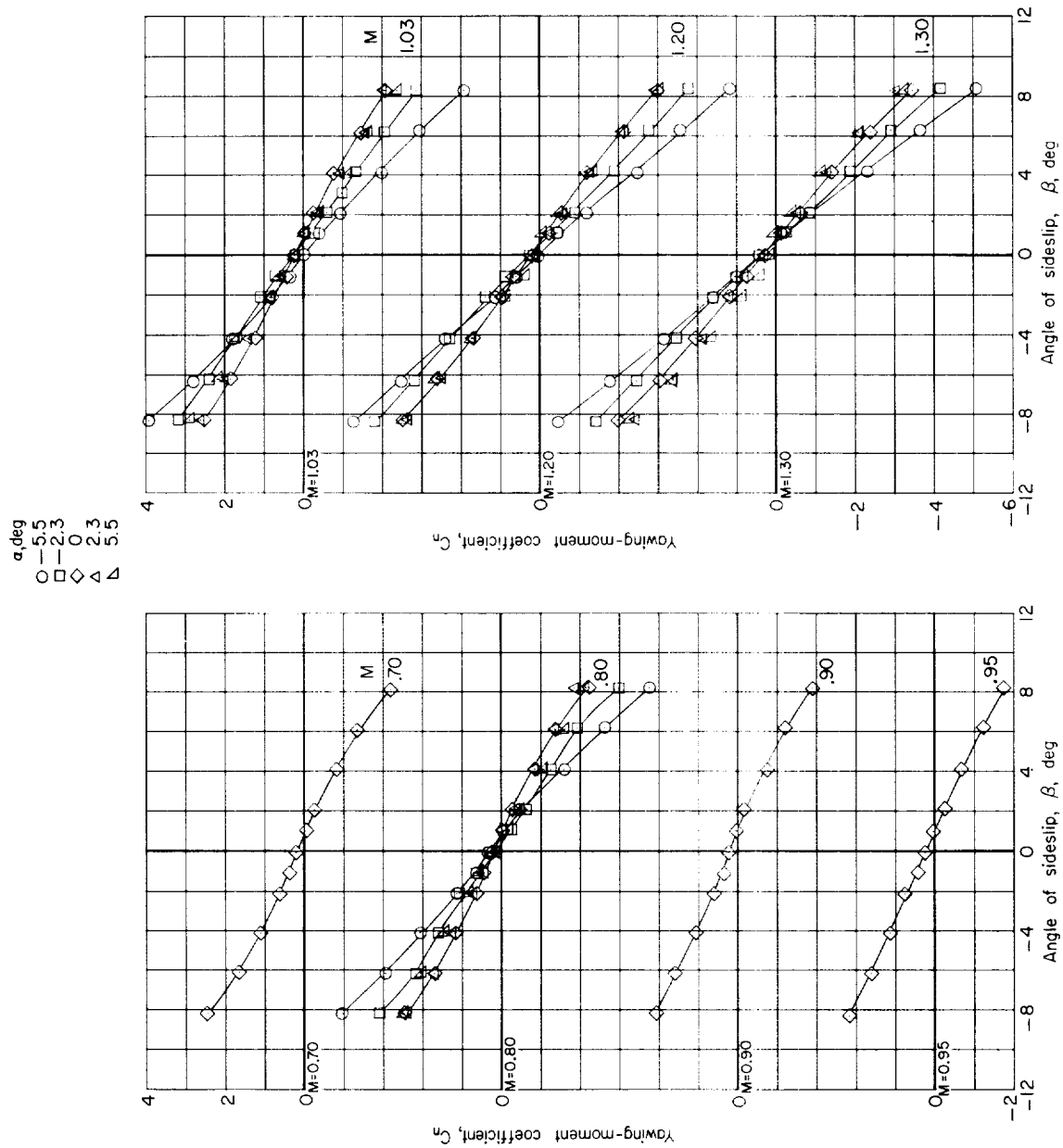
Figure 15.- Concluded.



(a) Rolling-moment coefficient.

Figure 16.- Aerodynamic characteristics in sideslip of the basic configuration with small fins.
 $\delta_e = 0^\circ$.

CONFIDENTIAL



(b) Yawing-moment coefficient.

Figure 16.- Continued.

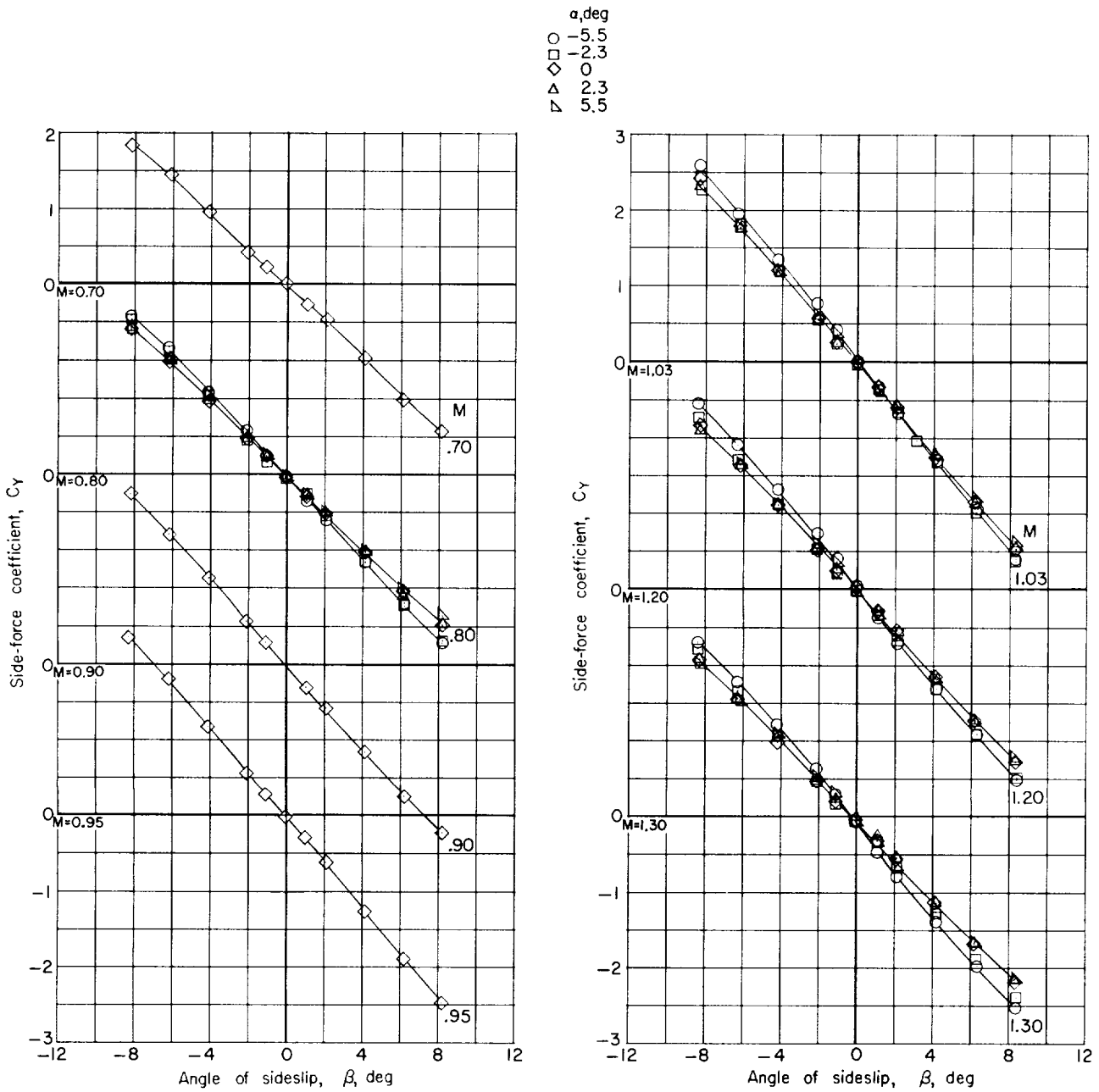
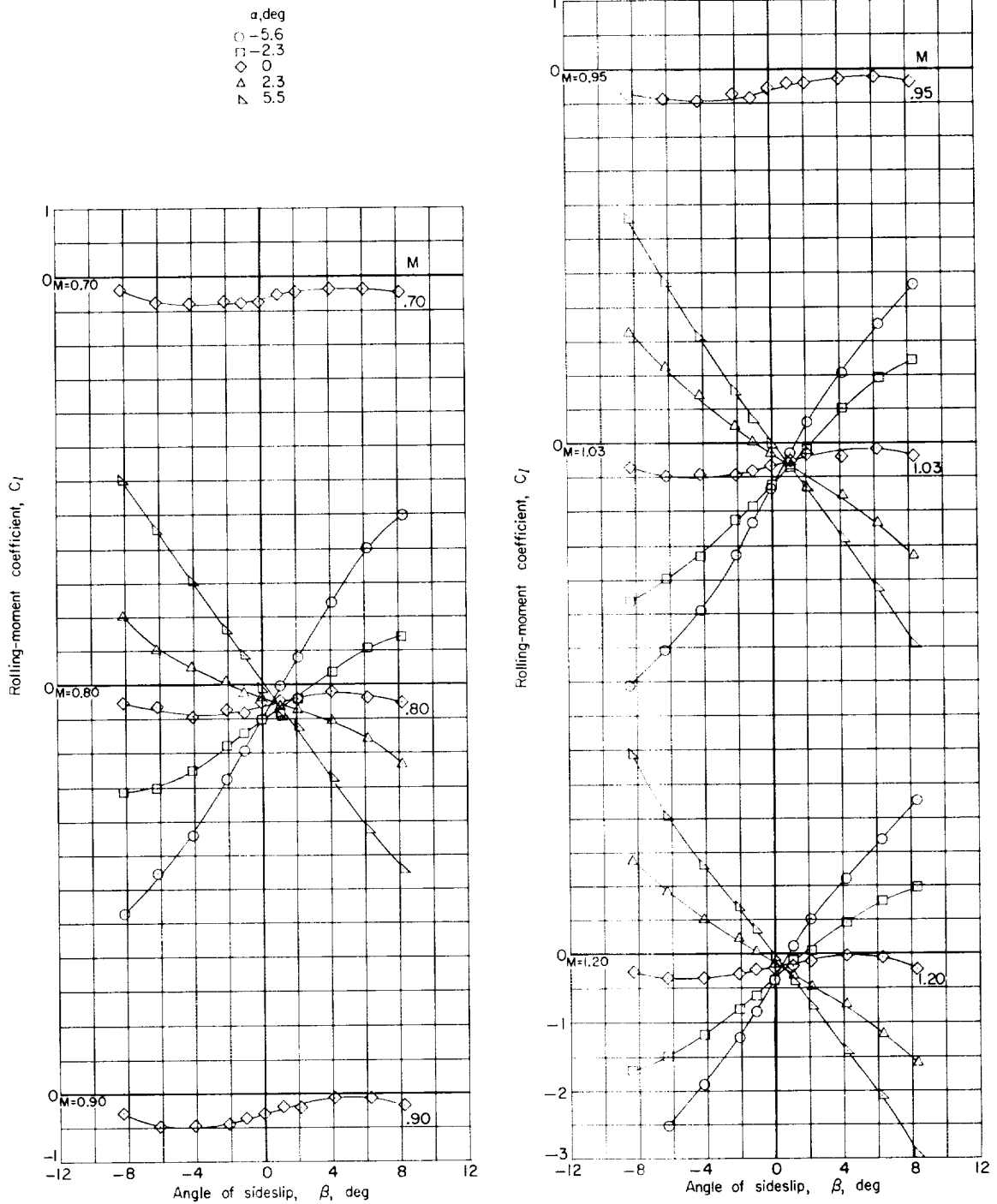
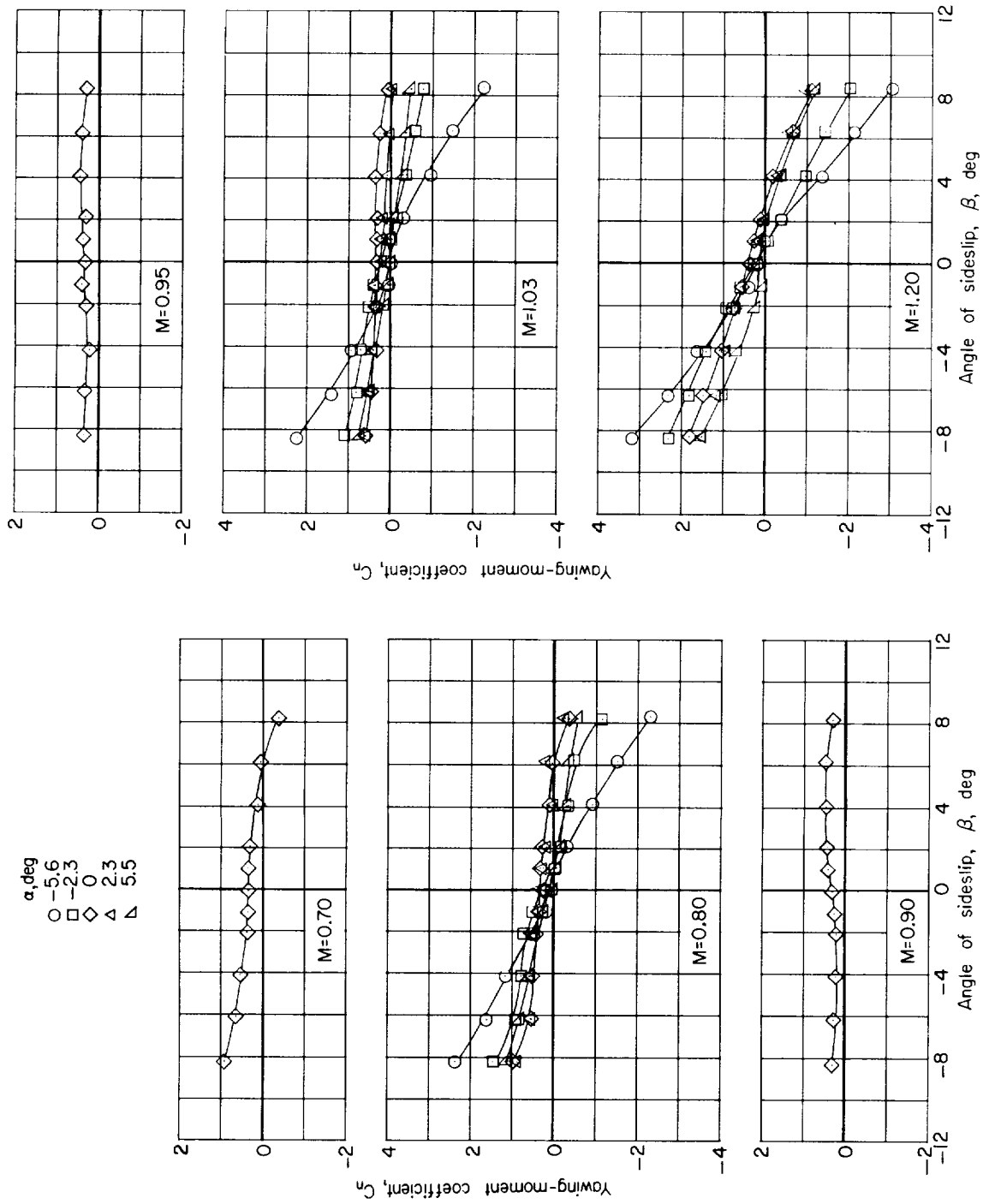


Figure 16.- Concluded.



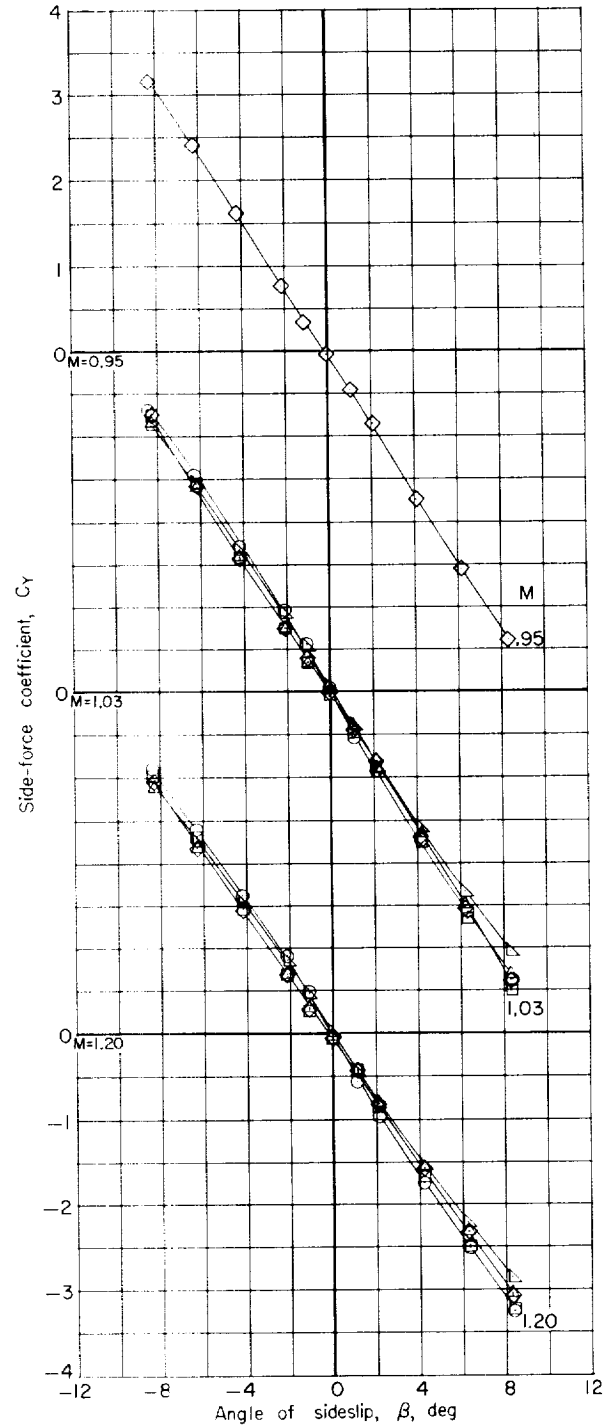
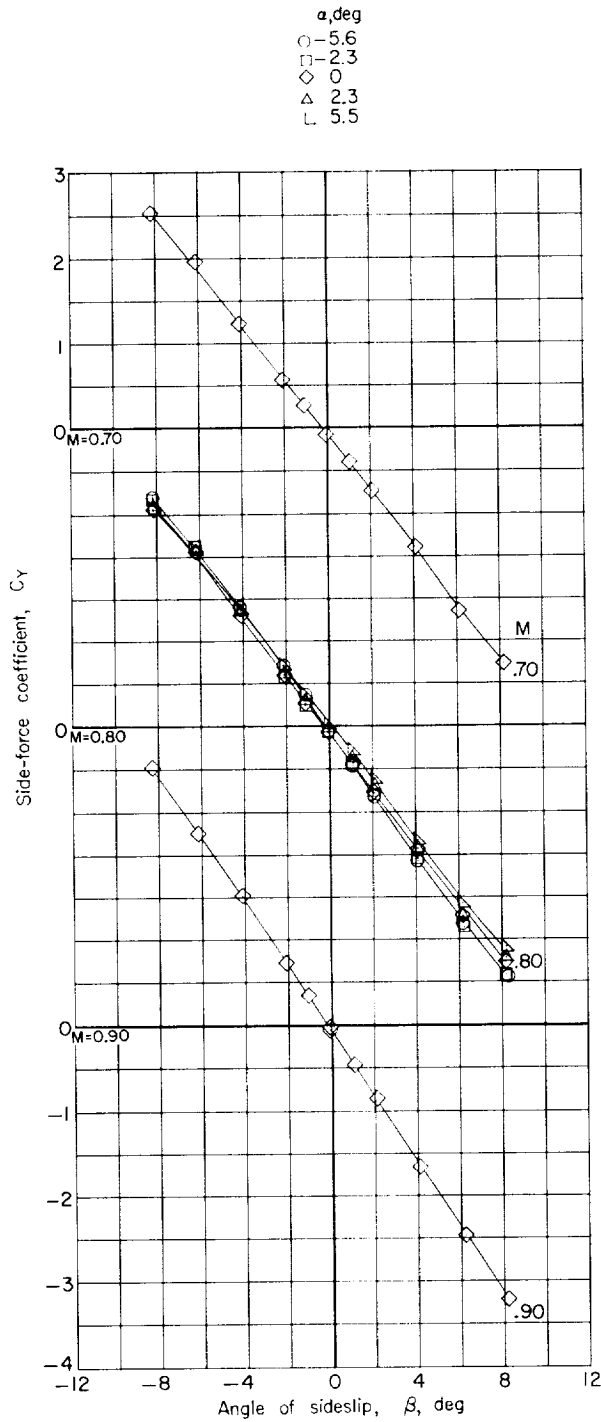
(a) Rolling-moment coefficient.

Figure 17.- Aerodynamic characteristics in sideslip of the basic configuration with medium fins.
 $\delta_e = 0^\circ$.



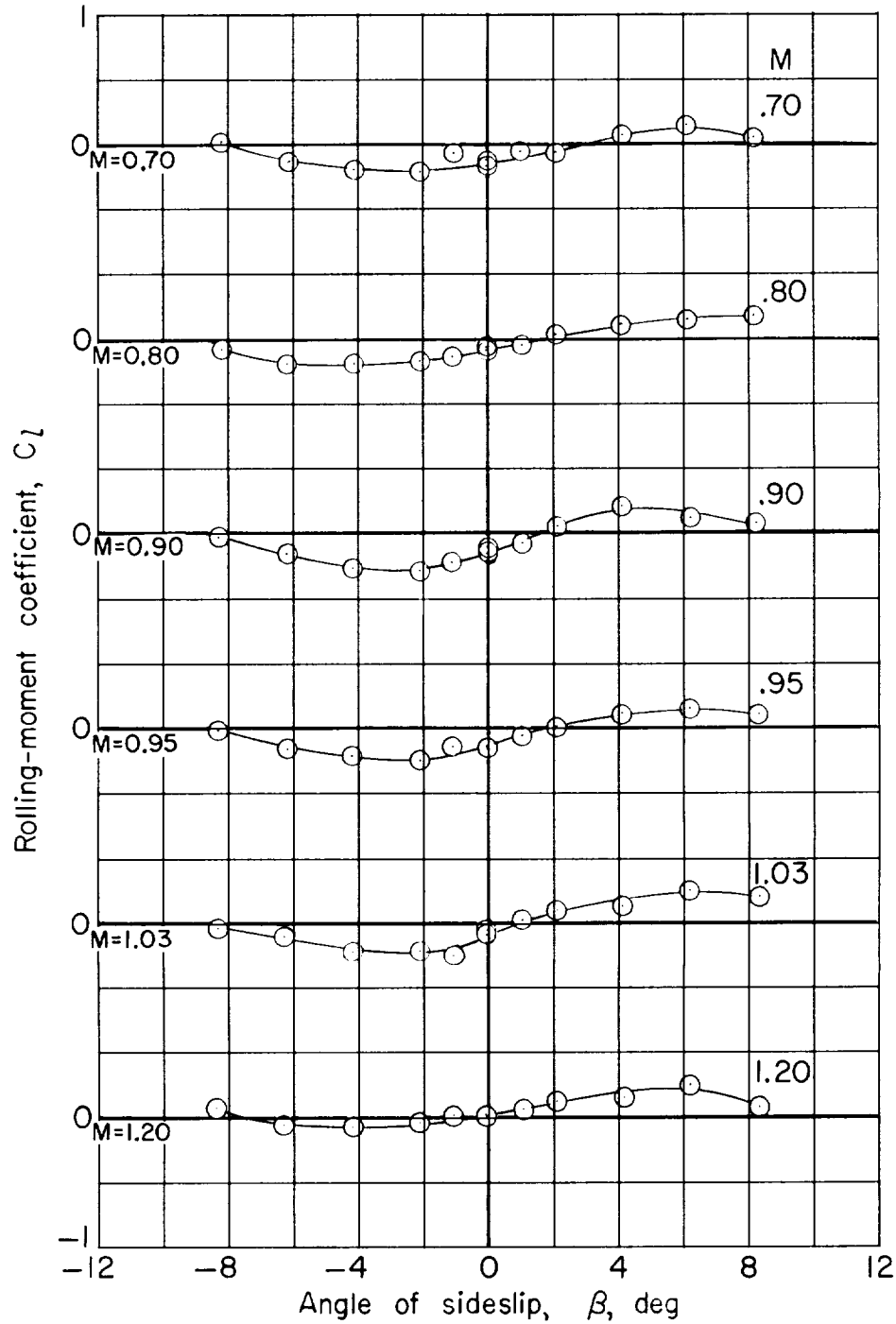
(b) Yawing-moment coefficient.

Figure 17.- Continued.



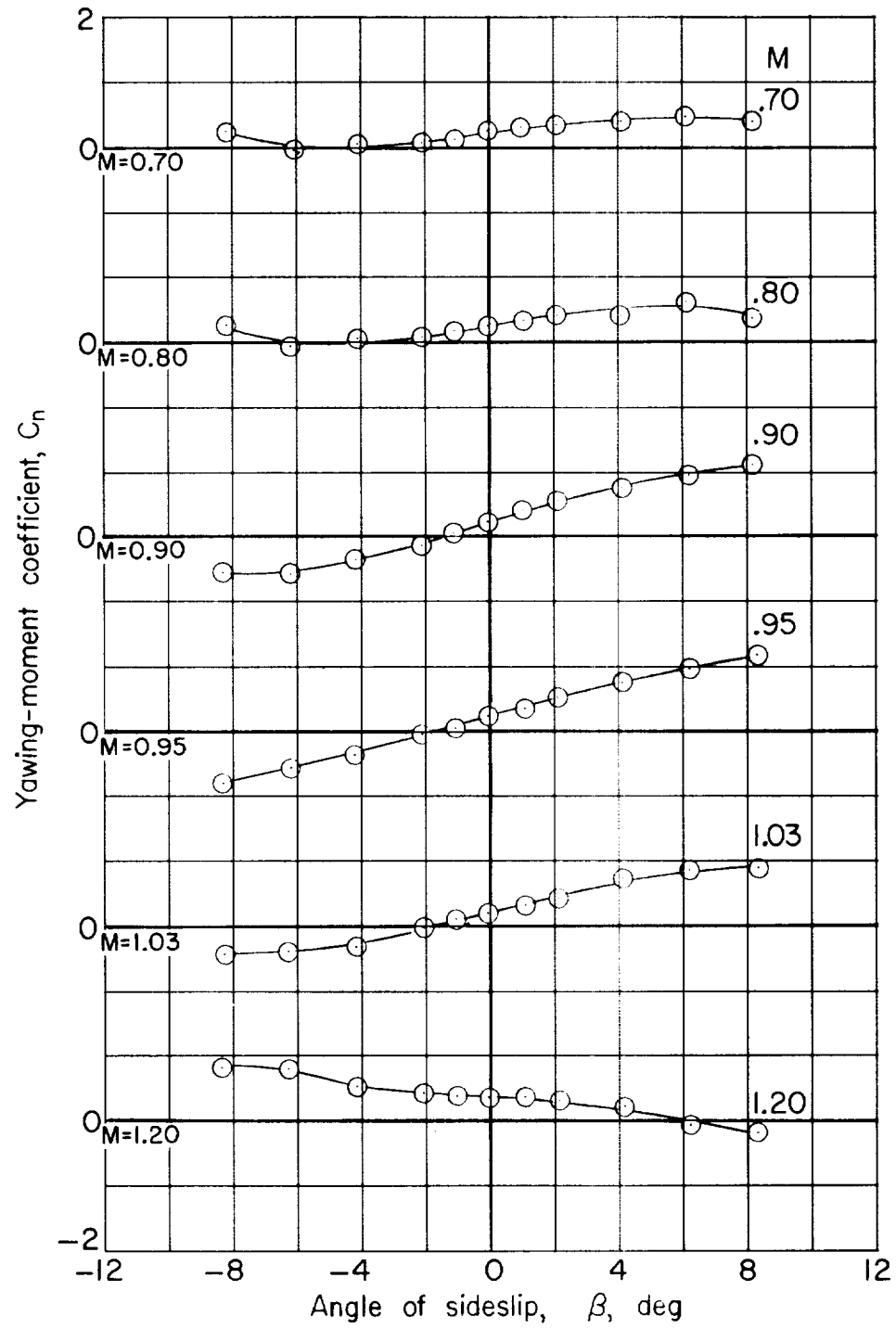
(c) Side-force coefficient.

Figure 17.- Concluded.



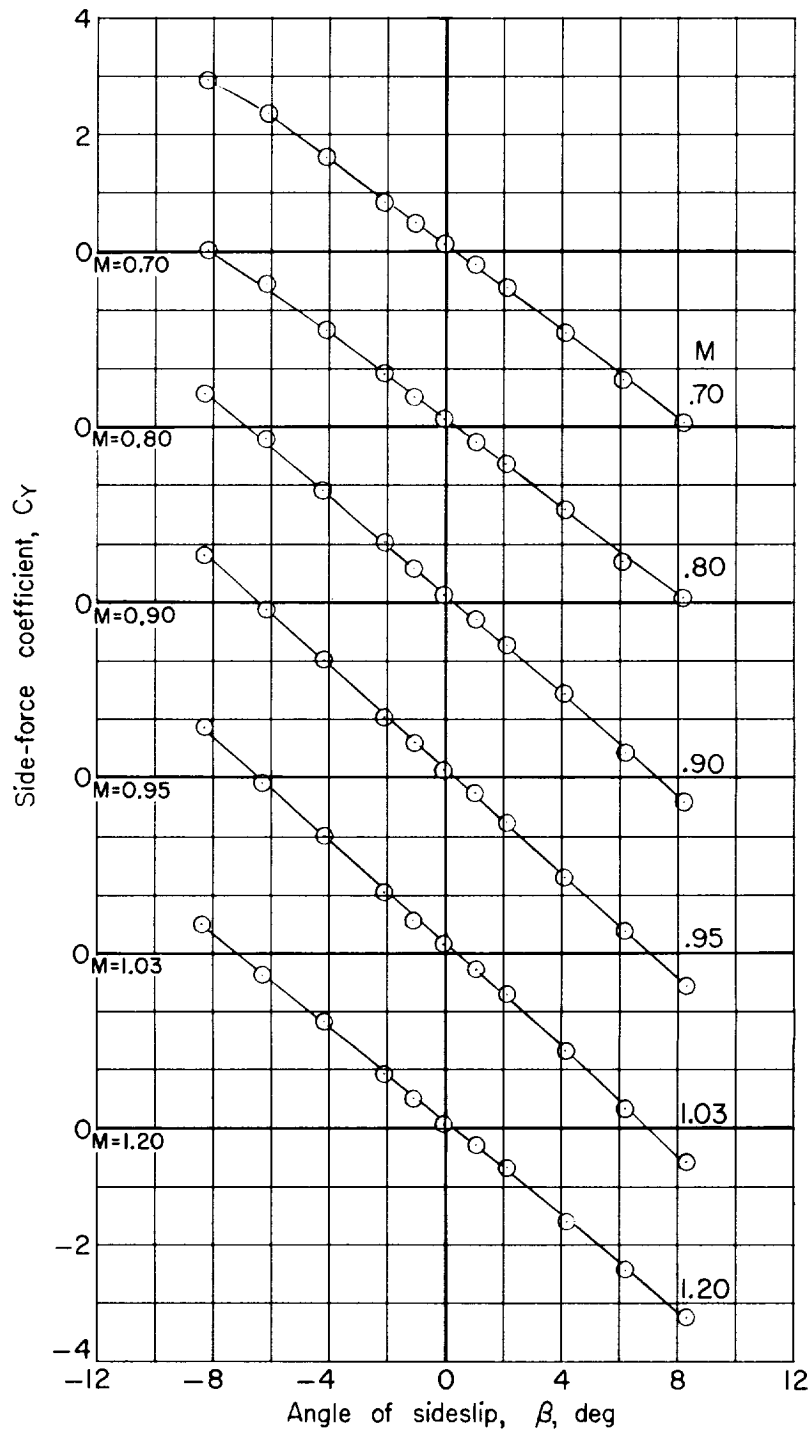
(a) Rolling-moment coefficient.

Figure 18.- Aerodynamic characteristics in sideslip of the basic configuration with large fins.
 $\alpha = 0^\circ$; $\delta_e = 0^\circ$.



(b) Yawing-moment coefficient.

Figure 18.- Continued.



(c) Side-force coefficient.

Figure 18.- Concluded.

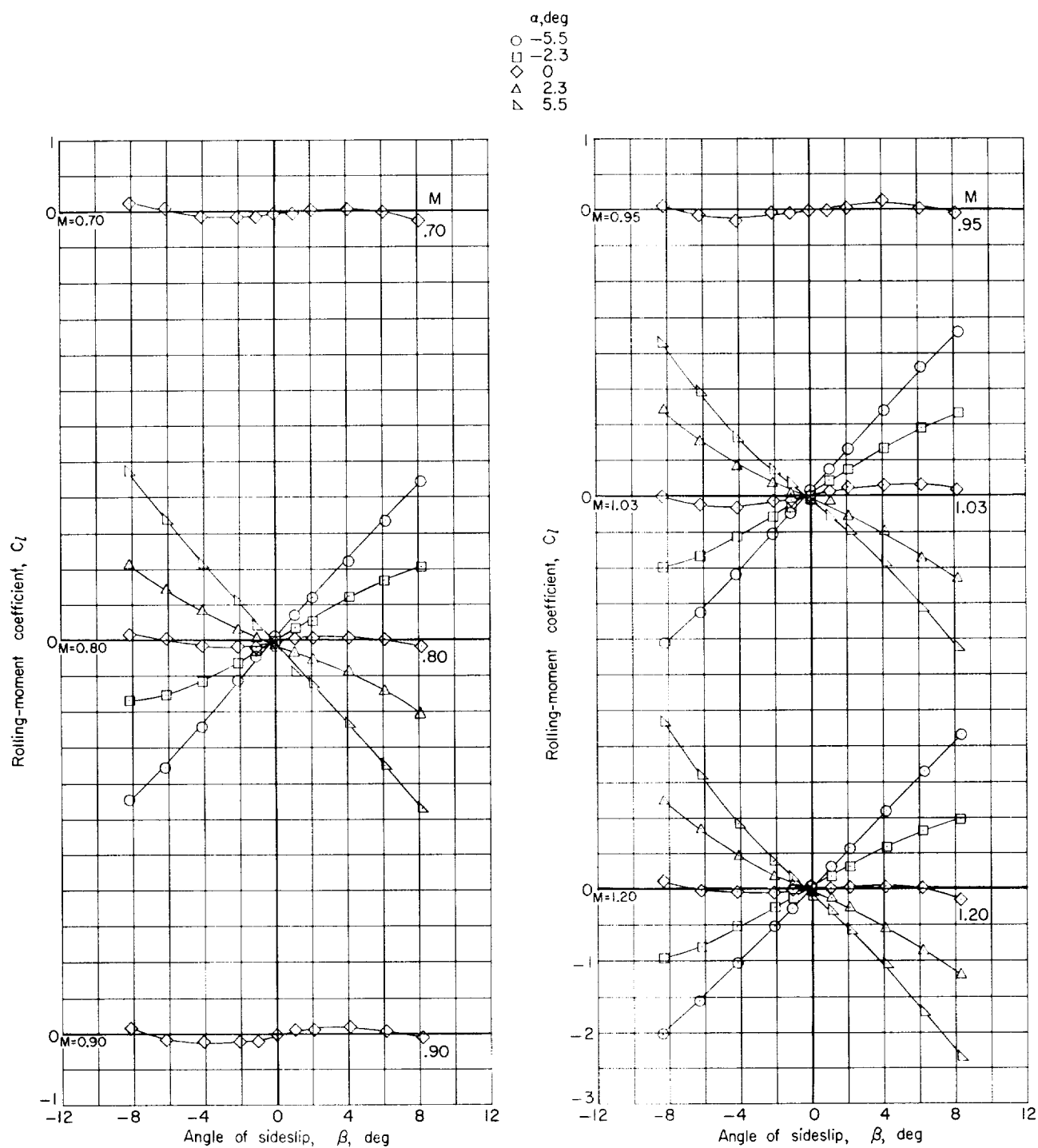


Figure 19.- Aerodynamic characteristics in sideslip of the basic configuration with small pitch fins on and yaw fins off. $\delta_e = 0^\circ$.

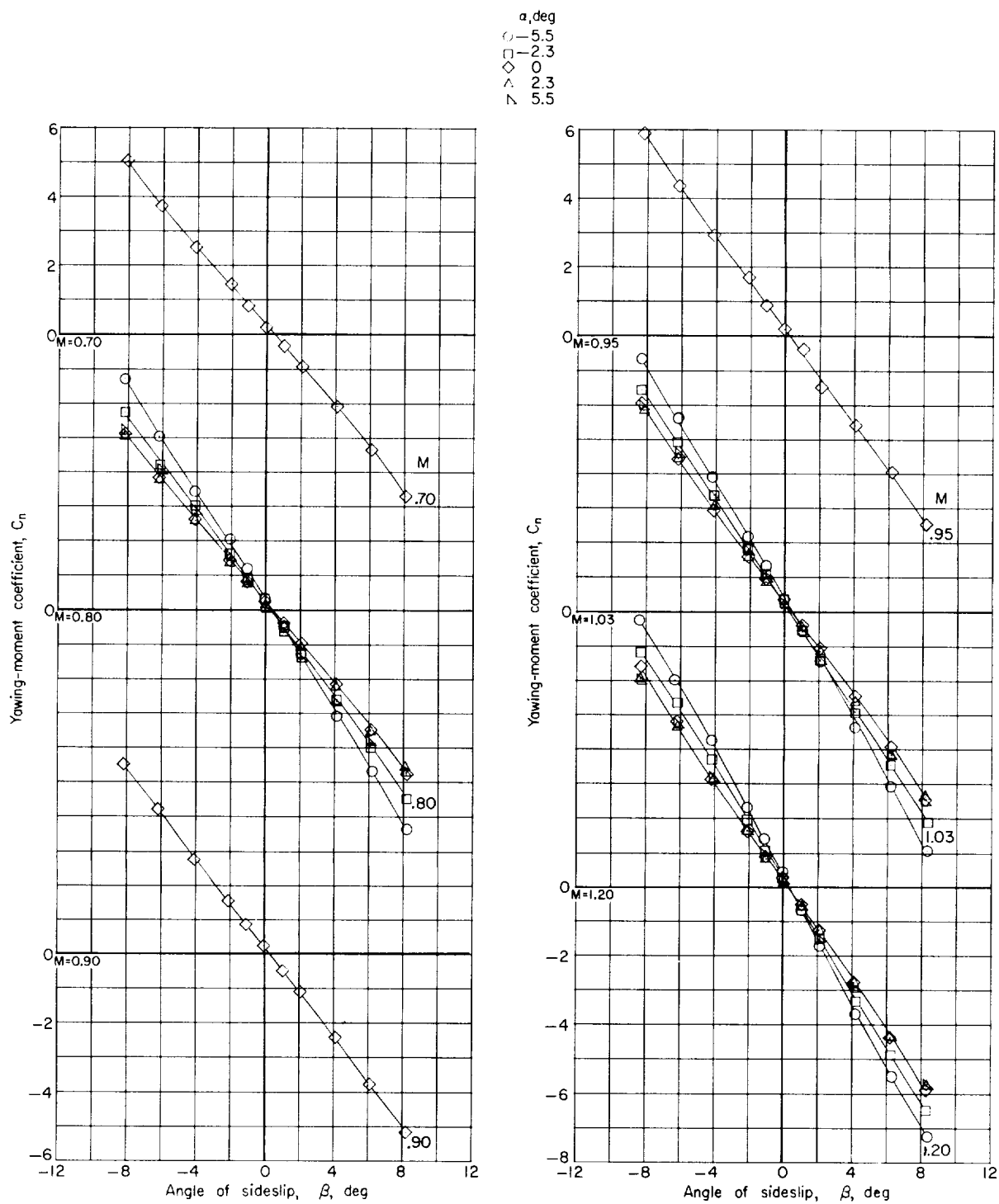
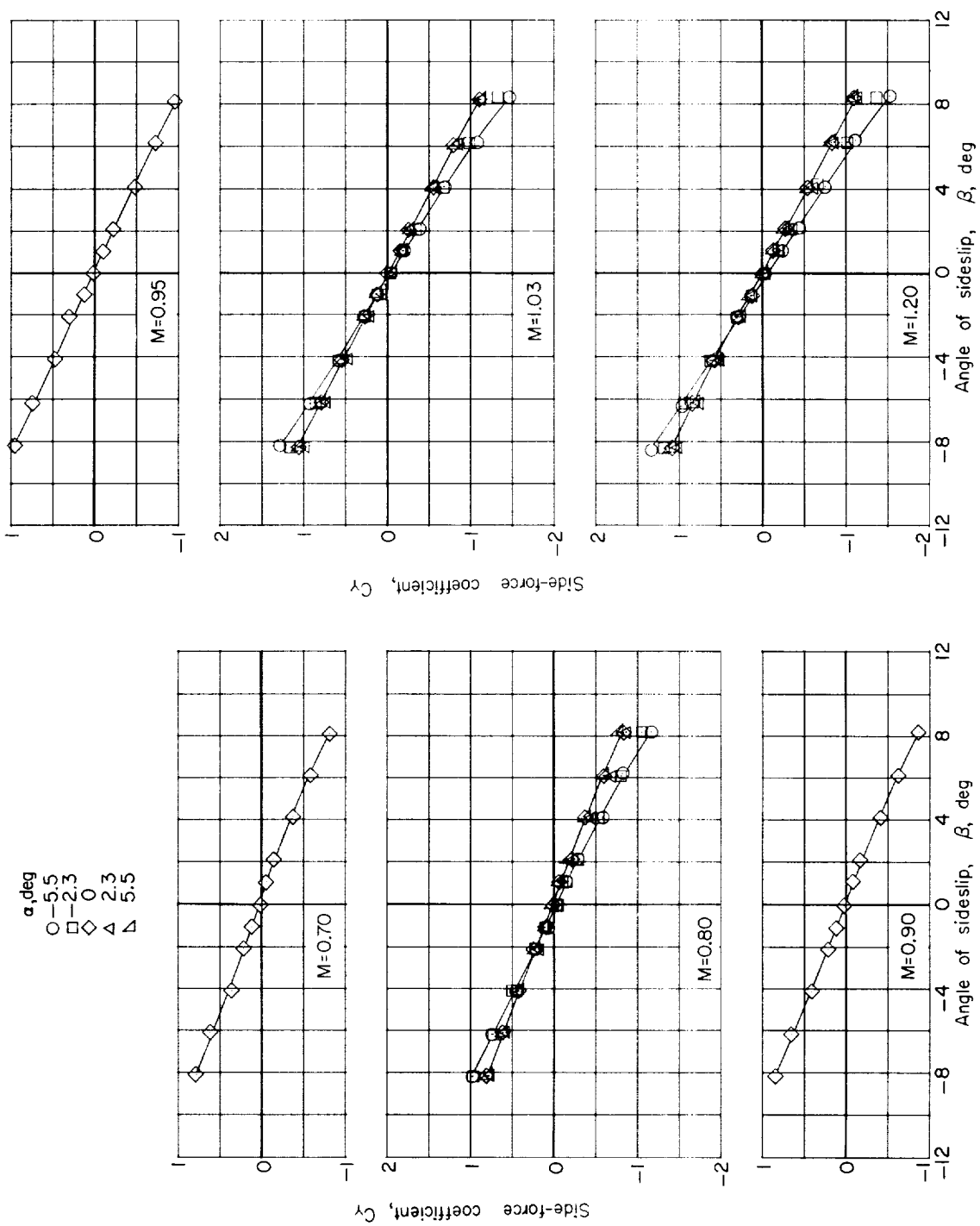


Figure 19.- Continued.



(c) Side-force coefficient.

Figure 19.- Concluded.

CONFIDENTIAL

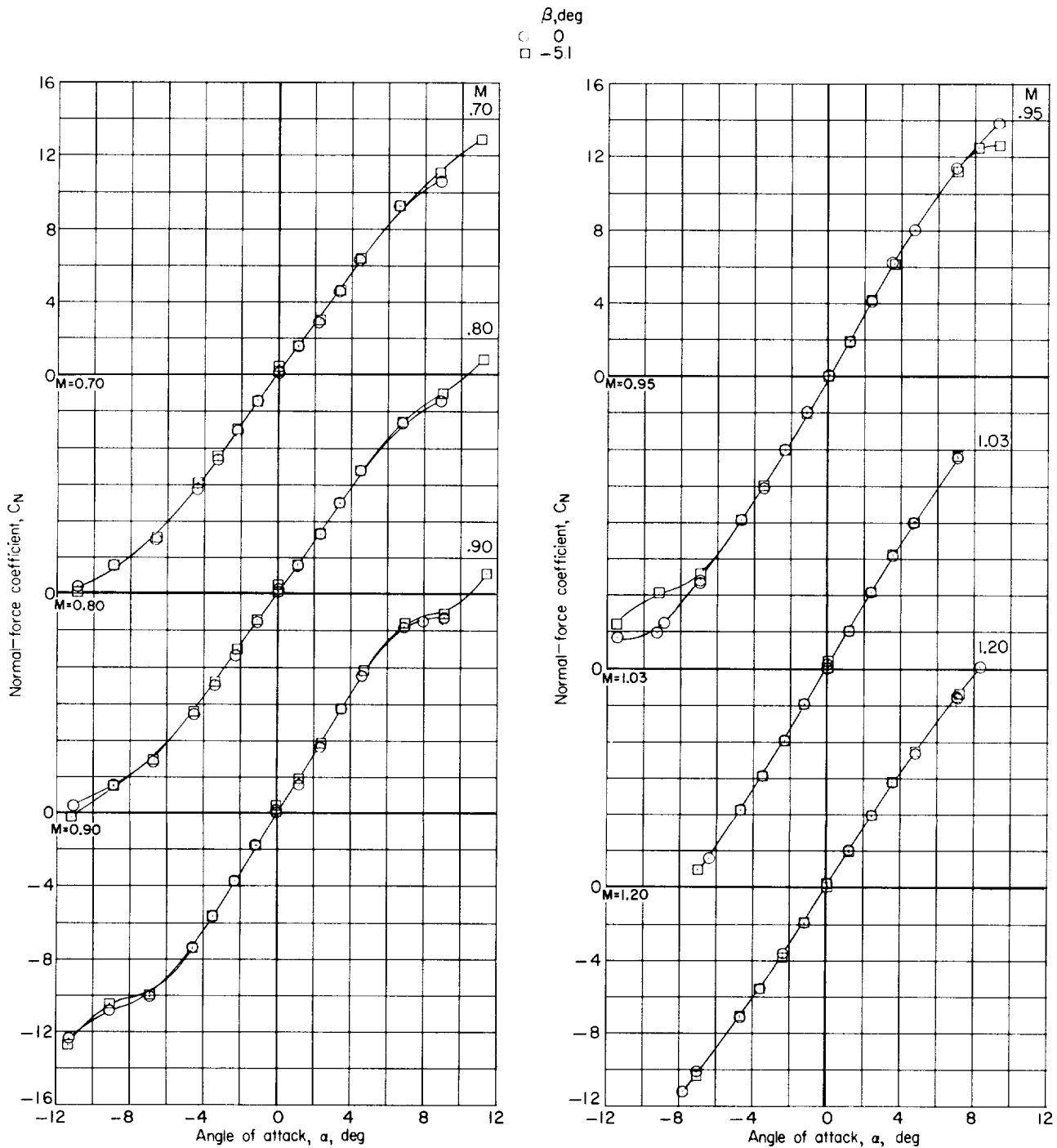
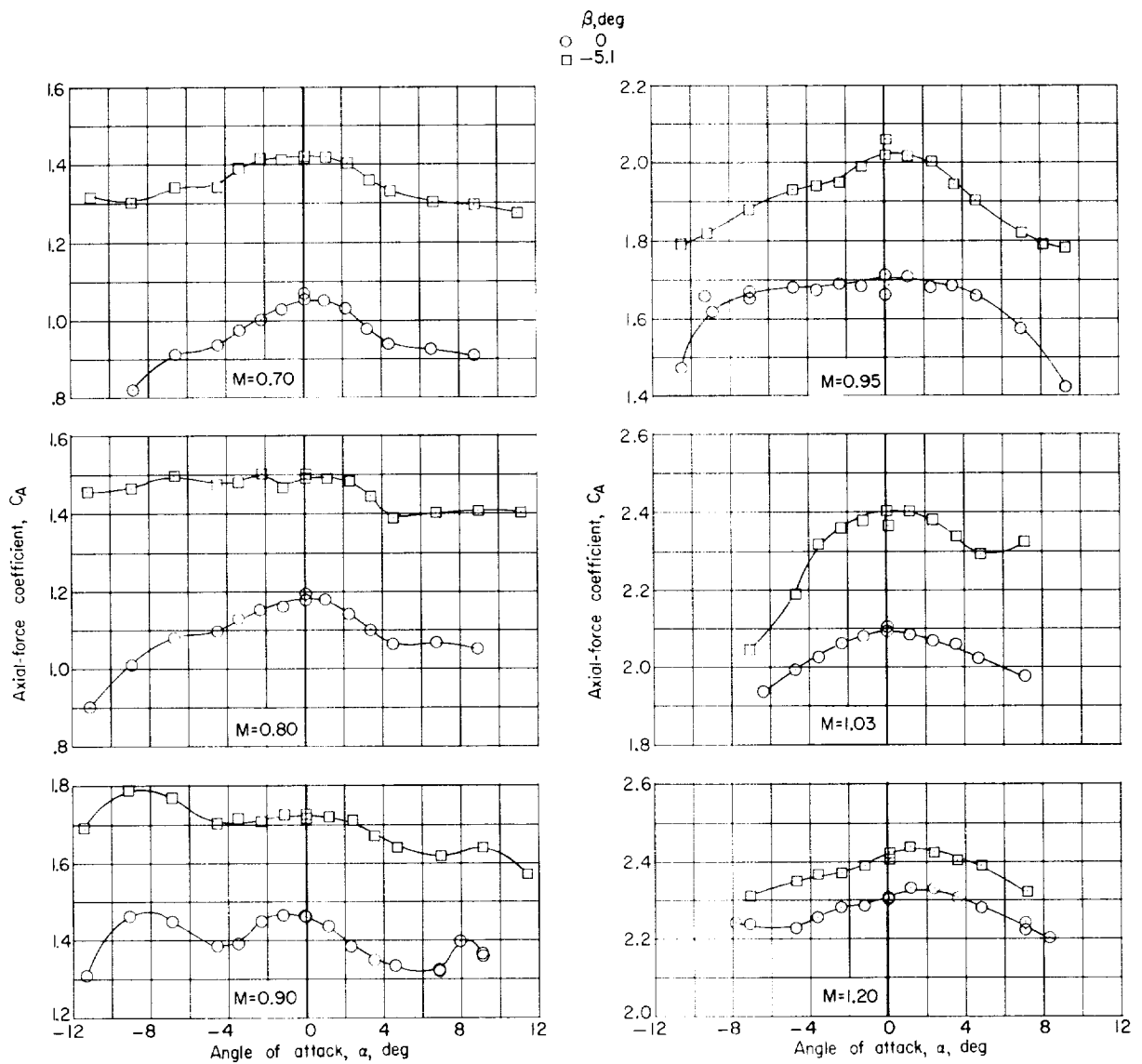


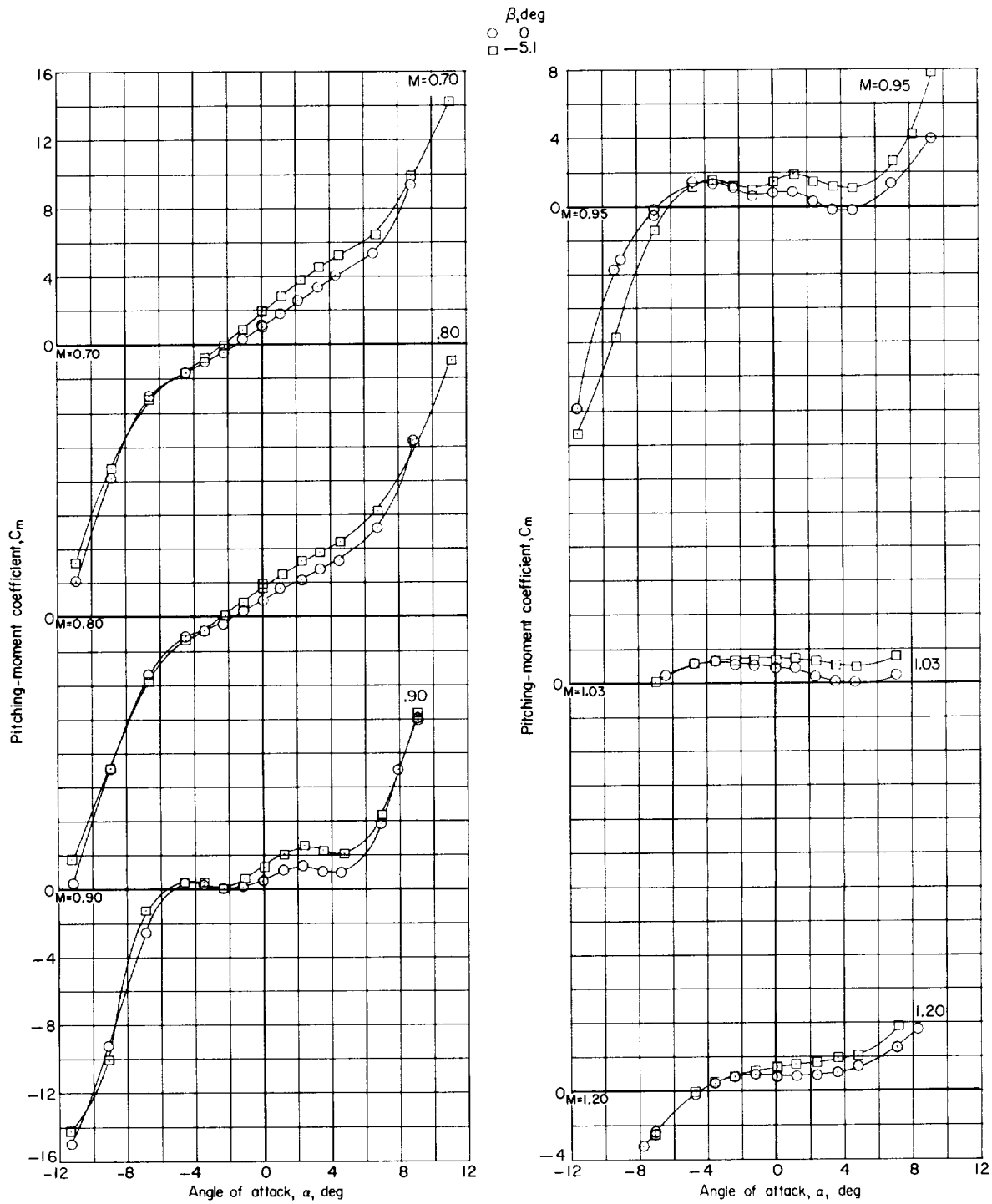
Figure 20.- Aerodynamic characteristics in pitch of the basic configuration with medium fins and core extension. $\delta_e = 0^\circ$.

CONFIDENTIAL



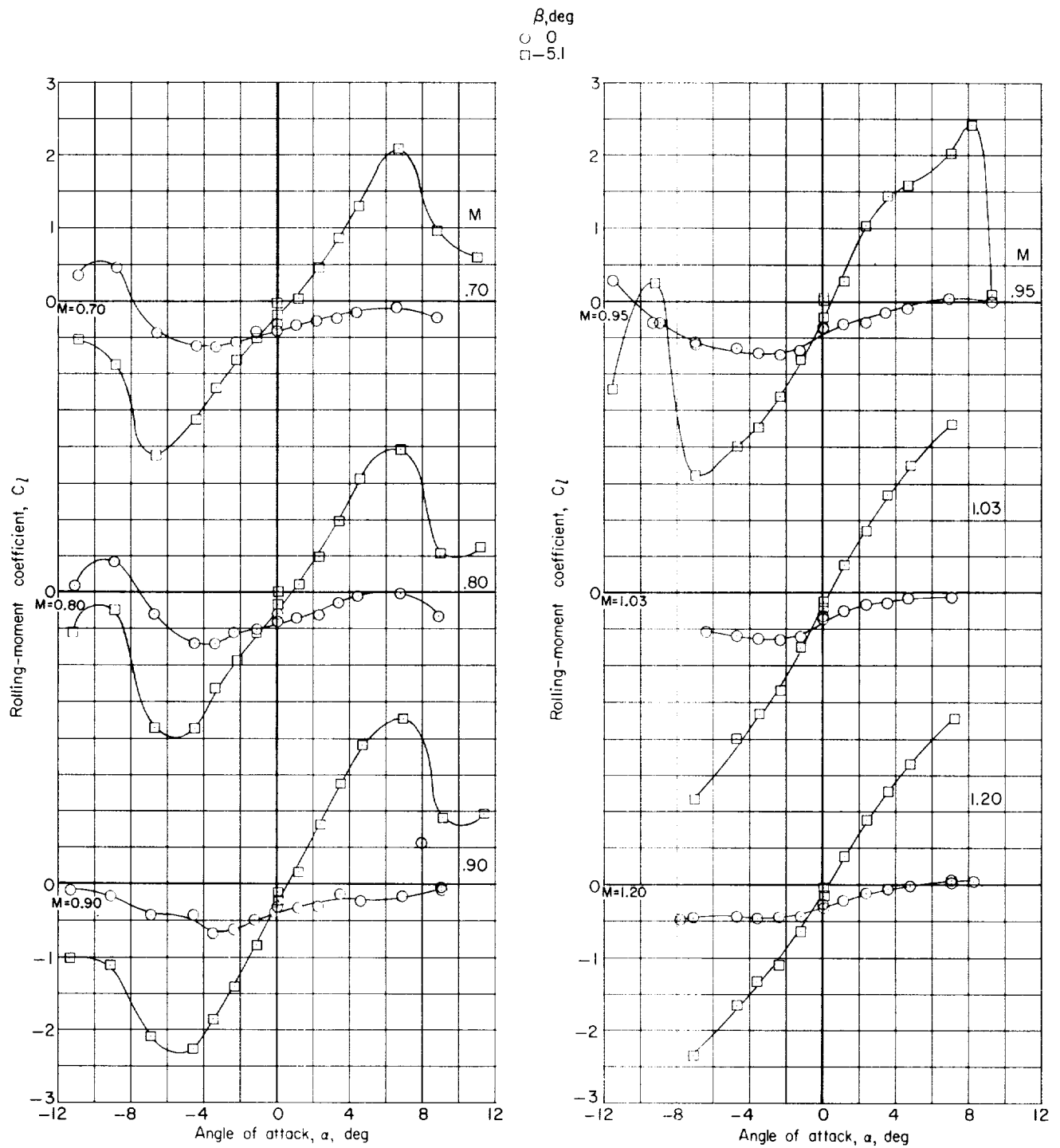
(b) Axial-force coefficient.

Figure 20.- Continued.



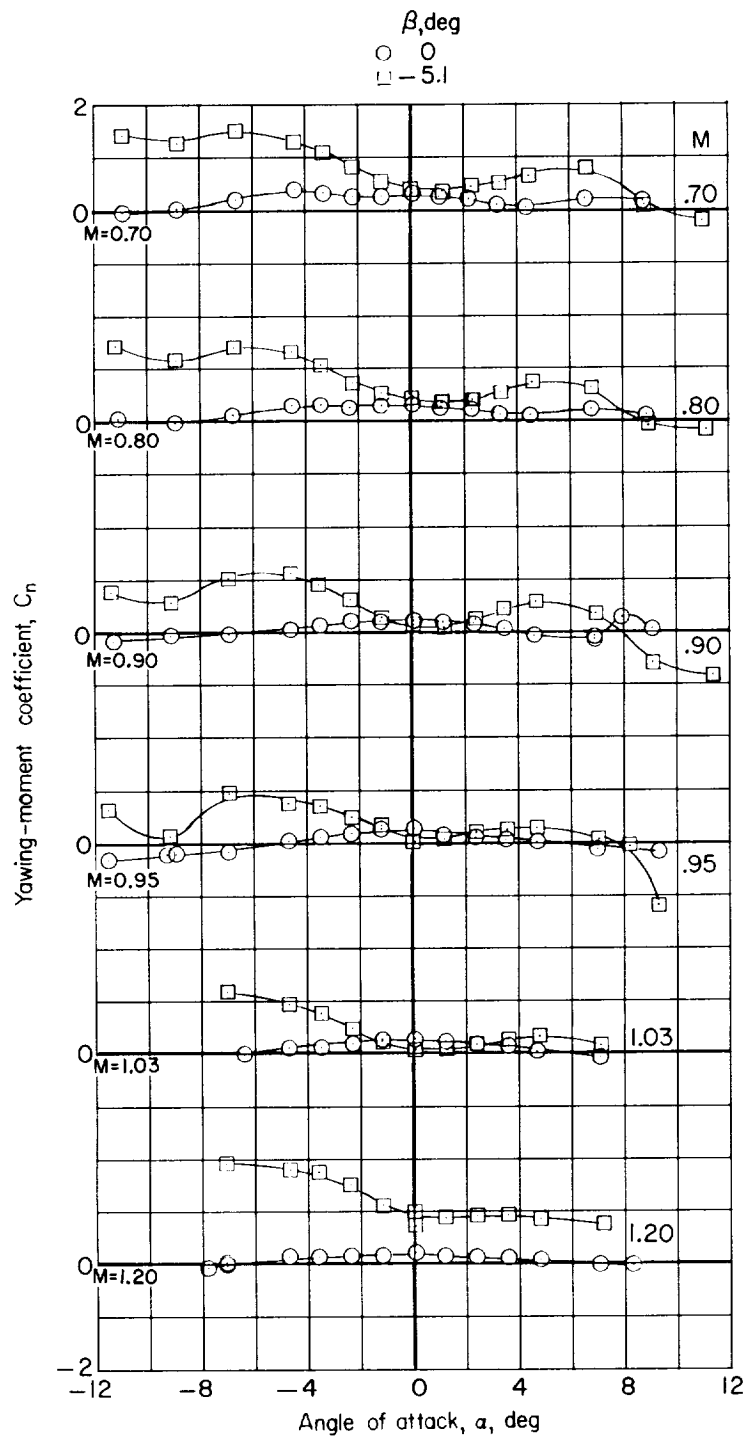
(c) Pitching-moment coefficient.

Figure 20.- Continued.



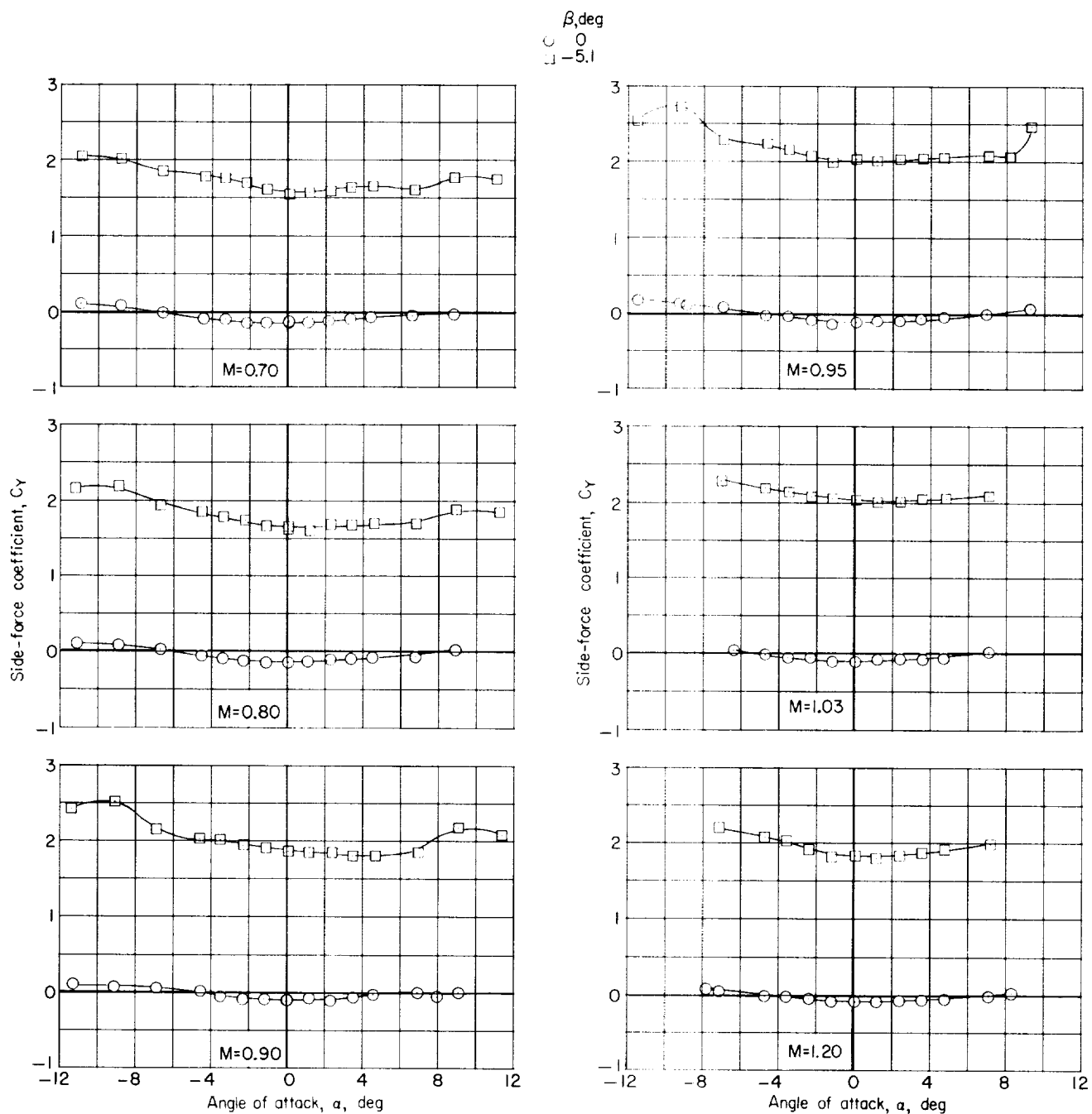
(d) Rolling-moment coefficient.

Figure 20.- Continued.



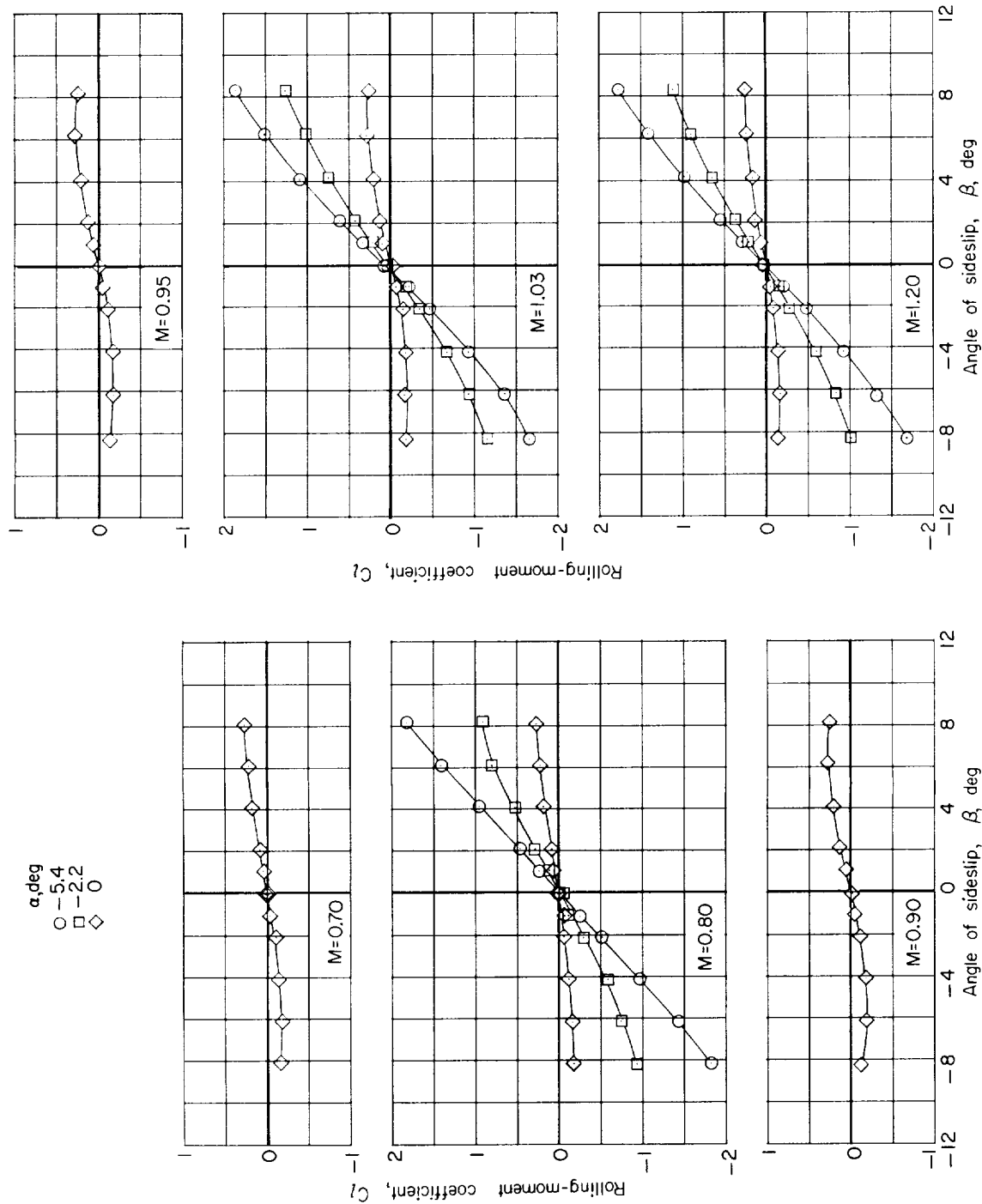
(e) Yawing-moment coefficient.

Figure 20.- Continued.



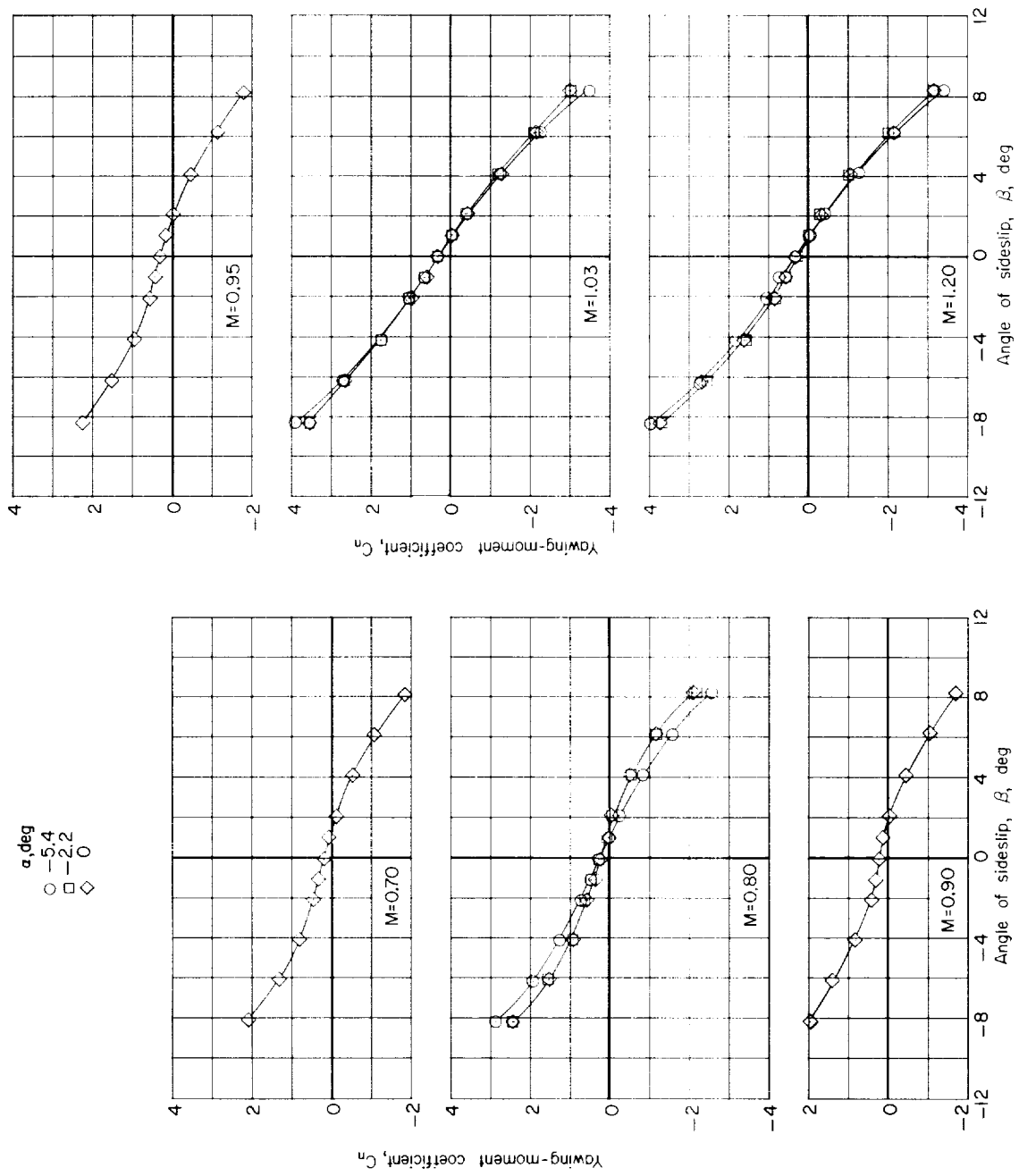
(f) Side-force coefficient.

Figure 20.- Concluded.



(a) Rolling-moment coefficient.

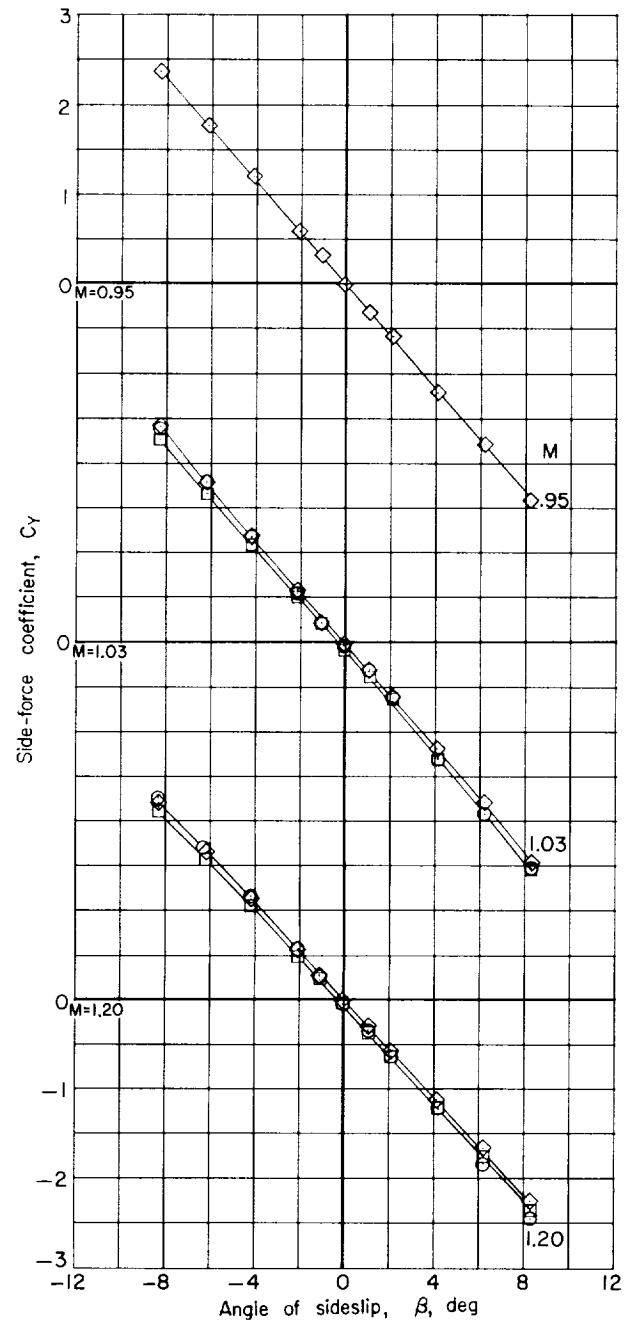
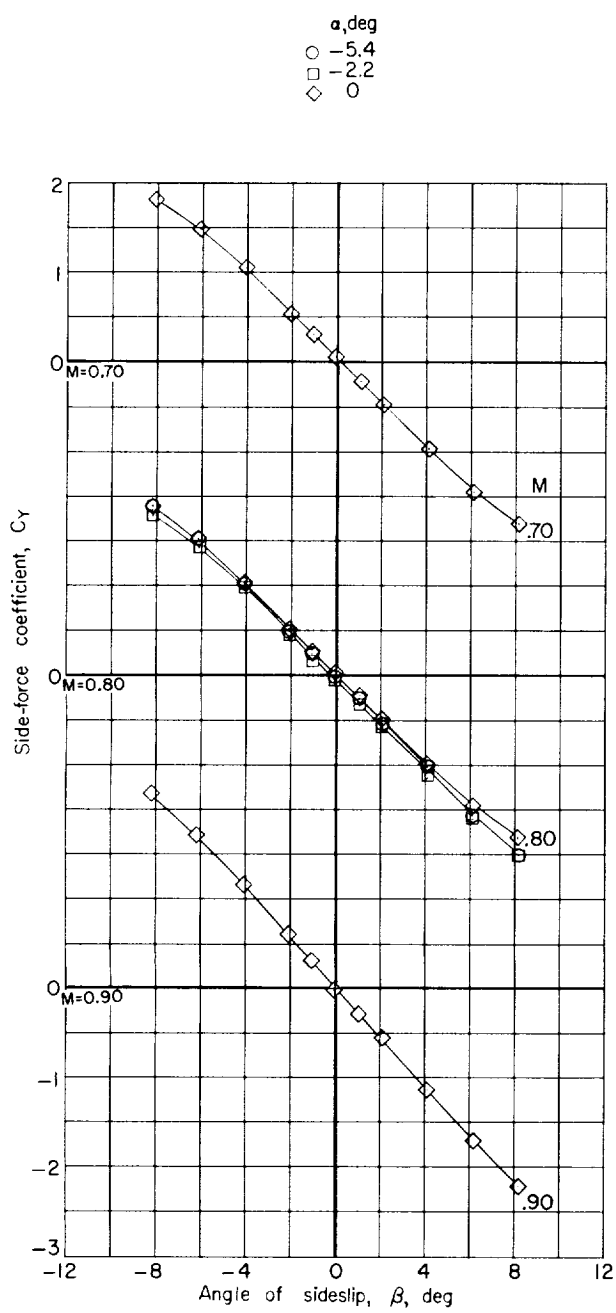
Figure 21.- Aerodynamic characteristics in sideslip of Titan III launch-vehicle configuration with small fins and bulbous nose shape.



(b) Yawing-moment coefficient.

Figure 21.- Continued.

CONFIDENTIAL



(c) Side-force coefficient.

Figure 21.- Concluded.

CONFIDENTIAL

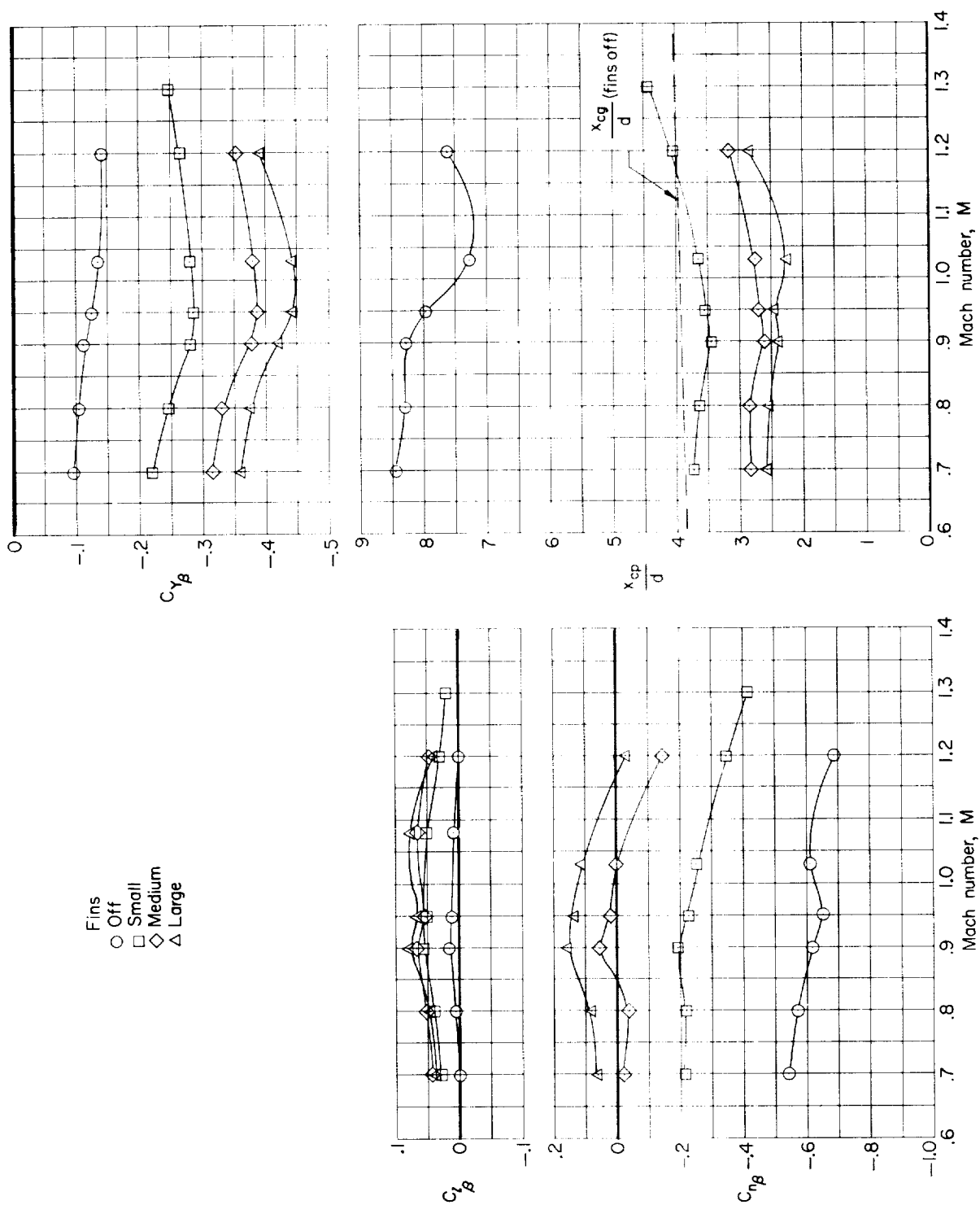


Figure 22.- Summary of the static lateral aerodynamic characteristics of several Titan III launch-vehicle and Dyna-Soar glider configurations. $\alpha = 0^\circ$.

Fins
 ○ Yaw off, pitch on
 □ On

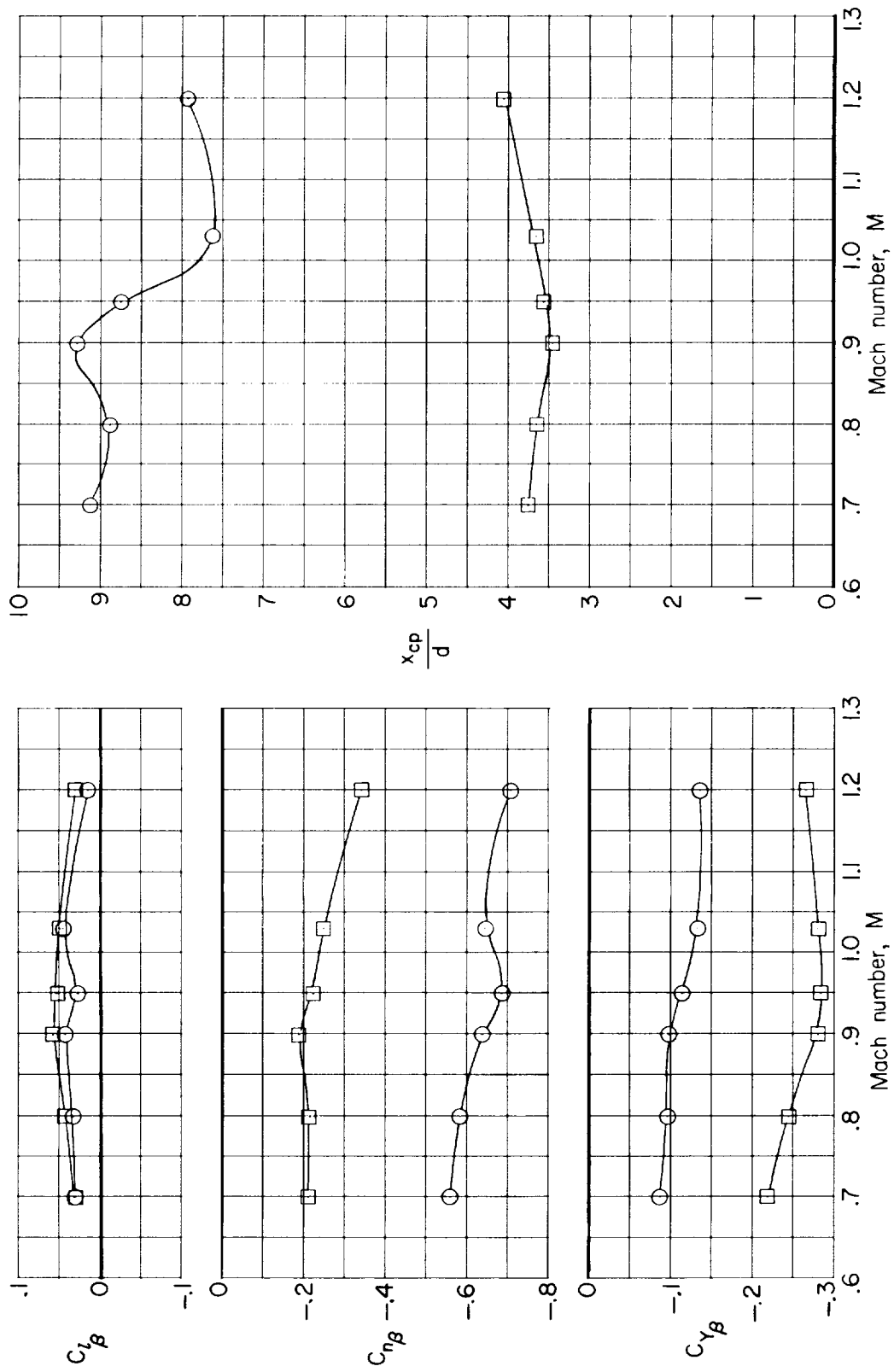


Figure 23.- Summary of the static lateral aerodynamic characteristics of the basic configuration with small fins. $\alpha = 0^\circ$.

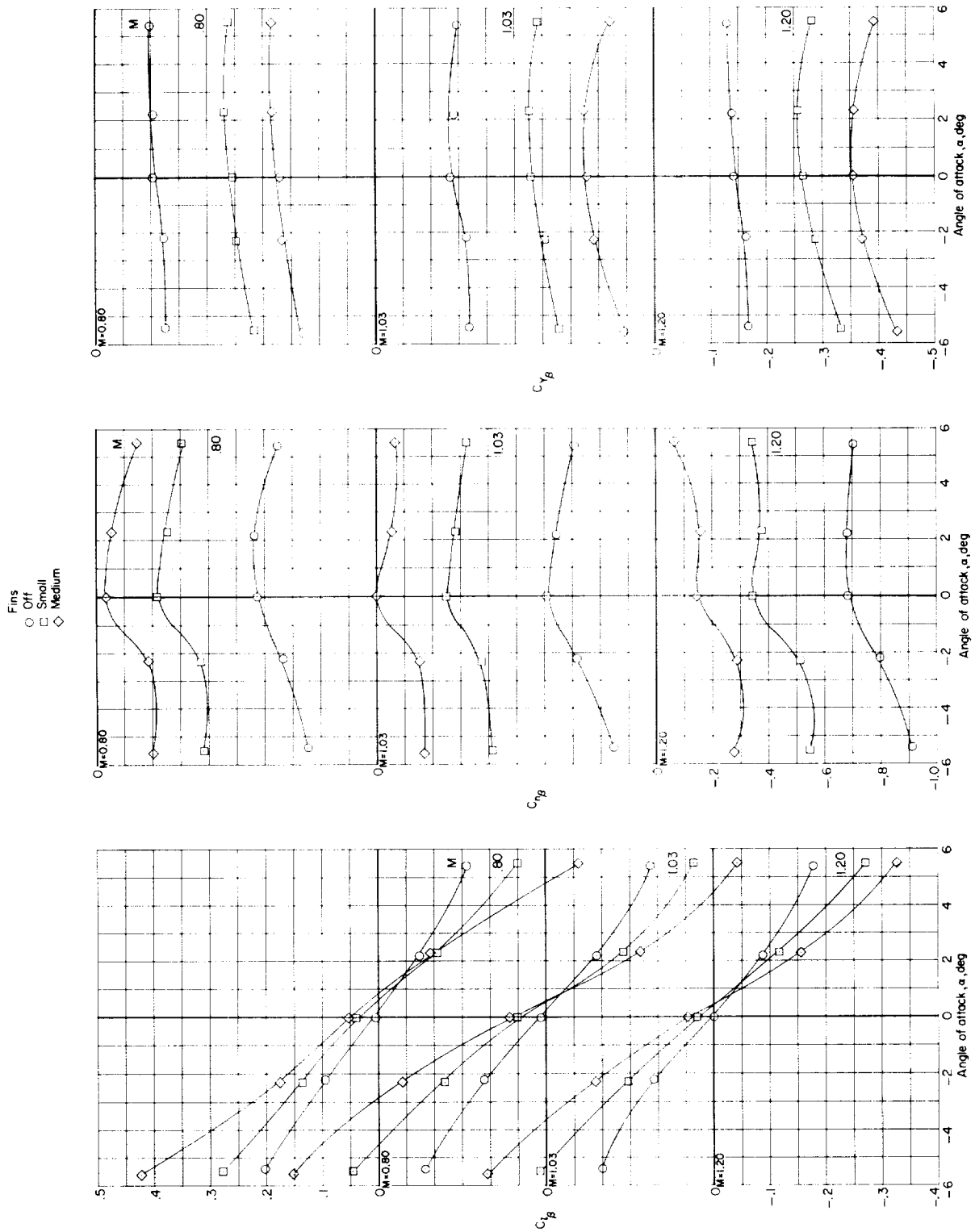


Figure 24.- Variation of the static lateral aerodynamic characteristics with angle of attack for various Titan III launch-vehicle and Dyna-Soar glider configurations.

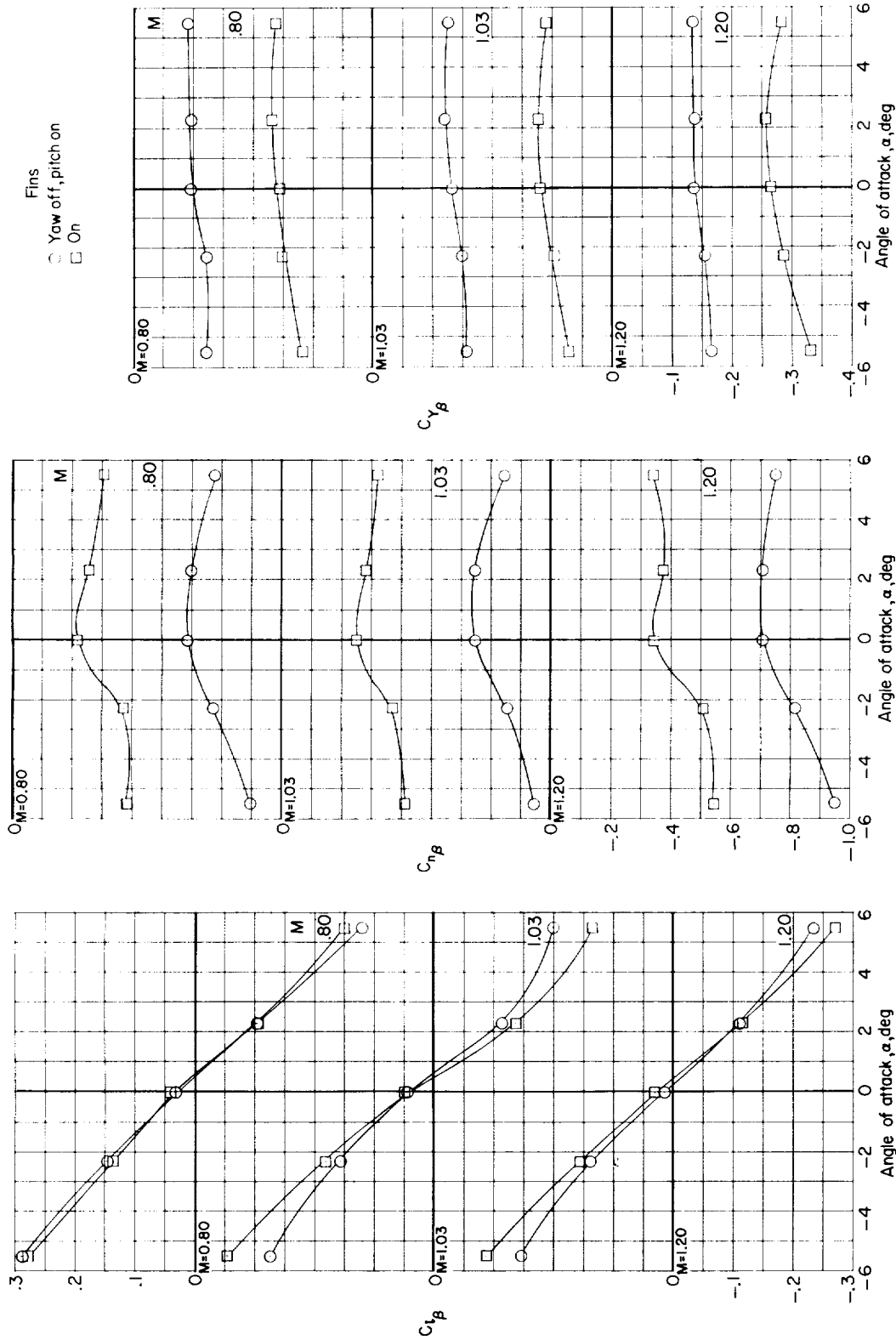


Figure 25.- Effect of yaw fins on the variation of the static lateral aerodynamic characteristics with angle of attack for the basic configuration with small fins.

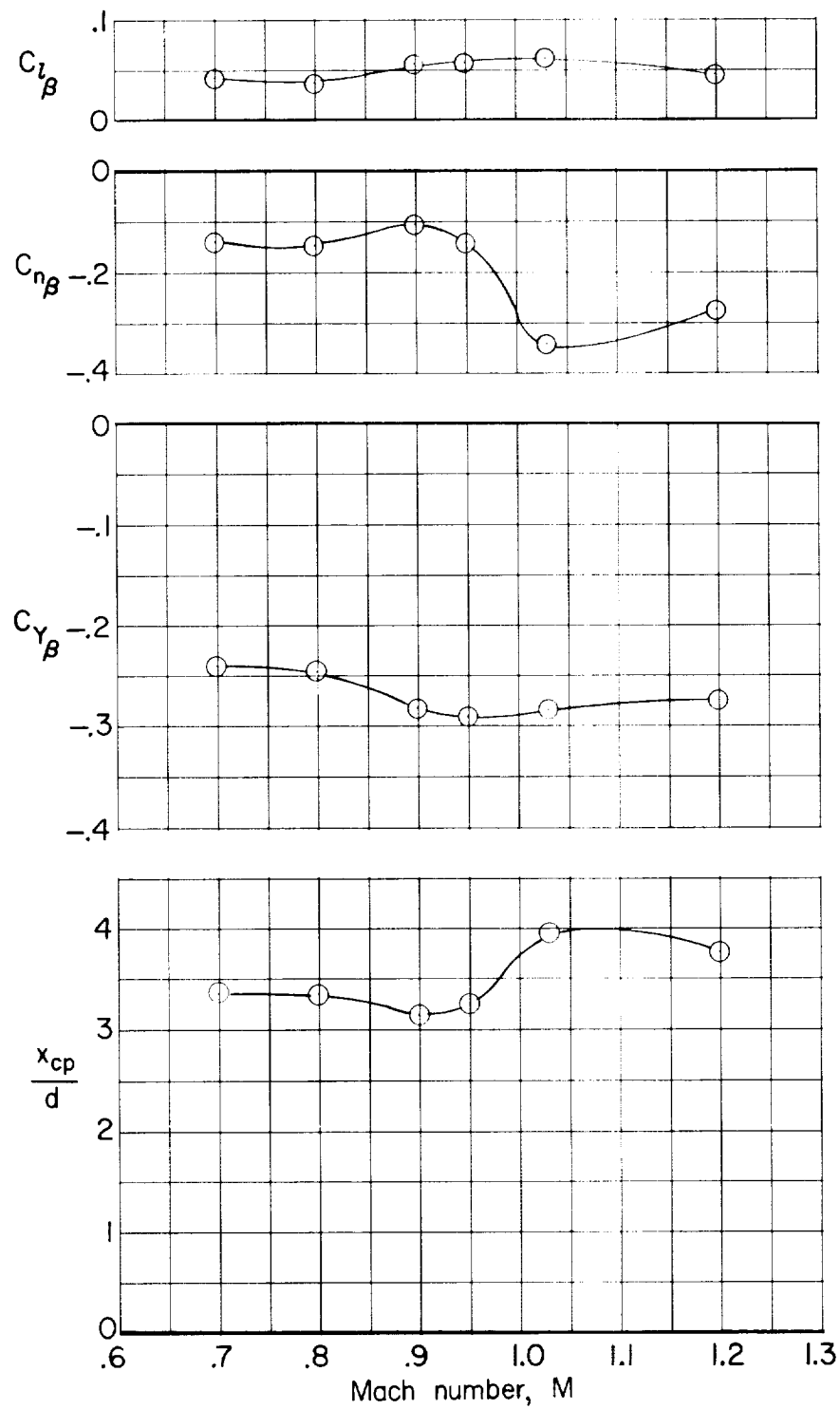


Figure 26.- Summary of the static lateral aerodynamic characteristics of the Titan III launch-vehicle configuration with small fins and bulbous nose shape. $\alpha = 0^\circ$.